MECHANOSENSOR-MEDIATED HSP70 PHOSPHORYLATION ORCHESTRATES THE LANDSCAPE OF THE HEAT SHOCK RESPONSE

by

Siddhi Omkar

A dissertation submitted to the faculty of
The University of North Carolina at Charlotte
in partial fulfillment of the requirements
for the degree of Doctor of Philosophy in
Biology

Charlotte

2024

Approved by:

_____
Dr. Andrew Truman

_____
Dr. Adam Reitzel

_____
Dr. Richard Chi

_____
Dr. Mehdi Mollapour

_____
Dr. Victor Cifarelli

ABSTRACT

SIDDHI OMKAR. Mechanosensor-mediated Hsp70 phosphorylation orchestrates the landscape of the heat shock response.
(Under the direction of DR. ANDREW W. TRUMAN)

Heat shock protein 70 is an evolutionary conserved molecular chaperone responsible for the protein quality control functions. It is involved in many critical cellular processes, including folding protein 'clients', modulation of protein-protein interactions, and transport of proteins across membranes. Hsp70s are critical for maintaining cell viability in response to a large variety of cellular stresses. Perturbation of the proteostasis network is implicated in many diseases ranging from cancer and neurodegeneration to genetic disorders. Hsp70s are highly modified at the post-translational level. All these modifications together are referred to as the "chaperone code. These modifications fine-tune chaperone function, altering chaperone activity, localization, and selectivity. Understanding the regulation of these modifications will provide new insights into the protein folding process as well as the characterizing the direct interplay between chaperones and major signal transduction pathways. This thesis investigates a critical post-translational modification (PTM) site on yeast Heat Shock Protein 70 (Hsp70) that undergoes phosphorylation during heat shock response. Here, we focus on threonine 492 (T492), a highly conserved residue on Hsp70, which is conserved across all domains of life. Elucidating its upstream regulation and downstream effects. Yeast cells respond rapidly to heat stress by activating multiple protective mechanisms to maintain proteostasis. These include Hsf1 and Msn2/4-mediated transcriptional activation, cell integrity signaling, stress-induced biomolecular condensate formation and resolution, and protein translation inhibition. However, these pathways' rapid activation and coordination

have remained poorly understood. Our findings reveal that heat-induced membrane stretch is detected by the Mechanosensor Mid2, triggering rapid phosphorylation of the cytosolic Yeast Hsp70 at T492. This phosphorylation event has several crucial downstream effects, which include altered interactome, altered dynamics of P-body resolution, maintenance of translational fidelity, amplification of the cell-wall integrity pathway, proper activation of heat-shock response, and regulation of clients Bck1 and Edc3. Together, these results provide a comprehensive, unified theory of the global yeast shock response mediated by the Hsp70 chaperone code.

DEDICATION

In the loving memory of my dearest Ajoba (Mr. Shrikrishna Patankar),

Your unwavering belief in the power of knowledge and your constant encouragement have always shown me a path forward

Your wisdom, resilience, and kindness continue to inspire me every day.

We miss you!

ACKNOWLEDGEMENTS

Firstly, I extend my deepest gratitude to my mentor, Dr. Andrew Truman. Your impact on my graduate career and personal growth has been immeasurable. Your dedication to helping students and advancing the chaperone code field has been truly inspiring. I will forever be grateful for the opportunity you gave me to be part of the lab. Despite beginning my PhD during the challenging COVID era of online interactions, your infectious enthusiasm motivated me to push my boundaries and helped transform me into a confident, critically thinking scientist. Your mentorship has not just shaped my academic journey but has fundamentally influenced my approach to scientific inquiry and professional development.

I extend my sincere gratitude to my committee members, Dr. Richard Chi, Dr. Mehdi Mollapour, Dr. Adam Reitzel, and Dr. Victor Cifarelli, for their support and guidance throughout my graduate research. Dr. Chi, your advanced cell biology class was exceptional, and your help with microscopy was invaluable. The collaborative atmosphere in Lab 1, created by you and Dr. Truman, made research truly enjoyable. Dr. Reitzel, thank you for patiently answering my numerous questions about graduate school and helping with RNA extraction. Dr. Mollapour, your inspirational research and dedication to growing the chaperone code community have been remarkable.

I am deeply grateful to all past and present members of the Truman lab. Special thanks to my undergraduates - Liz, Ishaan, and Ainella - for their assistance and for making Lab 1 such a happy workplace. To current members - Megan Mitchem, Dr. Chathura, Dr. Yevheniia, and all undergraduates - your support has been invaluable. Duhita Mirikar, my

lab sister, your friendship and support have made this journey a bit easy. To Chi lab members, especially Trey Grissom and Jacob, thank you for your support and generosity with reagents. Thank you to all faculty and staff in the Department of Biological Sciences and the Graduate School for their continuous support.

To my pillars of strength - Omkar, for loving me through good and bad days, making me laugh, and being my biggest supporter; Aai (Deepa Patankar), for your unwavering faith and being my anchor; Baba (Suhas Patankar), for your quiet confidence and lessons about integrity; and Sawani, my constant source of strength and joy. I couldn't have managed pregnancy and PhD together without you four. To my sweetest baby boy Athang, your arrival brought new meaning to everything - thank you for being my tiny lab partner and motivation. This thesis carries not just years of research but our story of growing together.

I am deeply grateful to all BHAKOPAs for their unwavering support and encouragement throughout this journey. A special thank you to Anandi, whose video calls brought light and joy to those long hours in the lab. My heartfelt gratitude extends to my family, who placed their trust in me and stood by my side unconditionally. And to those family members who questioned my capabilities - your doubts became the stepping stones to my success.

I extend my heartfelt thanks to my friends from Pune and Baroda, who made my scientific journey enjoyable and memorable. I am deeply grateful to my Charlotte family for creating a warm home away from home - your support, encouragement, and love have meant everything to me. A special note of gratitude to Shweta Dixit-Pingle, ma’am, who not only taught me laboratory skills but also instilled strong scientific ethics. I am indebted to all my professors at Fergusson College Pune and MSU Baroda for their excellent teaching that ignited my passion for science. I would also like to thank my mentors at the National

Institute of Virology, Vasantdada Sugar Institute, and Venkys, who guided and supported me at every step of my scientific journey.

Above all, I bow to the Almighty for bestowing me with the strength and courage to overcome every challenge on this journey.

Table of Contents

LIST OF FIGURES

LIST OF TABLES

LIST OF ABBREVIATIONS

Hsp70 – Heat Shock Protein 70

HSR- Heat shock response

Hsf1 - Heat shock factor 1

HSE -Heat shock element

CTA- carboxyl-terminal transactivation domain

CWI - Cell-wall integrity

BiP – Binding Protein

NBD - Nucleotide-binding domain

SBD - Substrate-binding domain

NTD – N terminal domain

CTD - C-terminal domain

PTM – Post Translational Modification

IP - Immunoprecipitation

NEF - Nucleotide Exchange Factors

LC-MS – Liquid chromatography-mass spectrometry

GO - Gene ontology

NLS – Nuclear localization signal

RNPs -ribonucleoproteins

IDR- Intrinsically disordered domain

PBs-P-body or processing body

SGs-Stress gran

CHAPTER 1: INTRODUCTION

Hsp70

The heat shock protein 70 (Hsp70) family represents a group of well-conserved yet functionally diverse crucial for various cellular housekeeping functions (1). Hsp70 is critical for the folding of newly synthesized proteins (2), the translocation of polypeptides, the disassembly of protein complexes, and the regulation of protein activity. Hsp70s also play a crucial role in promoting the clearance of misfolded denatured proteins and protein degradation and preventing stress-induced aggregation (3-5). Thus, Hsp70s act as sentinel chaperones, guarding cells against the deleterious effects of a wide range of proteotoxic stresses (3). Hsp70s are critical components of the proteostasis network and help cells cope with a wide range of cellular stresses, including high temperature, nutrient starvation, osmotic shock, oxidative stress, and DNA damage, for maintaining cell viability in response to a large variety of cellular stresses (2). The Hsp70 family of proteins represents a highly conserved group of molecular chaperones that spans the entire phylogenetic spectrum, from archaebacteria to prokaryotes and eukaryotes, including plants and animals (5-7). This widespread distribution suggests the fundamental importance of Hsp70s in cellular function across diverse life forms.

Domain structures of Hsp70

The Hsp70 molecular chaperone exhibits a modular design with distinct functional domains. The protein features two major regions: a 45-kDa nucleotide-binding domain (NBD) at the N-terminus (9) and a 28-kDa substrate-binding domain (SBD). These domains communicate through a flexible linker. The NBD's architecture includes four

essential subdomains (IA, I, IIA, and IIB) that orchestrate ATP binding and hydrolysis. The SBD's organization comprises three key elements: the substrate-binding region (SBDβ), a helical lid (SBDα), and a flexible C-terminal tail featuring a conserved EEVD (Glu-Glu-Val-Asp) motif (10). This EEVD sequence serves as a crucial docking site for co-chaperone interactions, while the interdomain linker facilitates allosteric communication between the major domains. ATP hydrolysis promotes conformational changes in NBD, which triggers the closure of SBDα over the SBDβ (11). This "closed" conformation effectively sequesters the bound client protein, minimizing its dissociation and providing a protected environment for folding processes to occur (9). The subsequent ADP release and binding of an ATP molecule reverses these conformational changes. The ATP-bound state promotes an "open" conformation, facilitating the release of the processed substrate (11-13). This ATP-driven allosteric mechanism enables Hsp70 to cycle between high and low-affinity states for substrate proteins, which is fundamental to its function in promoting proper protein folding and maintaining cellular proteostasis (1, 3).

Hsp70s in yeast

The cytosolic Hsp70 system in Saccharomyces cerevisiae encompasses multiple distinct families: Ssa, Ssb, Sse, and the atypical Ssz1 (stress seventy A, B, E, Z). These chaperones demonstrate functional specialization, falling into two main categories (14). The "generalist" category, represented by the Ssa family, exhibits broad substrate recognition, binding to various hydrophobic regions of unfolded proteins to assist in their folding. In contrast, "specialist" chaperones, exemplified by the Ssb family, perform targeted functions, such as ribosome-associated activities and cotranslational protein folding, demonstrating their evolution toward specific cellular processes and substrate interactions

(14). *Saccharomyces cerevisiae* contains seven cytosolic Hsp70 family proteins-cytosolic Ssa1-4 (the expression of at least one isoform is essential for viability), Ssb1-2 and Ssz1 (ribosomal bound) (15-17). In addition, there are three mitochondrial isoforms (Ssc1, Ssq1, and Ecm10) and one specific to endoplasmic reticulum (Kar2) (17). The Ssa protein family, a product of genome duplication events, exhibits remarkable sequence conservation among its members. While Ssa3 and Ssa4 share 88% sequence identity with each other and maintain 80% identity with Ssa1/2, they show distinct expression patterns, being activated only under stress conditions to protect cells from adverse effects (18). Under optimal growth conditions, Ssa2 maintains dominance, expressing approximately four times higher levels than Ssa1 due to partial repression of the SSA1 promoter in non-stress conditions. Importantly, cells maintain tight control over total Hsp70 levels through a compensatory mechanism where Ssa2 depletion triggers increased Ssa1 expression (18-19).

Regulation of Hsp70 function

The functional cycle of Hsp70 is precisely controlled through two critical steps: ATP hydrolysis and ADP-ATP exchange rates. This regulation involves two essential classes of cochaperones that interact with Hsp70's nucleotide-binding domain (NBD): J-domain proteins and nucleotide exchange factors (NEFs) (20,21). These cochaperones enhance the versatility and specificity of Hsp70 function, with J-proteins particularly notable for their ability to enhance Hsp70's ATPase activity (22-24). Together, these regulatory components create a sophisticated system for controlling chaperone function. Hsp70's substrate binding characteristics vary significantly depending on its nucleotide-bound state. Hsp70 displays reduced substrate affinity and accelerated exchange rates in its ATP-bound conformation.

Conversely, it exhibits enhanced substrate affinity and slower exchange rates when bound to ADP. This distinction primarily stems from positioning the C-terminal domain (CTD). The nucleotide-dependent positioning of Hsp70's C-terminal domain (CTD) is crucial in substrate retention. When ADP is bound, the CTD covers the substrate binding pocket, creating a secure environment that prevents premature substrate release. Nucleotide exchange factors facilitate this process by promoting ADP release from Hsp70's nucleotide-binding domain (NBD), thereby regulating the substrate binding and release cycle. This mechanism is fundamental to Hsp70's ability to control substrate handling effectively. The nucleotide-dependent positioning of Hsp70's C-terminal domain (CTD) is crucial in substrate retention. When ADP is bound, the CTD covers the substrate binding pocket, creating a secure environment that prevents premature substrate release. Nucleotide exchange factors facilitate this process by promoting ADP release from Hsp70's nucleotide-binding domain (NBD), thereby regulating the substrate binding and release cycle. This mechanism is fundamental to Hsp70's ability to control substrate handling effectively. (26,27). In Saccharomyces cerevisiae, nucleotide exchange factors (NEFs) comprise several key proteins: the Hsp110 family members (Sse1/2), Fes1, and Snl1. Within the Hsp110 family, Sse1 and Sse2 share 76% sequence identity and maintain approximately 70% similarity with Ssa1, positioning them as evolutionarily distant members of the Hsp70 family (28).

Hsp70 chaperone code

The cellular proteome gains remarkable functional diversity through post-translational modifications (PTMs), where proteins undergo chemical alterations after their initial synthesis. These modifications act as sophisticated molecular switches, attaching specific

chemical groups to proteins and fundamentally altering their properties. By modifying either individual or multiple amino acid residues, PTMs create dynamic changes in protein behavior, structure, and interactions (29,30). The chemical transformations at modification sites can profoundly impact protein function (31). Elucidating the precise patterns of these modifications - their locations, types, and effects on specific amino acids - remains crucial for understanding their roles in biological processes. The extensive array of post-translational modifications discovered on chaperone proteins suggests the existence of a sophisticated regulatory code that fine-tunes their function and activity (32). Recent investigations have revealed an intricate network of post-translational modifications in Hsp70 proteins (32-36). A landmark 2012 bioinformatic analysis identified two critical PTM hotspots: T36 in the nucleotide-binding domain (NBD) and another in the substrate-binding domain (SBD) encompassing residues T492, S495 and T499, where mutations significantly impaired chaperone function (29). A pivotal mechanistic breakthrough followed, demonstrating how cell-cycle kinase-mediated phosphorylation of a single Hsp70 site could influence cyclin stability and cell cycle progression (37). Subsequent studies uncovered additional regulatory mechanisms through C-terminal phosphorylation and methylation, leading to the emergence of the "chaperone code" concept (32,38), analogous to the histone code. This code suggests that PTMs orchestrate multiple aspects of chaperone function, including activity modulation, cellular localization, and substrate specificity (1). The conservation of these modifications across species indicates that PTM-based regulation of chaperones represents an evolutionarily selected mechanism for precise control of protein function.

Affinity purification combined with tandem mass spectrometry (AP-MS/MS) represents a powerful technological approach for studying protein modifications and interactions. This sophisticated analytical method enables detailed characterization of protein modifications and complexes. Additionally, bioinformatics-based approaches, isoelectric properties of the protein, and isotope labeling have uncovered several post-translational modifications on chaperones (1, 39). Modern research into Hsp70 modifications is facilitated by sophisticated online databases that track and analyze post-translational modifications. The comprehensive platform PhosphoSitePlus® (RRID: SCR_001837) serves as a central repository, documenting various PTMs - from phosphorylation and acetylation to methylation, ubiquitination, and O-glycosylation - while providing crucial context for their biological significance (40). Complementing this, the Global Proteome Machine Database (RRID: SCR_006617) offers daily updated PTM information (41). Deciphering the complete "chaperone code" remains challenging despite these powerful resources. Key obstacles include connecting specific modifications to chaperone function, identifying the stress conditions and enzymes that regulate these PTMs, and understanding how these modifications orchestrate various cellular pathways.

Hsp70 phosphorylation

Phosphorylation is adding a phosphate group to an amino acid such as Serine, Threonine, and Tyrosine (42). Members of the Hsp70 family exhibit extensive phosphorylation patterns, with remarkable numbers of modification sites identified across different family members: 88 sites in Hsc70, 87 in BiP, and 73 in yeast Ssa1 (1). A few sites which undergo post-translational modifications on molecular chaperones have been studied. Phosphorylation of Hsp70 is known to regulate important cellular processes, such as cell

cycle progression (37), apoptosis (43), Stabilizing kinetochore fibers, mitotic progression (44), protein degradation, and client triaging (38, 45-46), and host-pathogen interaction (47). In pathogenic yeast *Candida albicans*, phosphorylation regulates growth and hyphae formation (48). Similarly, the malarial parasite *Plasmodium berghei* displays phosphorylation of Hsp70 at the gametocyte stage. (49). The extensive phosphorylation patterns found on Hsp70 proteins may play a crucial role in host-parasite interactions, potentially providing protective mechanisms for parasites within their hosts. However, a fundamental question persists: the specific functions and biological significance of most of these numerous modification sites remain largely unexplored and poorly understood. Although chaperone code research is in its infancy, the study of the role and regulation of each site will form the foundation for future studies on global regulation of the code.

Heat Shock Response (HSR)

The Heat Shock Response (HSR), an evolutionarily conserved protective mechanism from yeast to humans, serves as a crucial cellular defense against stress-induced damage. As a component of the broader environmental stress response (ESR), HSR operates through two primary transcription factors, Hsf1 and Msn2/4 (14). This pathway simultaneously suppresses general protein synthesis while inducing heat shock protein (HSP) expression when activated. Heat Shock Factor 1 (Hsf1) plays a central role in maintaining protein homeostasis and cellular fitness during proteotoxic stress conditions. This fundamental cytoprotective mechanism exemplifies cellular adaptation to environmental challenges. Heat Shock Factor 1 (Hsf1) promotes protein homeostasis and cellular fitness under proteotoxic stress (19). HSR is an evolutionarily conserved program in eukaryotes from yeast to humans. The Heat Shock Factor (HSF) family in vertebrates and plants comprises

four distinct members - HSF1, HSF2, HSF3, and HSF4. Within this family, HSF1 emerges as the master regulator, playing the dominant role in orchestrating Heat Shock Protein (HSP). Unlike higher organisms with multiple heat shock factors, yeast and other invertebrates possess a single HSF that functionally parallels mammalian HSF1. In Saccharomyces cerevisiae, HSF1 exists as an essential single-copy gene encoding an 833-amino-acid protein (50-51). This system's simplicity and essential nature has established S. cerevisiae as a powerful experimental model for investigating heat shock response mechanisms. eukaryotic HSR in detail. The essential nature of HSF1 in yeast is demonstrated by the lethal phenotype of HSF1 deletion mutants, indicating its crucial role even during normal growth conditions. This vital function likely operates through HSF1's regulation of molecular chaperones like Hsp70 and its influence on other target genes. The yeast Hsf1 has the DNA-binding domain (DBD), three leucine zipper (LZ) repeats, Control element 2 (CE2) or regulatory domain, and a carboxyl-terminal transactivation domain (CTA) (14). Leucine zipper is responsible for the trimerization of the factor. DBD is the most conserved domain within the Hsf family. CTA is responsible for sustained responses. Saccharomyces cerevisiae Hsf1 contains a distinct transcriptional activation domain at its N-terminus (NTA), promoting transient transcriptional response. (49). Heat shock transcription elements (HSEs) in Hsf1 target genes are characterized by pentameric sequences (nGAAn) (50). The "perfect" HSE consists of three consecutive inverted repeats (nTTCnnGAAnnTTCn). At the same time, the "gap" type features a 5-base pair insertion between units [nTTCnnGAAn (5 bp) nGAAn], and the "step" type includes 5-base pair spacings between all units [nTTCn (5 bp) nTTCn (5 bp) nTTCn] (53-55). These spacing variations maintain the crucial 5-base pair orientation of the consensus sequences. While

human Hsf1 prefers perfect HSEs, yeast Hsf1 can recognize perfect and discontinuous arrangements. The regulation of Hsf1 follows a titratable chaperone repressor model originally derived from bacterial systems. (55). According to the proposed chaperone titration model for HSR, two major molecular chaperone families, Hsp70 and Hsp90, function as negative regulators of Hsf1 activity. Through this trans-acting repression, these heat shock proteins create a feedback loop that modulates the heat shock response. (56-57). An imbalance in protein homeostasis results in unfolded proteins accumulating, requiring increased chaperones to clear out the misfolded proteins. Under unstressed conditions, Hsf1 is bound to Hsp70. Upon heat shock, Hsf1 dissociates from Hsp70 and induces transcription. Basal levels of chaperones repress Hsf1 by direct binding (58-59). Induced chaperones, in turn, assist with protein folding (51 and 58-62). Heat stress is known to cause protein misfolding, thereby exposing hydrophobic regions (63). Hsp70 has a high affinity to these hydrophobic regions (64). HSF1 activity is controlled through multiple regulatory mechanisms that extend beyond simple chaperone titration. These sophisticated control mechanisms encompass spatial regulation via nuclear-cytoplasmic shuttling, diverse post-translational modifications (PTMs), and conformational changes within the HSF1 protein structure (65-67). In S. cerevisiae, HSF1 is nuclear and constitutively bound as a trimer even without stress (68); hence, the proposed model needs to be revised. Pincus and colleagues (59) revealed a finely calibrated feedback loop between Hsp70 and Hsf1 in Saccharomyces cerevisiae. Their research showed that Ssa1 (a yeast Hsp70) remains bound to Hsf1 under normal growth conditions. Upon heat stress, this interaction rapidly dissociates within 5 minutes, triggering the heat shock response. The Ssa1-Hsf1 binding is subsequently restored within 15 minutes, correlating with the attenuation of transcriptional

response (61, 65). Interestingly, the interaction between Hsp70 and Hsf1 occurs via the C-terminal substrate binding domain of Hsp70. SBD, thus, is required to maintain Hsf1 in an inactive state. Hsp70 was found to associate independently with the CE2 site in the Hsf1 C-AD, and a novel site was identified in the N-AD (49). It was demonstrated that Hsf1 activation can be regulated by increasing the rate at which Hsp70 releases substrates in the nucleus. They tested this by targeting NEF Sse1 to the nucleus, which activated Hsf1 and decreased the Hsp70-Hsf1 complex (65). They demonstrated that excess Hsp70 inhibits Hsf1 DNA-binding activity. Pincus and group also showed the role of localization of the J-protein Sis1 in regulating HSR activation in yeast. (69-70). However, the influence of the Hsp90 chaperone system on the HSR is predicted to be indirect rather than direct binding (14). Hsf1 is subjected to a large number of post-translational modifications like phosphorylation, acetylation, SUMOlytion, and ubiquitination, but the influence of these modifications on the heat shock response is still not clear (71). The role of hyperphosphorylation of Hsf1 to help regulate the yeast's heat shock response was evaluated. (58).

The role of condensates in the HSR

For decades, Hsf1 has been known to be the master regulator of heat shock response. However, recent studies from (61) suggest that the decade-old Hsf1 theory needs modifications. For a long time, toxic protein aggregates have been assumed to activate HSR (72). However, a new functional model is predicted, showing that adaptive biomolecular condensates activate HSR rather than aggregates. These adaptive condensates are known to be composed of orphan ribosomal proteins (oRP) and stress granule components that potentially act as Hsp70 clients. It is shown that upon heat shock,

condensates show dispersal in a Sis1- and Hsp70-dependent manner. Activation of HSR is propagated via the condensate cascade (73,74).

Msn2/4

The main regulators of the HSR in yeast are Hsf1, Msn2, and Msn4 (14 and 75). *MSN2/4* was initially identified as the multicopy suppressor of *SNF1* mutant with two zinc finger motifs (76). Msn2/4 and HSR are included in a general stress response pathway called the environmental stress response (ESR). ESR is activated in response to other stresses that include oxidative stress, osmotic shock, glucose starvation, high ethanol concentrations, temperature upshift, and freezing stress (77,78). There is an overlap of major chaperone-encoding genes that are regulated by both Hsf1 and Msn2/4 (79). During normal growth conditions, Msn2/4 transcription factors remain in the cytoplasm, where they are maintained in a phosphorylated state by PKA (cAMP-dependent protein kinase A). Environmental stress triggers rapid dephosphorylation of Msn2/4, prompting their translocation to the nucleus. Once nuclear, these factors bind to specific DNA sequences called stress-response elements (STRE; AGGGG) in target gene promoters, activating their transcription (14, 77). The treatment of amino acid analog AZC (azetidine-2-carboxylic acid) triggers a specific transcriptional response that aligns with the Hsf1-regulated gene set. while notably not activating genes controlled by the Msn2/4 stress response pathway. This selective activation demonstrates pathway-specific stress responses. (80). STRE has been found to control the activation of transcription of specific genes with protective functions. There is a set of genes whose activation depends on Ms2/4, including CTT1, DDR2, HSP12, TPS2, GSY2, and GPHI (81). These genes are used as reporters to track Msn2/4 inducibility. HSR and ESR are known to function in a compensatory manner (82).

The yeast cell integrity/PKC Pathway

The cell wall in Saccharomyces cerevisiae serves multiple vital functions. It acts as a primary architectural framework that maintains cellular morphology and structural stability while providing protection against mechanical forces (83,84). Additionally, this complex structure plays a crucial role in osmotic regulation and serves as a scaffold for surface-associated proteins (85). Remodeling of the cell wall is controlled by the Rho1p GTPase (86). The yeast cell wall features a distinctive dual-layer arrangement. The interior layer, identifiable by its electron-transparent properties, is built mainly of beta 1,3-glucan networks interconnected with chitin molecules through beta 1,6-glucan bridges. Meanwhile, the exterior layer, distinguished by its electron-dense characteristics, contains GPI (glycosylphosphatidylinositol) and Pir glycoproteins (87). The physical strength and stability of the cell wall stem from beta 1,3-glucan chains featuring beta 1,6 branching points, which are manufactured by glucan synthase (GS). The Cell Wall Integrity (CWI) pathway functions as a key stress response mechanism, triggering MAP kinase signaling cascade upon cell wall perturbation (83, 88). The activation of this pathway during acute heat exposure suggests its role in responding to temperature-induced destabilization of both cell-wall and membrane structures. Heat shock alters membrane fluidity and lipid composition. Sphingolipids are found to be accumulating rapidly after heat shock and play a role in heat shock signaling response (14).

CWI Pathway regulation

The Cell Wall Integrity (CWI) pathway initiates its response through specialized cell-surface sensors that detect wall stress. At the heart of this signaling network lies Rho1, which functions as the master regulator. Rho1 coordinates cellular responses by processing

signals from the cell surface and orchestrating essential outputs, including cell wall synthesis and actin cytoskeleton organization, to maintain wall integrity. (89), transcription, and exocytosis (90) Rho1 functions as a key regulatory component of the 1,3-β-glucan synthase (GS) complex while simultaneously activating protein kinase pathways. This dual role positions Rho1 as a central cell wall synthesis and signaling coordinator. The Cell Wall Integrity pathway employs a sophisticated surveillance system featuring five membrane-bound mechanosensors: Wsc1-3, Mid2, and Mtl1 (91, 92). These sensors trigger Rho1 GTPase activation through the exchange factor Rom2 (GEF) upon detecting wall perturbations. Signal amplification occurs through a sequential MAP kinase cascade, where Bck1 (MEKK) activates Mkk1/2 (MEKs), which in turn stimulates Mpk1 (MAPK), creating a powerful linear signaling response 93). Pkc1 is the first kinase in the signaling cascade (94). Different Pkc1 isoforms display slightly varied substrate sequence specificity; it is commonly accepted that the general motif is an arginine at the -3 position and a basic residue at the +2-position relative to the phosphorylation site (95). Pkc1 phosphorylates and activates Bck1, followed by activating Mkk1/2 via phosphorylation (96 and 97). This further can dual Tyrosine/Threonine-specific phosphorylation of Mpk1 (83,88 and 98).) (The activation state of Mpk1 can be monitored using antibodies that recognize phosphorylated mammalian ERK1/2 (p42/44), demonstrating the evolutionary conservation of these MAP kinase phosphorylation sites. This cross-reactivity provides a valuable tool for studying stress response pathways (99 and 100). The Mlp1 pseudo-kinase is also phosphorylated by Mkk1/2 (101). The pathway activates two known transcription factors- Rlm1(102 and 103), which is activated through phosphorylation of Mpk1(104). The transcription factor Rlm1 plays a central role in cell wall maintenance. This regulator

serves as a key downstream effector in the cell wall integrity pathway. The second is SBF, a dimeric transcriptional regulator comprising Swi4 and Swi6. (105). SBF is phosphorylated, which regulates the expression of cell-cycle genes. Mpk1 and its pseudo-kinase paralog, Mlp1, use a noncatalytic mechanism to activate SBF. The catalytic activity of the glucan synthase (GS) complex relies on two related genes, FKS1 and FKS2. However, when both genes are lost, the resulting defect proves lethal and cannot be rescued even with increased osmotic support (88). Fks2 is activated non-catalytically through SBF via the stable association of Mpk1 with SBF at the *FKS2* promoter (86 and 106). Mutations affecting any protein kinase downstream of Pkc1 lead to temperature-sensitive cell lysis, highlighting the critical nature of this signaling cascade. Notably, osmotic stabilizers such as 1M sorbitol can rescue these growth defects, indicating that the primary defect lies in cell wall construction rather than other cellular processes. (88). The activation of CWI signaling can be detected by measuring Mpk1 protein kinase activity, immunological detection of phosphorylated Mpk1, or by activation of transcriptional reporters (107-110).

Heat stress and CWI

Mutations of components in the cell integrity pathway cause temperature sensitivity at 37 °C, which can be rescued by an osmotic stabilizer (88). The deletion of PKC1 causes cell lysis regardless of growth temperature, demonstrating its fundamental role in maintaining cell wall integrity and cellular viability (96). Thus, Pkc1 is a regulator of additional targets separate from the MAP kinase cascade. Similarly, several Hsf1 and chaperone mutants are viable at growth temperatures but sensitive to high temperatures (111). This temperature-sensitive defect is also reversed by 1M sorbitol. This effect was shown to be linked to defects in Mpk1. Mpk1 was identified as a client of Hsp90. A reduction in Hsp90 function

led to decreased activity of Mpk1 (99 and 112). It was shown that Hsp90 binds exclusively to the dually phosphorylated form of Mpk1. Hsp90 function is crucial here to activate the downstream targets of CWI. Heat causes cell wall weakness. Weakened cell walls possibly have increased membrane fluidity. Activation of the CWI pathway at high temperatures plays a novel role in induced thermotolerance (107). It was demonstrated that the activation of the cell-wall integrity pathway does not regulate the heat shock gene expression (95). It was shown that the cell wall integrity pathway is activated under heat shock in a misfolded protein-independent manner. They used azetidine 2-carboxylic acid (AZC) to mimic misfolded protein. AZC treatment does not cause Pkc1 activation (113). The essential role of the Cell Wall Integrity pathway in thermal adaptation is demonstrated by genetic studies where overexpression of either Mpk1 (the terminal kinase) or the transcription factor Rlm1 can rescue growth defects in Hsf1-mutant cells at high temperatures. This genetic evidence confirms that CWI pathway activation is crucial for cellular survival under thermal stress. (114). Upon overexpression of Hsp90, cells deficient with the Hsf1 restored the ability to grow at high temperatures. The reduced expression of Hsp90 impairs cellular growth at elevated temperatures, demonstrating the critical role of this chaperone in high-temperature survival

CWI and chaperones

Few initial studies show the important connections between cell wall integrity and chaperone function in yeast, specifically through KAR2, which encodes an ER-resident Hsp70 chaperone. Mutations in KAR2 affect cell wall maintenance, demonstrating the crucial link between protein folding in the ER and cell wall biosynthesis. Decrease b1,6-glucan in the cell wall (115). It was discovered that overexpression of Mid2 in yeast lacking

co-chaperone Ydj1 rescued its viability at high temperatures by thickening the wall (116). They also demonstrated that temperature-sensitive mutants of Hsp82 (G313N and G170D) that exhibited cell-wall defects had improved growth at elevated temperatures by overexpression of Mid2 or Pkc1(116). However, overexpression of Mid2 or components in the CWI pathway is unable to rescue the Hsp70 thermosensitive mutant (Ssa1-45) phenotype.

Yeast HSFs has two distinct *trans*-activation domains: (amino-terminal (NTA) and c-terminal (CTA), respectively). Loss of the C-terminal domain of Hsf1 led to compromised viability at high temperatures (80 and 111). Further, it was demonstrated that loss of the CT domain of Hsf1 resulted in cell-wall integrity pathway defect at high temperatures. Studies have revealed that deletion of the amino acids 583-833 in *Saccharomyces cerevisiae* Hsf1 impairs proper heat-induced activation of Mpk1, demonstrating this domain's importance in stress response signaling. (114). This resulted in a lack of cell wall-related gene expression and weak cell walls at high temperatures. Hsp110 is a nucleotide exchange factor that is shown as *SSE1/2* genes in *Saccharomyces cerevisiae*. The chaperone Sse1 plays a crucial role in Cell Wall Integrity (CWI) pathway signaling through its cooperation with Hsp90 and interaction with the terminal kinase Mpk1. While studies have also confirmed that Sse1 forms a complex with Slt2 in living cells, this interaction is not essential for maintaining Slt2's stability or phosphorylation state. However, cells lacking Sse1 show a complete loss of Rlm1 activity. Sse1 functionally interacts with both Hsp90 and Mpk1, demonstrating how chaperone networks integrate with stress signaling pathways (68 and 117).

Biomolecular condensates

In eukaryotic cells, the regulation of gene expression extends beyond transcription through sophisticated post-transcriptional control of messenger RNA. This regulatory layer serves as a crucial mechanism for cells to rapidly adjust their gene expression patterns in response to environmental signals. (118). Stress granules and P-bodies, which are referred to as biomolecular condensates, are formed by the phase separation of RNAs and proteins. RNA granules are evolutionarily conserved and are reported in yeast, plant, nematode, fly, and mammalian cells (119). Saccharomyces cerevisiae serves as an excellent experimental system for investigating conserved stress response mechanisms. During stress conditions, cells exhibit two key responses: a global translational shutdown and the formation of distinct RNA-protein assemblies. Two types of granules emerge: stress granules, which contain ribosome-associated mRNAs and translation machinery components, and P-bodies, which accumulate translationally inactive mRNAs lacking initiation factors (119-120). Stress granules (SGs) and Processing bodies (PBs) maintain a dynamic equilibrium with translating ribosomes, showing quick adjustments in response to changes in the population of polysome-bound ribonucleoproteins (RNPs) (121-123). PBs are visible by microscopy under unstress and stress conditions, while SGs only become microscopically detectable under stress conditions. P-bodies and stress granules are distinct organelles, but due to the shared components, these organelles are thought to be linked functionally (123). The assembly of RNA granules is significantly influenced by Intrinsically Disordered Regions (IDRs) present in their associated proteins (124). A fascinating aspect of granule formation is that stress granules (SGs) emerge from existing P-bodies (PBs) during stress conditions, suggesting PBs act as storage sites for messenger ribonucleoproteins (mRNPs).

These two types of granules maintain dynamic interactions through common protein components and RNA molecules (125). P-bodies specifically function as concentration hubs for translationally inactive mRNPs, housing machinery for both translation suppression and RNA degradation, and contain a fundamental set of conserved proteins (119, 126). The components of the P-body include proteins from mRNA decapping machinery-Dcp1/Dcp2, the activators of de-capping-Dhh1, Pat1, Scd6, Edc3, the Lsm1-7 complex and exonuclease Xrn1 (127-130). P-bodies are sites for rapidly degrading defective mRNAs through the nonsense-mediated decay pathway. Their formation requires the presence of translationally repressed mRNAs, with their size and abundance directly correlating with the quantity of untranslated mRNA in the cell (119 and 125). Ribosomal subunits are not detected in PBs (131). The formation of P-bodies (processing bodies) is intricately linked to the Cell Wall Integrity (CWI) MAPK pathway, specifically requiring active Mpk1 kinase function. The temporal dynamics of P-body assembly precisely correlate with CWI pathway activation, demonstrating coordinated regulation between stress signaling and RNA processing. (132).

Stress granules (SGs) function as dynamic cellular structures that sequester mRNAs stalled in translation initiation. These complex assemblies incorporate multiple components: translationally repressed mRNAs, various translation initiation factors, poly(A)-binding protein (Pab1), diverse RNA-binding proteins like Ngr1, Pub1, Hrp1, Gbp2 and Additional regulatory factors like Pbp1, Nrp1, Eap1, Ygr250c (118, 133, 134). SGs maintain a dynamic equilibrium with polysomes and show sensitivity to translation inhibitors (135), functioning as crucial triage centers that direct mRNAs toward translation, storage, or degradation (136). Recent evidence suggests that pre-existing P-bodies may serve as

nucleation sites for SG assembly (118). The formation of these granules is enhanced by constitutively active Gcn2 kinase, which inhibits translation initiation through eIF2α phosphorylation, reflecting a mechanism conserved between yeast and mammalian cells (118, 137). The disaggregation of misfolded protein aggregates and dispersion of SGs is facilitated by molecular chaperones, specifically by Ssa1, Hsp26, and Hsp104 (138). The particular stress conditions influence the composition of SGs. Heat stress causes P-bodies or stress granules (SGs). In *S. cerevisiae* cells, growth at 39°C triggers P-bodies, and robust heat shock at 46°C leads to the formation of SGs (140 and 141). Yeast EGP bodies are another reported form of stress granule that functionally are analogous to SGs (139), which are reported to form during glucose-deprived (118) or cold-stressed (143).

The formation of protein aggregates during heat stress represents a sophisticated cellular adaptation mechanism rather than simply protein damage. When cells experience thermal stress, mature proteins undergo controlled aggregation, forming specific condensates that contribute to stress tolerance (144). A key feature of these endogenous protein assemblies is their reversible nature - they can be efficiently disassembled without requiring protein degradation once conditions normalize, highlighting their role in adaptive stress response rather than cellular damage In addition to this relatively slow transcriptional response (30+ mins),, recent studies have demonstrated the rapid formation of reversible quinary protein aggregates in response to acute heat exposure that occurs after only a few minutes (144). The formation of SGs is a cellular strategy to downregulate overall protein synthesis when environmental conditions become unfavorable, allowing cells to conserve energy and resources during stress. Chaperones may play a role in assembling or disassembling PBs and SGs (14).

Complex machinery of protein translation

Ribosomes are highly conserved ribonucleoprotein nanomachines with large and small subunits that synthesize polypeptides (145). In the model organism *Saccharomyces cerevisiae,* ribosomes consist of two distinct subunits with unique compositions: The small (40S) subunit incorporates 33 ribosomal proteins along with 18S ribosomal RNA, while the large (60S) subunit contains 46 ribosomal proteins and three different rRNAs - 25S, 5.8S, and 5S. (145). Hsp90 shows preferential binding to the small ribosomal subunit, while Hsp70, which interacts with newly synthesized protein chains, associates with all ribosomal fractions. (145-148). NAC and the Hsp70/Hsp40 dimeric chaperone system are called the ribosome-associated complex (149-151). RAC acts as a cofactor for Ssb (yeast ribosomal Hsp70) or cytosolic hsp70 in higher eukaryotes (152). Chaperones interact with the freshly emerging polypeptide chain from the ribosome to start folding it into an active 3D structure (152). Yeast ribosome associated Hsp70 is crucial for maintaining translational fidelity (153). The construction of ribosomes represents a major cellular investment, demanding significant energy and coordinated production of multiple components: ribosomal RNAs (rRNAs), ribosomal proteins (RPs), and various ribosome biogenesis (RiBi) factors. In Saccharomyces cerevisiae, disruptions in translation trigger a sophisticated cellular response known as RASTR (Ribosomal Assembly Stress Response). This pathway simultaneously activates Hsf1-dependent stress genes while suppressing ribosomal protein gene expression, representing a coordinated cellular adaptation to translation stress (154). During stress, ribosomal proteins that normally contact mRNA show reduced RNA binding. Additionally, key translation initiation factors - eIF4A, eIF4B, and Ded1 - demonstrate decreased RNA association, indicating a coordinated mechanism

for suppressing translation activity. (155). Heat shock induces the expression of heat shock proteins and leads to a global cessation of translation. This translational arrest is a protective mechanism that conserves energy and resources while the cell is under heat shock. During heat shock, the dissociation of Hsp70 from ribosomal components plays a pivotal role in halting translation. This dissociation causes a pause in translational elongation, preventing the accumulation of misfolded proteins that could overwhelm the chaperone machinery. Cells employ sophisticated mechanisms to modulate protein synthesis during stress conditions. At the molecular level, stress activates specific regulatory kinases like Gcn2, which phosphorylates eIF2α (initiation factor 2 alpha), leading to translation initiation suppression. Heat shock has long been recognized to impair protein synthesis, particularly affecting the elongation phase (156. During severe thermal stress, cells exhibit comprehensive translation suppression, accompanied by significant alterations in Hsp70's interactions with translation machinery, notably showing reduced ribosomal association (157).

In this study, we sought to understand the interplay between the Hsp70 chaperone code and proteostasis. We identified a novel rapidly heat-induced phosphorylation site on yeast Hsp70 at T492 that Pkc1 mediates during heat shock. Phosphorylation of T492 promotes interactome remodeling, which drives the dissociation of Hsp70-Hsf1 and the activation of HSR. T492 phosphorylation also altered Hsp70-ribosome interactions, explaining the long-established observation of heat-induced translational pausing. Finally, we identified the CWI protein Bck1 as a *bona fide* client of yeast Hsp70 whose activity is dependent on T492 status. Together, our data provide a novel paradigm for how cells can coordinate the

activation of diverse signaling pathways that respond to heat through modulation of the Hsp70 chaperone code.

CHAPTER 2:MATERIALS AND METHODS

Yeast strains

The parental yeast wild-type strain of all haploid derivatives used in this study is MH272 a/alpha (ura3/ura3 leu2/leu2 his3/his3 trp1/trp1 ade2/ade2). The strain lacks chromosomal versions of Ssa1, Ssa2, Ssa3, and Ssa4 (*ssa1–4*Δ). Although the Ssa1–4 function is required for cell viability, the *ssa1–4*Δ strain is kept viable through at least one of the isoforms. To keep the ssa1-4Δ strain alive, pYCPlac33-SSA1 (URA3) is needed (158) functionally complemented by *SSA1* expressed from a *URA3*-marked centromeric plasmid. The ssa1 ssa2 ssa3 ssa4 (ssa1-4) pYCPlac33-SSA1 strain was generated using the loxP-kanMX-loxP gene disruption cassette (159). Kinase deletes strains used were obtained from Dr. David Levin. The process for degron strain preparation was described in (160). A full table of used yeast strains can be found in Table 2.

Plasmids

Ssa1-4Δ strain was functionally complemented by pYCPlac33-SSA1 (URA3), which expresses *SSA1* from a *URA3*-marked centromeric plasmid. (158). All experiments used plasmid P210 under a Ssa2 constitutive promoter with Wild-type FLAG-SSA1 or a non-phosphorylatable mutant (FLAG-T492A). P210 is a (LEU) plasmid, which will be used to cure. Site-directed mutagenesis of Threonine 492 to an Alanine mutant (FLAG-T492A) was completed by Genescript (https://www.genscript.com/). The strain was transformed with a *LEU2*-marked plasmid bearing either wild-type FLAG-tagged Ssa1 or the non-phosphorylatable mutant ssa1-T492A. The *URA3* plasmid was evicted on 5-fluoro-orotic acid (5-FOA) media (161) to yield strains expressing wild-type Ssa1, Ssa1-T492A as the sole Ssa protein in the cell. A full table of used plasmids can be found in Table 1.

For epitope tagging the genomic copy of *HSP12, MKK1, and MKK2* with an HA epitope tag at the carboxy terminus, the pFA6a-3HA-His3MX6 plasmid was used. For Hsf1-Ssa1 IP, we used N-AD (50–100 Hsf1-GFP-FLAG (HGF) plasmid construct as previously described in (49). For HSE- Luciferase HSE-lucCP+ construct was used for real-time luciferase assay as described in (49). For the LacZ assay, The *URA3*-based *PRM5-lacZ* and *FKS2-lacZ* vectors were used as previously described in (86). For dual luciferase assay, plasmids used as described in (146 and 162)

Media and growth conditions

Yeast cultures were grown in either YPD (1% yeast extract, 2% glucose, 2% peptone) or grown in Synthetic dropout (SD) media (0.67% yeast nitrogen base without amino acids and carbohydrates, 2% glucose). It was supplemented with the appropriate nutrients and drop-out mix to select for plasmids and tagged genes. *Escherichia coli* DH5α was used to propagate all plasmids. E. coli cells were cultured in Luria broth medium (1% Bacto tryptone, 0.5% Bacto yeast extract, 1% NaCl) and transformed to ampicillin resistance by standard methods.

Plasmid curing on FOA

Ssa1-4Δ background yeast cells were transformed with the LEU plasmid expressing either wild-type Flag-Ssa1 or non-phosphorylatable mutant Flag-T492A under an Ssa2 constitutive promoter. Transformants were selected on SD media lacking leucine. Single colonies were restreaked on Leucine dropout media and incubated at 30 °C for at least 1 day. Further restreak yeast cells from previous to leucine dropout plates on SD media containing 5-fluoro-orotic acid (5-FOA) to counter-select for the *URA3*-based covering

vector. Cured strains are validated by spot assay (161). These cured strains are referred to as wild-type FLAG-Ssa1 or mutant FLAG-T492A.

Growth Assay

Yeast cells were grown to mid-logarithmic phase (OD600 nm = 0.5) in 10 ml of SD media in a 50 ml tube. Cells were 10-fold serially diluted (full concentration, 1/10 concentration, 1/100 concentration, and 1/1,000 concentration) in a clear 96-well plate using SD media. Cells are replica plated either onto solid media containing the aforementioned chemicals of known concentration or exposed to abiotic stressors, including heat stress, at 37 °C. Cells were plated onto SD solid media for the control plate without any drug or abiotic stress. For heat shock stress, the plates were pre-warmed at the desired temperature. Cells were replica plated onto prewarmed plates and immediately kept back at high temperature. After cells have dried, all plates except the 37 °C plate are kept upside-down in a 30 °C incubator for 3 days. Plates were checked regularly for growth (161).

Protein extraction from yeast

Protein lysates were prepared as previously described in (107). Yeast strains were cultured overnight in 10ml of SD media at 25°C. The following morning, the cells were diluted into 50ml of fresh media and incubated until an OD_{600} of 0.5-08 was reached. The cells were harvested by centrifugation (5 minutes at 3000 rpm), and pellets were washed with sterile, distilled water. Pellets were then resuspended in yeast protein extraction buffer (1M Tris HCl, pH 7.5, 5M NaCl, 1M DTT, supplemented with NP-40 and glycerol) with a protease inhibitor cocktail (Pierce). Glass beads with a 0.5mm diameter were added to lyse cells using a bead beater (Biospec products). The supernatant was then centrifuged for 10

minutes at 12,800 rpm to remove any cellular debris and transferred to a 1.5ml Eppendorf. Protein extraction was stored at -80℃.

Western blotting

Protein extracts were made as described (Kamada et al., 1995). 15 µg of protein was separated by 4%–12% NuPAGE SDS-PAGE (Thermo). Proteins were detected using the following antibodies; Anti- PhosphoT492 (21st-century biochemicals), Anti-PGK1 (Thermo #22C5D8), Anti FLAG (Sigma, #F1365), Anti-His (QIAGEN #34670) Anti-GAPDH(Thermo MA5-15738), Anti-Hsc70 (Rockland immunochemicals #200301F64), Anti-HA(Thermo #26183), Anti-Ydj1 (StressMarq #SMC-166D), Anti-Sis1(), Anti-Hsp26 (Gift from Dr. J Buchner), Anti-GFP (Roche #1814460), Anti-Mpk1 (Santacruz 133189) and Anti-phosho Mpk1 (Cell-signaling #4695). Blots were imaged on a ChemiDoc MP imaging system (Bio-Rad) after being treated with Super Signal West Pico PLUS Chemiluminescent Substrate (Thermo). For multiplex blots, fluorescent secondary antibodies (Bio-Rad Starbright #12004159 and #12005867) were added to the blots and imaged on the ChemiDoc MP imaging system (Bio-Rad) using multiplex settings.

The blots were then subsequently stripped and re-probed with relevant antibodies using a mild or harsh stripping buffer (glycine, SDS, Tween20, pH 2.2, or 10% SDS, 0.5M Tris HCl, pH 6.8 with β-mercaptoethanol, respectively).

Heat shock conditions

Ssa1-4Δ background expressing either wild-type Flag-Ssa1 or non-phosphorylatable mutant Flag-T492A were used. Cells were grown in SD-LEU at 25℃ overnight, re-inoculated into a larger culture of selectable media, and grown to mid-log phase (until an OD_{600} of 0.5-08 was reached). The cells were kept at 25℃ for unstressed conditions or

stressed at 39℃ for one hour. Cells were harvested, and protein was extracted via bead beating in 500 µl binding buffer (50 mM Na-phosphate pH 8.0, 300 mM NaCl, 0.01% Tween-20). Extracted protein was analyzed via SDS-PAGE/Western Blotting for T492 activation (Phospho T492 antibody), and a PGK1 loading control (PGK1 antibody) or FLAG loading control (FLAG antibody) for longer time-course aliquots of cells were collected at 0, 1,2, and 4 hours. Aliquots were collected at 0,5,15,25, and 45 minutes for the shorter time course to study the rapid heat response.

Chlorpromazine (CPZ) experiments

Wild-type FLAG-Ssa1 or mutant FLAG-T492A cells were grown in SD-LEU at 25℃ overnight and grown to the mid-log phase. To study the effect of the membrane, stretch mid-log phase yeast cells were treated with 250 micromolar of chlorpromazine (CPZ) for 2 hours at 25℃ (07). Untreated cells were used as control. Cells were harvested, and extracted protein was analyzed via SDS-PAGE/Western Blotting for T492 activation (Phospho T492 antibody) and a PGK1 loading control (PGK1 antibody) or FLAG loading control (FLAG antibody).

Azetidine 2-carboxylic acid (AZC) experiments

Wild-type FLAG-Ssa1 or mutant FLAG-T492A cells were grown in SD-LEU at 25℃ overnight and grown to the mid-log phase (until an OD_{600} of 0.5-08 was reached). To study the effect of misfolded proteins, mid-log phase, yeast cells were treated with 10mM azetidine 2-carboxylic acid (AZC) for four hours (113) at 25℃. Aliquots of cells were collected at 0, 1,2, and 4 hours. Untreated cells were used as control. Cells were harvested, and protein was extracted via bead beating in 500 µl binding buffer (50 mM Na-phosphate pH 8.0, 300 mM NaCl, 0.01% Tween-20). Extracted protein was analyzed via SDS-

PAGE/Western Blotting for T492 activation (Phospho T492 antibody) and a PGK1 loading control (PGK1 antibody) or FLAG loading control (FLAG antibody).

Immunoprecipitation of FLAG-tagged Ssa1 from yeast

Wild-type FLAG-Ssa1 or mutant FLAG-T492A cells were grown in SD-LEU at 25°C overnight and grown to the mid-log phase. Cells were harvested, and FLAG-tagged proteins were isolated as follows: Protein was extracted via bead beating in 500 µl binding buffer (50 mM Na-phosphate pH 8.0, 300 mM NaCl, 0.01% Tween-20). In low-retention microcentrifuge tubes, 25 µl of anti-Flag M2 magnetic beads (Sigma) were aliquoted. Tubes were placed on a magnetic stand and washed with 500 µl TBS solution 3 times. Further, all the TBS were removed, and the beads were washed with 500 µl of yeast protein extraction buffer twice. All traces of the buffer were removed from the magnetic beads, and 1000 µg of protein extract was added to the anti-Flag M2 magnetic beads (Sigma). The beads with protein lysate were incubated at 4° C overnight. On the next day, tubes were placed on a magnetic stand, and the supernatant was discarded. Anti-Flag M2 beads were then washed 5 times with 500 µl TBS solution. After the final wash, the buffer was aspirated. The beads were incubated with 65 µl Elution buffer (binding buffer supplemented with 10 µg/ml 3X FLAG peptide (Apex Bio)) for 30 minutes at room temperature. Next, beads were collected via a magnet stand. The supernatant containing purified FLAG-tagged protein was transferred to a fresh tube. 25 µl of 5x SDS-PAGE sample buffer was added, and the sample was denatured for 5 min at 95° C. 20 µl of the sample was analyzed using SDS-PAGE/Western Blotting for T492 activation (Phospho T492 antibody), and a PGK1 loading control (PGK1 antibody) or FLAG loading control (FLAG antibody).

Immunoprecipitation of HA-tagged PKC1 from yeast

Wild-type FLAG-Ssa1 or mutant FLAG-T492A cells were grown in SD-LEU at 25℃ overnight and grown to the mid-log phase. Further, the cured strains were transformed with a plasmid expressing HA-Pkc1 under a galactose promoter. (95) Cells were grown in SD-URA Galactose at 25℃ overnight and grown to the mid-log phase. Protein was extracted via bead beating, and HA-tagged proteins were purified as follows: For HA IP, cells were harvested and HA-tagged proteins were isolated as follows: Protein was extracted via bead beating in 500 µl binding buffer (50 mM Na-phosphate pH 8.0, 300 mM NaCl, 0.01% Tween-20). 200 µg of protein extract was incubated with 30 µl anti-HA magnetic beads (Thermo Fisher Scientific) at 4˚C for 30 minutes. The magnet collected Anti-HA beads and then washed 5 times with 500 µl binding buffer. After the final wash, the buffer was aspirated, and beads were incubated with 65 µl Elution buffer and 15 µl of 4X loading dye and boiled at 100˚C for 10 minutes; then, beads were collected via magnet. The supernatant containing purified HA-protein was transferred to a fresh tube, 25 µl of 4X SDS-PAGE sample buffer was added, and the sample was denatured for 5 min at 95˚C. The eluates were separated by SDS-PAGE (7.5–10%) and visualized by immunoblotting.

Purification of GFP-tagged Hsf1 from yeast

Wild-type FLAG-Ssa1 or mutant FLAG-T492A cells were transformed with a plasmid expressing GFP-HSF1(N-AD fusion (50–100HGF)) (49). Cells were grown in SD-HIS at 25℃ overnight, re-inoculated into a larger culture of selectable media, and grown to mid-log phase (until an OD_{600} of 0.5-08 was reached). Protein was extracted via bead beating. Protein was isolated, and GFP-tagged proteins were purified as follows: In low-retention microcentrifuge tubes, 25 -30 µl anti-GFP magnetic beads (Chromotek). Let it stand, and

then the supernatant was removed. A total of 200 µg of protein extract was incubated with 30 µl anti-GFP magnetic beads at 4°C overnight. The magnet collected Anti-GFP beads and then washed 5 times with 500 µl binding buffer. After the final wash, the buffer was aspirated, and beads were incubated with 65 µl Elution buffer and 15 ul of 4× loading dye and boiled at 100°C for 10 min; then, beads were collected via magnet. The supernatant containing purified GFP-protein was transferred to a fresh tube. The eluates were separated by SDS-PAGE (7.5% to 10%) and visualized by immunoblotting for T492 activation (Phospho T492 antibody), GFP antibody, and a PGK1 loading control (PGK1 antibody) or FLAG loading control (FLAG antibody).

In vitro kinase assay

Wild-type FLAG-Ssa1 were transformed with a plasmid expressing HA-Pkc1 under a galactose promoter. (95) Cells were grown in SD-URA Galactose at 25℃ overnight and grown to the mid-log phase. Protein was extracted via bead beating. For HA pulldown, anti-HA antibody-conjugated beads (Thermo Fisher Scientific) were washed 3 times with kinase buffer.100 µg of protein extract was added to the beads, which were incubated at 4℃ for 1 hour. The supernatant was removed, and the beads were supplemented with 40 µl of kinase buffer along with 10 µg of purified full-length His-Ssa1 (gift from DR. C Prodromou). After substrate addition, 100µM of ATP is added to initiate kinase reaction. The reaction was incubated for 1 hour at room temperature. The reaction was terminated by adding 60 µl of loading buffer, followed by boiling for 10-15 minutes. Samples were then separated using 4-12% SDS-PAGE gel and immunoblotted using phospho T492 antibody, His antibody, and HA antibody.

HSE Luciferase assay

Wild-type FLAG-Ssa1 or mutant FLAG-T492A cells were transformed with a real-time luciferase reporter pHSE-lucCP+ plasmid. (49). Cells were grown in SD-URA at 25℃ overnight and grown to the mid-log phase (until an OD_{600} of 0.5-08 was reached). Luciferase assay was done as given in 150-µl of yeast culture (WT and mutant added into separate wells) and was aliquoted into a white 96-well plate (Lumitrac 200, Greiner). The activity of Hsf1 was determined by adding luciferin (final concentration 0.5 mM). Cells were incubated in a Synergy H1 Microplate reader (37 °C for 90 min) and shaking and luminescence were read every 3 minutes (49). The graph was prepared using GraphPad Prism 7. All experiments were conducted with at least three biological replicates.

β-Galactosidase assays

For the *PRM5*-LacZ and *FKS2*-LacZ reporter experiments, Wild-type FLAG-Ssa1 or mutant FLAG-T492A cells were transformed with either *PRM5-LacZ* (104) or *FKS2-LacZ* (101) expressing plasmids. Yeast cells were grown overnight in SD-URA media at 25°C, re-inoculated at OD600 of 0.2–0.4, and then grown for 4 hours. Cells were heat shocked at 39 °C for 1 hour, and LacZ fusion assays were carried out as described previously in (100). Briefly, the protein was extracted through bead beating and quantified via Bradford assay. The b-Galactosidase reaction containing 50 µg of protein extract in 1 ml Z-Buffer (30) was initiated by addition of 200 µl ONPG (4 mg/ml) and incubated at 28°C until the appearance of a pale-yellow color was noted. The reaction was quenched by adding 500 µl Na2CO3 (1M) solution. The optical density of the reaction was measured at 420nm. β-Gal activity was calculated using ((OD420 x 1.7)/(0.0045 x protein x reaction time)), where protein is measured in mg, and time is in minutes. The mean and standard deviation from three

independent transformants were calculated. The graph was prepared using GraphPad Prism 7. All experiments were conducted with at least three biological replicates.

Dual luciferase assay

pFJZ1052 (AUG) and pFJZ1054 (UUG) dual luciferase plasmids were used here. Wild-type FLAG-Ssa1 or mutant FLAG-T492A were transformed with each plasmid, and four single colonies were assayed for dual luciferase activity as described in (146). Cells were grown in SD-URA at 25℃ overnight and grown to the mid-log phase (until an OD_{600} of 0.5-08 was reached). Luciferase assay was done as given in (146). Aliquots (2 µl) of the cultures were added to 50 µl 1x Passive lysis buffer (PROMEGA) and incubated at room temperature with shaking for 50 min. Firefly luciferase activity was measured by the addition of 50 µl luciferin in substrate buffer (15 mM Tris pH 8, 25 mM glycylglycine, 4 mM EGTA, 15 mM MgSO4, 1 mM DTT, 2 mM ATP, 0.1 mM CoA, 75 µM Luciferin). Followed by the measurement of Renilla luciferase activity by the addition of 50 µl coelenterazine substrate (0.22 M citric acid-sodium citrate pH 5, 1.1 M NaCl, 2.2 mM EDTA, 1.3 mM NaN3, 0.44 mg This/This mL BSA This This This, 1.43 µM Coelenterazine) to the same wells. Reading was taken in Synergy H1 Microplate reader

To calculate UUG utilization, UUG and AUG Firefly luciferase values were first normalized to their respective AUG Renilla luciferase values to determine the FUUG and FAUG values. FUUG was then normalized to FAUG for the final UUG utilization value.

F_{UUG} = UUG Firefly / AUG Renilla F_{AUG} = AUG Firefly / AUG Renilla

UUG utilization = F_{UUG} / F_{AUG}

Polysome profiling

To grow cells for polysome profiling, 200 mL of yeast were grown in SCD-Leu overnight with shaking at 25°C until they reached an OD600 = 0.4. Cells were collected onto a 0.45 µM filter (Cytiva #60173) using vacuum filtration (Sigma #Z290432) and immediately transferred to 100 mL of SCD-Leu prewarmed to 25°C or 39°C. After 10 minutes of incubation with periodic swirling the cells were either cooled back to 25°C in a water bath and then transferred to a shaking incubator at 25°C or harvested immediately via vacuum filtration onto a filter, followed by scraping the cells (Fisher #8100241) and plunging directly into liquid N2. The frozen cells were transferred to a pre-chilled 2 mL tube (Eppendorf #022363352). Cells were lysed with a pre-chilled 7 mm stainless steel ball (Qiagen #69990) using four 90 sec, 30 Hz pulses in a Retsch MM 400 mixer mill, chilling in liquid N2 between pulses. The sample was resuspended in 900 µL polysome lysis buffer (20 mM HEPES-KOH pH 7.4 (Sigma #H4034), 100 mM KCl (Fisher #BP366), 5 mM MgCl2 (Sigma #M2670), 200 µg/mL heparin (Calbiochem #375095), 1% triton X-100 (Sigma #T8787), 0.5 mM TCEP (Goldbio #TCEP25), 100 µg/mL cycloheximide (Thermo #J67043AD), 40 U/ml RNase inhibitor (NEB #M0314L), 1:100 EDTA-free Halt protease inhibitor (Thermo #PI78437)). The lysate was clarified by centrifugation at 3000 rcf for 2 min, and the clarified lysate was transferred to a new tube. The OD260 of each lysate was measured using an LVis plate on a CLARIOstar Plus (BMG) and the concentrations were normalized across samples using lysis buffer. Finally, aliquots were flash frozen in liquid N2, and total samples were collected by mixing 20 µL of sample with 2x LDS buffer (500 mM Tris pH 8.5, 4% lithium dodecyl sulfate, 20% Glycerol, 1 mM EDTA, 0.2%(w/v) orangeG, 2.5% 2-Mercaptoethanol). A 10–50% continuous sucrose gradient in polysome gradient buffer (5 mM HEPES-KOH pH 7.4, 140 mM KCl, 5 mM MgCl2, 100 µg/ml

cycloheximide, 0.5 mM TCEP) was prepared in SW 41Ti tubes (Seton #7030) using a Biocomp Gradient Master with the 10-50% short sucrose program and cooled to 4°C. Clarified lysate (200 µL) was loaded on top of the gradient, and gradients were spun in a SW41Ti rotor at 41,000 rpm for 105 minutes at 4°C. Gradients were fractionated into 0.8 mL fractions using a Biocomp Piston Gradient Fractionator with a Triax flow cell monitoring at 260 nm. Polysome to monosome ratios were calculated using background subtracted values. Proteins were precipitated from fractions using Trichloroacetic acid (TCA). First, 5 µL of 1 mg/mL BSA was added to each fraction as a carrier protein. Then TCA was added to a final concentration of 10%, samples were vortexed and frozen at -20°C for at least one hour. Samples were then centrifuged at 4°C, 21,000 rcf for 15 minutes and the supernatant was removed. Fractions were combined by centrifugation in the same tube before a final wash with 10% TCA. Each tube was then washed twice with chilled acetone and dried for 5 minutes at 70°C before being resuspended in 2x LDS sample buffer (500 mM Tris pH 8.5, 4% lithium dodecyl sulfate, 20% Glycerol, 1 mM EDTA, 0.2%(w/v) orangeG, 2.5% 2-Mercaptoethanol), incubated with shaking at 70°C for 10 minutes, vortexed and finally centrifuged at 21,000 rcf for 1 minute. Samples were then run on a Bis-Tris, 4-12% gel with MES buffer (Genescript #M00654), transferred to PVDF membrane (Millipore Sigma #IPFL85R) using a Trans-blot turbo transfer system (Bio-Rad #1704150) in transfer buffer (0.3 M glycine, 0.3 M Tris, 0.1% SDS, 20% methanol). Membranes were blocked with 5% milk for 1 hr. before incubating with specified primary antibodies overnight. Westerns were then visualized using donkey anti-mouse 800CW (LI-COR #925-32212) and goat anti-rabbit 680 (LI-CRO #925-68071) on a LI-COR Odyssey M imager.

Sample preparation for proteomic analysis

Immunoprecipitations were eluted from beads using 8M Urea,10mM DTT in 50 mM tris pH 8.5 for 45 min at room temperature with mixing at 600 rpm before alkylation with 50 mM IAA for 30 min in the dark. Samples were diluted 6x with 50 mM tris pH 8.5. 2 M Urea concentration and digested with 0.4 µg of trypsin-LysC mix (Promega) overnight at 37˚C. Tryptic peptides were desalted with Pierce C18 Desalting Spin Columns (Thermo Fisher Scientific) according to the manufacturer's protocol, dried down on SpeedVac, and resuspended in mobile-phase A (0.2% formic acid in water) immediately before mass spectrometric analysis. Liquid chromatography-tandem mass spectrometry peptide analysis. Resuspended cross-linked peptides were separated by nanoflow reversed-phase liquid chromatography (LC). An Ultimate 3000 UHPLC (Thermo Scientific) was used to load ~1 ug of peptides on the column and separate them at a 300 nL/min flow rate. The column was a 15 cm long EASY-Spray C18 (packed with 2 µm PepMap C18 particles, 75 µm i.d., Thermo Scientific). The analytical gradient was performed by increasing the relative concentration of mobile phase B (0.2% formic acid, 4.8% water in acetonitrile) in the following steps: from 2% to 30% in 32 min, from 30% to 50% in 5 min, and from 50 to 85% in 5 min (for washing the column). The 4 min wash at high organic concentration was followed by moving to 15% in 2 minutes, increasing to 70% in 1 min for a secondary wash before re-equilibration of the column at 2% B for 7.5 min, for a total run time of 68 min. A 2.2 kV potential was applied to the column outlet using an in-house nanoESI source based on the University of Washington design for generating nano-electrospray. All mass spectrometry (MS) measurements were performed on a tribrid Orbitrap Eclipse (Thermo Scientific). Broadband mass spectra (MS1) were recorded in the Orbitrap over a 375-1500

m/z window, using a resolving power of 120,000 (at 200 m/z) and an automatic gain control (AGC) target of 4e5 charges (maximum injection time: 50 ms). Precursor ions were quadrupole selected (isolation window: 1.6 m/z) based on a data-dependent logic, using a maximum duty cycle time of 3 s. Monoisotopic precursor selection and dynamic exclusion (60 s) were applied. Peptides were filtered by the intensity and charge state, allowing the fragmentation only of precursors from 2+ to 7+. Tandem mass spectrometry (MS2) was performed by fragmenting each precursor passing the selection criteria using both higher energy collisional dissociation (HCD) with normalized collision energy (NCE) set at 30% and electron transfer dissociation – higher energy collisional dissociation (EThcD), with ETD reagent target set at 5e5, reaction time calculated based on a calibration curve and supplemental collisional activation set at NCE=10%. The AGC target for HCD and EThcD MS2 was set at 8e4 (maximum injection time: 55 ms), and spectra were recorded at 15,000 resolving power.

Proteomic Data analysis

HCD fragmentation data were processed with Protein Discoverer 2.4 utilizing Sequest HT and MS Amanda search engines for general identification of all proteins included in the samples. For both precursor mass tolerance, it was 10 ppm, and for fragment mass tolerance, it was 0.2 Da. Carbamidomethylation (C) was allowed as a static modification and dynamic modifications were as follows: Oxidation(M) and acetyl (protein N-term). Identified peptides were validated using Percolator and the target FDR value was set to 0.01 (strict) and 0.05 (relaxed). Finally, results were filtered for high-confidence peptides using consensus steps. A control peptide error rate strategy was used and 0.01 (strict) and 0.05 (relaxed) values were used for Target FDR for both PSM and Peptide levels. Changes

in protein abundance between the two strains were statistically tested by ANOVA using the built-in function within Proteome Discoverer.

Gene ontology analysis

Gene Ontology analysis was performed as previously described in (164) using GO Slim Mapper on the SGD Database (http://www.yeastgenome.org/cgi-bin/GO/goSlimMapper.pl). Interactome visualization was performed using Prism 7 graphing software for individual interactomes and comparative interactomes. Functional classification of the WT Ssa1 and T92A under heat shock interactome. Interactors were categorized by cellular function using GO Slim analysis, and relative enrichment was calculated compared to occurrence in the non-essential genome. The top 10 enriched cellular processes are shown for each interactome.

Microscopy

Yeast cells from cultures grown to log phase (OD600 ≈ 0.5) were mounted in selective growth medium (C-URA), and 3D image stacks were collected at 0.3 μm z increments on a Delta Vision Elite Workstation (Cytiva) based on an inverted microscope (IX-70; Olympus) using a 100×1.4NA oil immersion lens. Images were captured at 22°C with a 12-bit charge-coupled device camera (Cool Snap HQ; Photometrics) and deconvolved using the iterative-constrained algorithm and the measured point spread function. Image analysis and preparation were done using Softworx 6.5 (Cytivia) and FIJI ImageJ. For heat shock experiments as described in (163), cells were incubated in growth media in a 39°C water bath (New Brunswick Scientific) for 15 minutes, 30 minutes, 1 hour, or 2 hours, then immediately mounted on slides for imaging. To quantify the presence of Pab1 and Edc1 foci, a minimum of 100 cells were analyzed for each time point. Wildtype or T492A cells

were visually scored for the presence of internal fluorescent puncta from z-stacks collected at 0.3 μm intervals. Timepoints for the presence of foci were compared via single-factor ANOVA analysis. All experimental conditions were repeated in biological triplicate.

CHAPTER 3: RESULTS

Heat shock induces rapid phosphorylation of Ssa1 T492 in yeast

To understand chaperone code alterations in response to heat, yeast expressing FLAG-tagged Ssa1 were grown to exponential phase and then treated for 1 h at 39 ˚C. Ssa1 was immunoprecipitated using FLAG beads and was subjected to phosphoproteomic analysis using Mass spectrometry. Only one Ssa1 phosphorylation site was identified to be upregulated under heat-shock induced. The site was not identified in untreated cells. The only site upregulated on Ssa1 was Threonine T492. The site T492 on Ssa1 is located in the substrate-binding domain of Ssa1 close to the region responsible for client binding (Figure 6A). The mammalian homolog for this site is (T495 on Hsc70). It is surprisingly well-conserved throughout evolution (Figure 6B), which probably indicates this residue is important for chaperone function. Phosphorylation of this site has been detected in both yeast and humans. Although T495 on Hsc70 can be phosphorylated by the *Legionella* protein LegK4 (46), the native regulation and role of this site remain unclear. To validate our MS data, we examined T492 phosphorylation in yeast treated with a range of stresses using a custom phospho-specific antibody.

For antibody validation, we tested the mutant of T492, which cannot get phosphorylated. Ssa has four isoforms (Ssa1-4) which are highly similar. To remove confounding effects of the highly similar Ssa2, 3, and 4 proteins, we used the well-established MH272 *ssa1-4* yeast strain for all our experiments. In the strain, all four *SSA* genes have been deleted and complemented by *SSA1* expressed from a *URA3*-marked centromeric plasmid under *Ssa2* constitutive promoter (158). Further, this strain was transformed with a *LEU2*-marked plasmid bearing either wild-type FLAG-tagged Ssa1 or the non-phosphorylatable mutant

Ssa1-T492A. The *URA3* plasmid was cured on 5-fluoro-orotic acid (5-FOA) media to yield strains expressing wild-type Ssa1 or Ssa1-T492A as the only Ssa in the cell, hereafter referred to as Wild-type FLAG-Ssa1 or mutant FLAG-T492A cells. Cells were grown to the mid-log phase and then were exposed to 39˚C. Aliquots of cells were taken after 0, 1, 2, and 4 hours for protein lysate preparation, at which T492 phosphorylation was assessed via Western Blotting. Ssa1 T492 phosphorylation was not detected in unstressed cells but was observed in cells heat-stressed for 1 hour (Figure 7A). Ssa1 T492 phosphorylation was seen to drop at later time points- 2 hours and 4 hours post-heat shock.

To examine whether T492 phosphorylation occurs at shorter time scales, aliquots of cells were taken at 0, 5, 15, 25, 45, and 60-minute time points for protein lysate preparation, at which T492 phosphorylation was assessed via Western Blotting. A robust increase in T492 phosphorylation was observed even after 5 minutes, suggesting this response is an early-stage response to heat shock (Figure 7B). The heat-induced T492 phosphorylation was seen for each time-point until 60 minutes, and no phosphorylation was detected in unstressed conditions (Figure 7B).

The Ssa isoforms are also phosphorylated in response to thermal stress

The four Ssa in yeast are highly similar in amino acid sequence and appear to have at least some functional overlap. Ssa1/2 is expressed constitutively at high levels, whereas Ssa3/4 is only expressed during cell stress (17 and 165). Although yeast can survive on the loss of any of 3 Ssas if the 4th is expressed at high levels (15). Given that the T492 site is conserved for all Ssas, we queried whether T492 is phosphorylated in all Ssa1, 2, 3, and 4. We first generated *Ssa1-4*Δ background yeast cells expressing either Flag-tagged Ssa1, 2, 3, 4 on constitutive Ssa2 promoters as the sole Ssa in the cell and assessed T492 phosphorylation

in these cells after 1 hour of heat shock at 39˚C. Heat-induced T492 phosphorylation was observed in all Ssas (Figure 8).

Heat-shock-induced phosphorylation T492 is independent of protein unfolding

Heat elicits a variety of effects on cells, including protein denaturation. To determine whether heat-induced phosphorylation of Ssa1 was promoted by protein misfolding, we utilized AZC (azetidine-2-carboxylic acid)), a proline analog that is incorporated in proteins during protein synthesis and triggers protein unfolding (113 and 65). Wild-type FLAG-Ssa1 or mutant FLAG-T492A cells were treated with AZC, and lysates were analyzed using Western Blotting. Treatment with AZC did not promote Ssa1 T492 phosphorylation even over extended periods (up to 4 hours), suggesting that protein unfolding is not the primary stimulus for T492 activation (Figure 9).

T492 phosphorylation is mediated by membrane stretch

Heat activates the CWI by causing the stretching of the plasma membrane (107). To determine if heat-activated phosphorylation of Ssa1 T492 was caused through a similar mechanism, we used a membrane stretching agent chlorpromazine (CPZ) and assessed T492 phosphorylation. Chlorpromazine (CPZ), a cationic amphipathic molecule, exhibits specific membrane interactions by preferentially inserting into the inner (cytoplasmic) layer of the plasma membrane's lipid bilayer. This selective insertion creates membrane stretch, making it a valuable tool for studying membrane stress responses. This agent effectively induces inward membrane stretch in vivo (107). Cured Ssa1-4Δ background yeast cells expressing wild-type Flag-Ssa1 or mutant Flag-T492A were treated with CPZ, and T492 phosphorylation was analyzed using Western blot. Robust T492 phosphorylation was observed after one hr. of CPZ treatment in WT cells. No T492 phosphorylation was

seen in mutant samples (Figure 10). Data suggests that Ssa1 T492 phosphorylation is not mediated by protein misfolding. However, the T492 phosphorylation is activated by membrane stretch that is detected through the Mid2 mechanosensor.

Heat-induced T492 phosphorylation is dependent on the Mid2 mechanosensor

Heat triggers the activation of the yeast cell wall integrity MAPK pathway (105). To determine whether activation of Ssa1 phosphorylation was dependent on CWI signaling, we queried each protein in the CWI cascade, starting with the mechanosensors. We analyzed whether the semi-redundant mechanosensor Wsc1 or Mid2 loss impacted T492 phosphorylation. Yeast strains deleted for 1 of the 2 mechanosensors were analyzed for T492 phosphorylation using Western blotting. Although heat induced Ssa1 T492 phosphorylation was unchanged in the *wsc1*Δ strain, cells lacking Mid2 could not induce T492 phosphorylation (Figure 11). This result is consistent with the earlier finding that AZC does not activate mechanosensor Mid2 or the rest of the cell integrity pathway (113).

Yeast Protein Kinase C (Pkc1) directly phosphorylates Ssa1 T492

The requirement of the mechanosensor Mid2 for Ssa1 T492 phosphorylation suggested the potential involvement of the CWI pathway. This raises the question of which of the kinases from the CWI cascade- Pkc1, Bck1, Mkk1/2, and Mpk1 phosphorylating Ssa1(Figure 5). Several indirect lines of evidence implicated Pkc1 as the potential kinase that can phosphorylate Ssa1 T492. In 2013, a quantitative phosphoproteomic approach identified Ssa1 T492 as a novel putative phosphorylation target of Pkc1. It was identified that Ssa1 T492 was phosphorylated upon Pkc1 overexpression in an Mpk1-dependent manner. (166). In addition, Ssa1 has an arginine at the -3 position and a basic residue at the +2-position relative to the T492 site, which is the preferred substrate sequence for PKC proteins (167).

To examine whether Pkc1 catalyzed T492 phosphorylation, we assessed T492 phosphorylation when Pkc1 function was ablated. As the Pkc1 function is essential for cell viability, we utilized the auxin-inducible degron (AID) system (160). After genomically tagging Pkc1 on the C-terminus with AID, we checked the system's functionality by plating the WT and Pkc1-AID cells on media containing or lacking Auxin. Although both strains grew on YPD, only WT was able to grow on media containing Auxin. The Pkc1-AID strain was, however, able to grow on auxin media when osmotic support was provided in the form of sorbitol. These results were consistent with Pkc1 being degraded in the presence of Auxin. We grew the Pkc1-AID strain to the mid-log phase at 25˚C and added Auxin to ablate the Pkc1 function. For each indicated time point, yeast was shifted to 39˚C for 30 minutes, and then T492 status was assessed via Western Blotting. Robust T492 phosphorylation was observed post-heat shock in WT and Pkc1-AID pre-auxin addition. Post-auxin addition, the ability of heat shock to stimulate T492 phosphorylation diminished over time, being barely observable 4 hrs. after auxin treatment (Figure 12). Pkc1 is part of a kinase cascade consisting of Pkc1, Bck1, Mkk1/2, and Mpk1. To rule out the possibility that Pkc1-dependence of T492 phosphorylation was via these other kinases, we assessed T492 phosphorylation in cells lacking either Bck1, Mkk1/2, or Mpk1. Cells lacking these kinases could still activate T492 phosphorylation in response to heat stress (Figure 13), indicating that Pkc1 directly phosphorylates this site. We performed an *in vitro* kinase assay with purified Pkc1 and recombinant Ssa1 to complement these results. Purified Pkc1 was able to phosphorylate Ssa1 on T492 (Figure 14). These data suggest that Pkc1 can directly phosphorylate Ssa1 on T492 in response to heat shock.

Phosphorylation of T492 fine-tunes the Hsp70 interactome

Interactions of chaperones are highly dynamic and vary depending on internal and external cues, all of which modulate the chaperone code (1, 147, and 168). We considered the possibility that phosphorylation of Ssa1 at T492 may dictate the breadth and specificity of the Ssa1 interactors. Using FLAG-Dyna beads, we purified Flag Ssa1 complexes from heat-shocked WT and T492A cells. These complexes were digested via trypsin and peptides and then compared their composition using mass spectrometry (Figure 15A). Analysis was done on samples from three biological replicates; only interactors seen in two were counted as genuine interactors. Interactome visualization was performed using Prism 7 graphing software for comparative interactomes. The volcano plot was plotted where the x-axis is the log2 ratio of WT/T492A, and the y-axis is -log(p-value) (Figure 15B). The proteins on the left side of the volcano plot are downregulated in the WT but unregulated in the mutant. Meanwhile, those on the right side are upregulated in the WT and downregulated in the mutant. The interacting proteins that are significantly downregulated were defined as $p < 0.05$ and have a $\log2 < -1$. For the significantly upregulated proteins, they have $p < 0.05$ and a $\log2 > 1$. We identified 647 proteins (1% FDR) and quantified 560 of those. 35 proteins were significantly downregulated, and 48 were significantly upregulated. Of the total interactors identified, 24% were enriched in the WT sample, 23% were enriched in the T492A samples, and 54% showed an equal affinity for both versions of Ssa1. For functional classification of the Ssa1 interactome, Gene Ontology analysis was performed using GO Slim Mapper on the *Saccharomyces* Genome Database (http://www.yeastgenome.org/cgi-bin/GO/goSlimMapper.pl). The study analyzed Ssa1's protein interactions using GO Slim analysis, comparing the relative enrichment of different

cellular processes against their occurrence in the nonessential genome. The top 10 enriched cellular processes are shown for each interactome. The GO process term most enriched in WT was endocytosis, ribosome assembly, and cytoplasmic translation, suggesting a role of T492 phosphorylation in translation fidelity. The GO process term most enriched in mutants was protein folding, reflecting the wide range of increased chaperones and co-chaperones identified (Figure 16 A and 16B). Studies have demonstrated quantitative changes in chaperone interactions upon phosphorylation, observing substantial differences in co-chaperone binding and selected client proteins, which may impact chaperone activity and specificity (36,169 and 170). 15 chaperones and co-chaperone proteins were identified to interact differently with Ssa1 under phosphorylation. These interactors were analyzed using the STRING database and grouped based on function. Among chaperones/cochaperones known to bind Ssa1 directly, those displaying preferred interaction with WT included nucleotide-exchange factors Sse2, Fes1, and Lhs1. T492A mutant displayed preferred interaction with J-protein-Ydj1, Hsp70 paralog-Ssz1, Hsp82, and its co-chaperones Sgt2 and Sti1 and mitochondrial chaperone Hsp10. Interestingly, other Hsp70 paralogs-Ssb1, Ssc1, Kar2, J-protein-Sis1, and mitochondrial chaperone-Hsp60 showed equal interaction with WT and mutant under heat shock (Figure 17A). We also validated the interactome result of altered co-chaperone binding using co-immunoprecipitation (Figure 17B).

Phosphorylation of Ssa1 T492 is critical for the activation of the heat shock response

Molecular chaperones are critical for refolding heat-denatured proteins and, thus, survival at high temperatures. Although viable at 30˚C, T492A cells could not grow on solid media at either 37˚C or 39˚C, suggesting a possible defect in the heat shock response (Figure

18A). To investigate this possibility, we assessed the expression of Hsf1 using a real-time luciferase reporter assay. The reporter used is an HSE-driven destabilized luciferase reporter (49). WT and T492A cells were transformed with the reporter, and Hsf1 activity was assessed using a luciferin substrate. WT cells exposed to 39˚C mounted a rapid and robust HSR within minutes, reaching a maximum after 30 minutes of heat exposure.

In contrast, T492A cells did not induce significant expression of the HSE-luciferase construct (Figures 18B and 18C). We assessed the Hsp26 induction in WT and T492 with Western blotting to complement our HSE-reporter result. Research demonstrates that Hsp26 plays a specific protective role during thermal stress, where its binding to client proteins enhances their stability at elevated temperatures (171). This small heat shock protein shows enhanced effectiveness in maintaining protein solubility during heat shock compared to normal growth conditions, highlighting its specialized function in thermal stress protection. Hsp26 induction was seen in WT upon exposure to heat shock at 39˚C; mutant T492A cells did not respond to exposure to 39 ˚C, and no Hsp26 induction was seen (Figure 19A). Thus, confirming that T492 phosphorylation is critical for the heat shock response.

T492 phosphorylation controls the interaction between Ssa1 and Hsf1

The traditional model of chaperone titration is seen in both yeast and humans. The model for HSF regulation involves the attenuation of Hsf1 optimal conditions, chaperone titration under proteotoxic stress, and then, finally, increased expression of molecular chaperones, leading to eventual HSR attenuation. (49). Recent work by Pincus and co-workers (58) have demonstrated the existence of a Hsp70–Hsf1 regulatory circuit in *S. cerevisiae*. However, the kinetics of Hsf1 activation and the role of chaperone PTMs in regulating

HSR are still unknown. The lack of heat-induced transcriptional response in T492A cells suggested a defect in Hsf1 regulation. Ssa1 regulates the response to heat shock through its interaction with the Heat Shock Factor, Hsf1 (58). Ssa1 has been shown to directly bind Hsf1 within the CE2 motif in the C-AD (59). A second Ssa1-interacting region localized to the N-AD, which resides between residues 50 and 100, was also identified (49). To understand whether the T492A mutation impacted Ssa1-Hsf1 interaction, we measured Ssa1-Hsf1 affinity in WT and T492A cells under unstressed and heat shock-treated conditions via co-immunoprecipitation. We used the fragment N-AD 50-100 Hsf1-GFP-FLAG (HGF) as previously described in(49), which resides between residue 50 and 100 (49**).** As expected, in WT cells, Ssa1 was seen to be interacting with Hsf1 under unstress conditions, and the interaction between Ssa1 and Hsf1 was disrupted by heat shock (Figure 20A). Consistent with earlier studies (58), the decrease in interaction upon heat shock suggests the dissociation of Hsf1 from Ssa1, thereby leading to HSR induction as seen in the HSE luciferase assay(Figure 18C). In contrast, in the T492A mutant, the Ssa1-Hsf1 interaction was similar to WT under unstress conditions. However, Hsf1 was locked onto Ssa1 under heat shock and failed to dissociate from Ssa1. This inability of Hsf1 to dissociate from Ssa1 explains the lack of HSR induction. These data demonstrate that T492 phosphorylation is required for Ssa1-Hsf1 dissociation upon heat shock and appropriate activation of heat shock-induced transcription (Figure 20A).

Accelerating Hsp70 substrate release suppresses the temperature sensitivity of T492 cells

In yeast cells, nucleotide exchange factors (NEFs) play a crucial role in accelerating substrate release from Hsp70 proteins. These important regulators are primarily

concentrated in the cytosolic compartment, where they modulate Hsp70 chaperone cycling (14). Our data suggested the primary cause of the heat sensitivity of T492 cells may be an inability of Ssa1 to release Hsf1. Release of Hsp70 from Hsf1 can be accelerated by overexpression of the nuclear-targeted Sse1 co-chaperone protein (65). To test if Sse1-NLS would rescue the Hsf1 defect in the T492 mutant, thereby rescuing its temperature sensitivity. WT and T492A mutant cells were transformed with a plasmid expressing Sse1-NLS. For control, an empty vector was used. Transformed cells were checked using spot assay on a pre-warmed solid media plate. As seen in (Figure 20B), mutant cells expressing empty control could not grow at high temperatures. However, mutant cells expressing Sse1-NLS were able to grow at high temperatures. These data demonstrate that T492 phosphorylation is important for Ssa1-Hsf1 dissociation upon heat shock and, thus, appropriate activation of heat shock-induced transcription.

Ssa1 T492 mutant has an altered Msn2/4 regulation to compensate for defective Hsf1

(The cellular response to heat stress involves two complementary pathways: the Heat Shock Response (HSR) mediated by Hsf1 and the Environmental Stress Response (ESR) controlled by Msn2/4. These pathways operate in a compensatory fashion, ensuring robust stress protection through parallel but distinct mechanisms. 65). As seen in the western blots, the native expression of chaperones (Ssa1, Hsp82) and co-chaperones (Ydj1) in the Ssa1 T492 mutant was high compared to that of WT. Additionally, we identified a defect in Hsf1 binding and HSR induction in mutant Ssa1 T492. We questioned whether the parallel ESR pathway is activated compensatively, increasing the expression of essential chaperones and co-chaperones that allow mutants to survive under heat shock. We analyzed the Hsp12 expression level as a reporter of Msn2/4 activity. *HSP12* represents a

classic example of a general stress response gene regulated by the transcription factor Msn2/4. While maintaining low expression levels during normal growth, HSP12 shows dramatic induction (100-fold increase) when cells encounter severe heat stress, demonstrating its crucial role in stress adaptation. (14). Hsp12 was genomically GFP epitope-tagged in Ssa1-4Δ background yeast cells. Epitope-tagged strains were further transformed with LEU-based plasmids Flag-Ssa1 or Flag-T492A and then cured on FOA. Levels of Hsp12 were analyzed using Western blotting. Hsp12 induction was seen only under heat shock in WT. However, the Hsp12 basal induction was observed to be high under both unstressed and heat shock in mutant Ssa1 T492. This might suggest an altered regulation of Msn2/4 in mutants to compensate for a defective Hsf1(Figure 21).

Hsp70 phosphorylation fine-tunes protein translational fidelity

Chaperones bind newly translated proteins and help them achieve their native, active state. In our interactome analysis, Ssa1 co-purified with proteins involved in protein translation, translation initiation and elongation, ribosome assembly, and RNA processing in our proteomics screen. Interesting interactors were identified which included cytoplasmic translation proteins(Rpl4a and Rpl7a had increased interaction in WT while Rps10 and Rps12 had preferred interaction with mutant) RNA processing proteins(Rps18a, Rps22, and Rpl8a had increased interaction in WT while Rps20 had preferred interaction with mutant, ribosomal assembly proteins(Rpl10a and Rps11b had increased interaction in WT, translation elongation (Rpl3 showed increased interaction with WT) and initiation components(Ded1 and Tif4631 showed increased interaction with WT) (Figure 22A). To investigate spatial patterns in phosphorylation dependent Ssa1 interactions, we mapped the identified interacting proteins onto the three-dimensional structure of the yeast ribosome

(using PDB structure 4V88) [39]. This structural mapping approach helped reveal the spatial organization of Ssa1's ribosomal interactions. (Figure 22). As these changes in ribosomal protein interaction were Ssa1 T492 phosphorylation-dependent we considered the possibility that it might also impact translational fidelity. We assessed translational fidelity in WT and Ssa1 T492 mutant cells using a well-established dual luciferase assay. In this system, Renilla luciferase (Rluc) and firefly luciferase (Fluc) are under the control of separate constitutive promoters. The firefly luciferase mRNA has a non-traditional start codon (UUG), which is only used when translational fidelity is lost (146). The Renilla luciferase mRNA has a classic AUG start codon and acts as a control for alterations in overall translation. Using this dual-luciferase system, we observed an increase in UUG utilization in the T492A mutant cell compared to the WT. Thus, suggesting a loss of translational fidelity in the Ssa1 T492A mutant (Figure 24). The data shown for the assays and blots are the mean and standard deviation of three biological replicates. Statistical significance was calculated via ANOVA. (*p < 0.05; **p 0.01).

Hsp70 phosphorylation is critical for protein translation and ribosome association

One role that Hsc70 plays in the cell is to assist in folding nascent polypeptides during translation (80). Hsp70's dissociation from the ribosome during extreme heat shock inhibits global protein synthesis (157). The extent of global translational repression during temperature stress was quantified in the two strains (WT and Ssa1-T492A) using the polysome-to-monosome signal ratio in polysome profiles. Both strains showed a similar decrease in translation upon 10-minute stress at 39°C, and both strains recovered to nearly unstressed levels after 30 minutes at 25°C. To track chaperone association with translating ribosomes during stress, we purified proteins from the polysome fractions and quantified

the abundance of chaperones by western blotting. While at 25°C, chaperone association with polysomes was similar across strains, after 10 minutes at 39°C, levels of polysome-bound Ssa1-T492A increased while levels of polysome-bound WT Ssa1 and other chaperones remained steady. (Figure 23)

T492 phosphorylation is required for P-body disassembly

Our interactome analysis revealed several protein interactors that are components of the stress granules, P-bodies, or both (Figure 21A). Both of these types of cytoplasmic RNA-protein granules are induced under heat stress. Proteins involved in P-body formation and stress granule components were also identified in the interactome. P-body marker Edc3 was identified to have increased interaction with WT. Stress granule component Ded1 showed an increased preference for WT, while Tif34 had an increased preference for mutant. Also, stress granule marker Pab1 interacted equally with WT and mutant under heat shock (Figure 21A). We queried whether the T492 phosphorylation state may impact stress granule and P-body formation. Our interactome study identified Edc3 (a P-body marker) as having increased interaction with WT upon phosphorylation. On the under hand, the stress granule marker (Pab1) had equal interaction with WT and mutant. Thus, we decided to understand the dynamics of Edc3-mCherry (P-body marker) and Pab1-GFP in WT and T492A cells under unstressed, heat shock, and recovery conditions. To examine stress granules and P-bodies, Ssa1-4Δ background yeast cells expressing FLAG-Ssa1 or FLAG-T492A were transformed with a centromere plasmid expressing Pab1-GFP from its own promoter (a stress granule marker) and Edc3-mCherry from its promoter (a P-body marker) (118). All experimental conditions were repeated in biological triplicate. We observed that the formation and resolution of Pab1 foci were not dependent on T492

phosphorylation. Upon heat shock, both WT and mutant demonstrated an increase in Pab1 and Edc3 foci consistent with earlier reports (118) followed by a decrease in Pab1 foci during the recovery phase (Figure 25B and 25C). However, a striking observation was seen for Edc3-foci during recovery time points. The mutant T492A was defective in Edc3-foci disassembly at 2 hours of recovery. The disassembly of stress granules was seen to be normal. The foci were quantitated and plotted (Figures 25D and 25E).

Heat-induced phosphorylation of yeast Hsp70 promotes CWI signal amplification

To understand the role of T492 phosphorylation on CWI, we first screened if sorbitol rescues the temperature-sensitive phenotype of mutant T492A. It was observed that the mutant cells, when supplemented with 1M sorbitol, could grow at high temperatures, suggesting that the mutant had defective cell-wall integrity signaling and that T492 phosphorylation may govern cell integrity (Figure 26A). We assessed the activity of this pathway in WT and T492 cells via *PRM5* and *FKS2* promoter-lacZ reporter assays. While both *PRM5* and *FKS2* expressions depend on cell integrity, their activation modes differ. *PRM5* expression is dependent on Rlm1 phosphorylation, catalyzed by the Mpk1 kinase. In contrast, FKS2 expression requires dual phosphorylation of Mpk1 but is independent of Mpk1 catalytic activity (86). T492A cells could not recapitulate WT levels of heat induced *FKS2* and *PRM5* transcription (Figure 26B and 26C).

Mpk1 activation is dependent on Ssa1 phosphorylation under heat shock

Mpk1 is dually phosphorylated with the activation of cell integrity signaling (172). Yeast Hsp90 binds to the dually phosphorylated form of Mpk1 and supports Mpk1 stability and kinase activity (86, 99, and 106). The high overlap between Hsp90 and Hsp70 clients makes it likely that Ssa1 also binds and impacts the Mpk1 function. We tested the stability

and activity of Mpk1 in Wild-type and mutant cells under heat shock. Western blotting was used for the analysis of dually phosphorylated Mpk1, we utilized a commercial antibody originally designed to recognize dual phosphorylation (Thr202/Tyr204) of mammalian p44/42 MAP kinase. This antibody effectively cross-reacts with yeast Slt2 MAP kinase when phosphorylated at equivalent sites (Thr190/Tyr192) in yeast cell extracts, demonstrating the evolutionary conservation of these phosphorylation sites.173). We also analyzed the native Slt2 stability using a mpk1 antibody. Mpk1 levels were unchanged in both WT and T492A mutant under heat shock (Figure 27). Interestingly, WT cells showed Mpk1 activation, but T492A mutant cells were defective in Mpk1 dual phosphorylation under heat shock (Figure 27).

Bck1 levels are compromised in Ssa1 T492 mutant under heat shock

As Hsp90 is required for yeast's catalytic activation of the CWI signaling pathway. We wondered if yeast Hsp70 would play a similar role in regulating other upstream CWI kinases. So, we decided to query Bck1 and Mkk1/Mkk2 to underpin the defect caused in the CWI in the absence of T492 phosphorylation. Mkk1 and Mkk2 are fully redundant, and their kinase domains are interchangeable. Slt2 is known to retro phosphorylate MKK1 and MKK2 (174). Studies have shown that a chaperone is required to stabilize Mkk2 (175) in Candida albicans. We queried the total levels of Mkk1 and Mkk2. We integrated HA epitope tags on Mkk1 or Mkk2 in Ssa1-4Δ background yeast cells. Epitope-tagged strains were further transformed with LEU-based plasmids Flag-Ssa1 or Flag-T492A and then cured on FOA. Levels of Mkk1 and Mkk2 remained the same in both WT and mutant under heat shock(Figure 28). So, we focused our attention further upstream on the Bck1. Bck1 is a 147kDa protein that consists of a kinase domain and a large intrinsically disordered

domain of unknown function. We initially tried to determine the impact of the T492A mutation on full-length WT Bck1 but were unsuccessful in detecting Bck1 even in WT cells (data not shown). We attribute this difficulty to the largely disordered nature of this protein and may explain why, since its discovery in 1992, there are no reports containing Western blots of this protein (96). To bypass these issues, we separately expressed the N- and C--terminal domains of Bck1 (amino acids 1-738 and 739-1478), each with an HA tag on a GPD constitutive promoters in WT and T492A cells (Figure 29). Stability of both halves was tested under unstress and heat shock conditions using Western blotting. Levels of N-terminal Bck1 remained unchanged in both WT and mutant. However, steady-state levels of the C-terminal Bck1 were compromised in the T492 mutant (Figure 29A and 29B) under heat shock.

Bck1 is a novel client of Ssa1

The stability of the catalytic domain of Bck1 was impacted in the T492 mutant under heat shock. Earlier studies in *Candida albicans* have shown that Bck1 is a client of Hsp90 (176), so we sought to determine if Bck1 interacts with yeast Hsp70. We co-immunoprecipitated Ssa1 from WT cells and probed for Bck1 using an HA antibody. We observed a robust interaction of Ssa1 with both Bck1 fragments, independent of heat shock. Thus, we identified Bck1 as a novel interactor and a bonafide client of the chaperone system (Figure 30).

CHAPTER 4: DISCUSSION

Regulation of Hsp70 through phosphorylation

Hsp70 is a well-conserved molecular chaperone crucial for protein homeostasis, according to the traditional model that suggests that Hsp70 expression in cells is regulated by stress, altered binding of co-chaperones, and the different isoforms. However, with advances in proteomics, many post-translational modifications have been discovered on Hsp70, which are predicted to fine-tune chaperone function. Chaperone code research is still in its infancy. Despite the large number of PTM sites detected on Hsp70, less than ten have been fully characterized in their role and regulation (1 and 147).

This study describes Hsp70 regulation mediated by direct phosphorylation. Via phosphoproteomic analysis, we identified a single site of Threonine 492 on yeast Hsp70, which was upregulated under heat shock. Ssa1 T492 lies on the SBD of Ssa1, and the location of this site is likely to influence chaperone-client interaction (29 and 46). Considering these data, this site is conserved through all domains of life. Interestingly, the site is conserved and phosphorylated under heat shock in all Ssa isoforms, Ssa1, 2, 3, and 4. These isoforms are partially redundant, and constitutive expression of even one isoform can maintain cell viability in the absence of the other three (17). This study demonstrates that all four Ssa1 isoforms can be phosphorylated on T492 under heat stress, making it the first example of conserved phosphorylation in yeast Hsp70. Thus, suggesting all 4 Ssa isoforms may be similarly regulated

Chaperone phosphorylation fine-tunes the well-conserved HSR

Our mass spectrometry data observed distinct patterns in chaperones and co-chaperone interactions upon Hsp70 phosphorylation. Upon phosphorylation of Ssa1 T492, a decreased interaction was seen for co-chaperone Ydj1, but the interaction with Sis1 remained unchanged. There are some similarities between T492 to another well-characterized Ssa1 phospho-site T36. Although these sites are differentially regulated (T36 by nutrient availability, T492 by heat), their phosphorylation leads to similar co-chaperone interaction changes. Both the phosphorylation of T36 and T492 lead to the loss of Ssa1-Ydj1 interaction while preserving interaction with Sis1 (36). In contrast to T36, alteration of T492 doesn't appear to impact cell cycle control. Our analysis revealed altered Ssa1, Hsp82, and Ydj1 expression levels in T492 mutants compared to wild-type cells. While Hsf1 controls chaperone and co-chaperone expression, heat shock doesn't expand its target gene repertoire but rather intensifies chaperone expression. heat shock triggers two parallel pathways – Hsf1-mediated Heat Shock Response (HSR) and the Environmental Stress Response (ESR) controlled by Msn2/4. These pathways demonstrate remarkable compensatory behavior, where inactivation of one pathway leads to enhanced activation of the other, ensuring robust stress protection through functional redundancy (82). Our study revealed a similar compensatory mechanism between transcription factors Hsf1 and Msn2/4 under heat shock. In T492 mutant cells, Hsf1 failed to dissociate during heat shock, resulting in an imbalance in chaperone expression and an impaired heat shock response (HSR). T492 mutant demonstrated increased basal activity for Msn2/4 (tracked by Hsp12 inducibility) under unstressed and stressed conditions compensated for the Hsf1 defect. Thus, this suggests that an increased inducibility enabled the mutants to produce higher

levels of chaperones, which is necessary for survival. The elevated activity of Msn2/4 in the Ssa1 T492 mutant appears to be an adaptive response. Thus, allowing the mutant cells to maintain adequate chaperone levels is crucial for survival even without Hsf1 activation. The initiating events of HSR have still not been fully uncovered. How cells fundamentally sense heat and how they respond so fast to changes in temperature have been a source of debate. The chaperone titration model, as described, proposes that heat shock protein (HSP) activation occurs when denatured proteins accumulate, drawing Hsp70 away from the heat shock factor (HSF) (65). This allows HSF to become active and induce heat shock genes. However, this model does not account for the rapid kinetics of Hsf1 activation observed in response to heat shock, which occurs faster than the time required for significant protein unfolding and chaperone sequestration. While the chaperone titration model has provided valuable insights into HSR activation, it likely represents only a part of a more complex and dynamic regulatory system (58). Krakowiak et al. (59) demonstrated that Ssa1 directly binds to Hsf1 within the CE2 motif in the C-terminal activation domain (C-AD). Peffer et al. 2019 (49) also identified a second Ssa1-interacting region situated to the N-AD between residues 50 and 100 (49). Interaction between Hsp70 and Hsf1 occurs via the C-terminal substrate binding domain of Hsp70 where T492 lies. Thus, it suggests the importance of the T492 phosphorylation in mediating the correct dissociation of Hsf1, thereby activating HSR. The phosphorylation of T492 occurs rapidly, within minutes of heat shock, and is not initiated by protein misfolding. This rapid response suggests the existence of an additional regulatory mechanism for the heat shock response (HSR). This mechanism appears to operate alongside the conventional Hsf1-Ssa1-unfolded protein titration system rather than replacing it. In this study, we have uncovered a novel paradigm of rapid yeast

Hsf1 activation that occurs through phosphorylation of Ssa1. The model integrates direct heat-sensing mechanisms with sophisticated interactions among chaperones, co-chaperones, and Hsf1. These interactions are modulated by phosphorylation at the Ssa1 T492 site, highlighting the intricate nature of cellular stress response systems.

Chaperone phosphorylation controls translational fidelity

As newly synthesized yeast proteins exit the ribosome, they are bound by ribosome-associated chaperones, including Ssb1, Ssz1, and Zuo1, to promote client folding (150) chaperone interactions on the ribosome. However, the yeast ribosome itself is an extremely complex structure consisting of 4rRNA molecules and 79 ribosomal proteins (145). Many of these proteins are highly aggregation-prone, and the process of assembling a ribosome must be tightly controlled to ensure translational fidelity. Thus, several studies have demonstrated chaperone control of the ribosome and translation. mutations in Ssa1, a yeast Hsp70 chaperone, cause cells to become hypersensitive to translation-inhibiting compounds like hygromycin B and cycloheximide. This increased susceptibility suggests an important role for Ssa1 in maintaining proper translation processes. (178). Yeast ribosome-associated Hsp70 is crucial for maintaining translational fidelity. Any mutation or deletion of the chaperone leads to translation defects. (153). Studies also show that the absence of ribosome-associated Hsp70 causes ribosome aggregation and impacts ribosome biogenesis (134) via TORC1 signaling (179). Heat Shock Factor 1 (Hsf1)-dependent upregulation of chaperone is required for adapting to ribosomal protein assembly (180). Two cross-linking mass spectrometry studies recently uncovered many direct Hsp90/Hsp70-ribosomal protein interactions (146-147). ribosome assembly is initiated in the nucleolus with rRNA transcription, followed by intricate processes including rRNA

folding, nucleotide modifications, and association with ribosomal proteins. Many of the interactors of Ssa1 identified in the interactome were structural components of the ribosome, both from the small and large subunits. In our studies, mutation of T492 substantially impacted Ssa1-ribosomal interactions and translational fidelity. Essential translational initiation factor Ded1 can repress translation by segregating mRNAs into phase-separated RNA–protein granules during cell stresses. (181). It is also important to scan the pre-initiation complex to the AUG start codon and subsequent formation of the initiation complex (182). Interestingly, we identified that the interaction of Ded1 was decreased in the mutant, suggesting the reason for the defect in translational fidelity seen in the mutant. Secondly, Ribosomal protein L10 (Rpl10) is the last protein assembled during ribosome biogenesis. Rpl10, plays essential roles in ribosome biogenesis and translational fidelity (185). Interestingly, we identified that the interaction of Rpl10 was decreased in the mutant. Heat shock causes global pausing of translational elongation (157 and 183). This heat-mediated pausing responds to Hsp70 dissociation with ribosomal machinery (157). The predicted mechanism that causes ribosome stalling during heat shock is the chaperones that are associated with the emergent nascent peptide, which somehow clog the peptide exit tunnel; in our study, we saw in the WT that upon heat shock, Ssa1 was seen to be dissociated from the polysome, thus pausing translation. However, in the mutant, upon heat shock, an increase in Ssa1 was seen on the polysome. Notably, phosphorylation of the equivalent site in human Hsc70 by the Legionella LegK4 kinase can exert a similar effect on mammalian translation (46). Minimally, our findings linking T492 phosphorylation to Ssa1-ribosome interaction explain how yeast can rapidly manipulate translation under heat stress.

Chaperone phosphorylation drives P-body dynamics

Stress granules (SGs) and processing bodies (PBs) are distinct cytoplasmic RNA structures that emerge as functional consequences of mRNA metabolism. While these structures share certain dynamic properties related to their substrate mRNA and contain overlapping protein components, they also possess unique elements and fulfill separate cellular roles (137). Processing bodies (PBs) maintain a baseline presence in unstressed yeast cells while showing dramatic induction under various stress conditions - including glucose deprivation, oxidative stress, and heat shock - all of which trigger global translation suppression (118). Interestingly, stress granules (SGs) emerge from existing PBs, suggesting that PBs serve as initial storage sites for messenger ribonucleoprotein complexes (mRNPs). Observations that intrinsically disordered domains of proteins promote the assembly of these biomolecular condensates. It was also suggested that interactions necessary for stress granule or P-body formation are regulated by chaperones, specifically, Hsp70 and Hsp40 (118). Studies also have shown that defects in Hsp70 or Hsp40 function inhibited the disassembly of stress granules during the post-stress recovery phase but not the P-body (184). The observation that stress granules emerge from existing processing bodies (PBs) in yeast suggests that defects in PB disassembly could impair proper mRNP exchange and subsequent stress granule formation. While the importance of Hsp70 phosphorylation in RNA granule dynamics remains unexplored, this relationship warrants investigation, particularly focusing on P-body and stress granule behavior during heat shock conditions. The deletion of Edc3 compromises cells ability to form Processing bodies (P-bodies), (124). Our interactome data identified important proteins (Pab1 and Edc3) that are involved in biomolecular condensate formation. We studied the foci

formation and the localization of Edc3-mCherry (P-body marker) and Pab1-GFP (stress granule marker) in WT and T492A cells under unstressed heat shock and recovery conditions. A striking observation was seen during the recovery time points. The mutant T492A was defective in Edc3-foci disassembly even at 2 hours of recovery. However, the disassembly of stress granules was seen to be normal. This suggests that Ssa1 T492 phosphorylation is required for P-body disassembly. In the interactome study, we saw that P-body marker Edc3 ad increased interaction with WT compared to mutant, while stress granule marker Pab1 had equal interaction. This might explain the impact seen on the disassembly dynamics of Edc3 but not Pab1. Lack of disassembly defect seen for stress granule for T492 mutant, we strongly believe that other phosphorylation sites on Hsp70 may contribute to altered stress granule dynamics. Studies have shown that (132). The assembly of Processing bodies (P-bodies) depends specifically on the catalytic function of Mpk1, the MAP kinase component of the cell wall integrity pathway. This requirement directly links stress signaling and RNA granule formation (132). Similarly, the case of the T492 mutant, which had a defect in the Mpk1 activation, showed altered P-body dynamics. Studies show that when cells return to lower temperatures, Hsp104 and Hsp70 play a crucial role in the resolution of the condensates (138). The failure of Ssa1 to bind substrates effectively leads to an inability to resolve mRNPs after stress removal (184). Thus, evidence is provided that the Hsp70 function is required for condensate resolution. This might explain the Edc3 disassembly defect seen in the mutant. As Ssa1 T492 lies on the substrate-binding domain, it can interfere with client binding activity and thus show a defect in condensate resolution. Our interactome identified a few proteins that were earlier reported to show heat-triggered aggregation. Ded1 is a crucial component of heat-induced

stress granules. The components of the granule that aggregate after 2 min of heat shock at 46°C are referred to as “super aggregators” (144). This supper aggregator showed increased interaction with WT. However, as we didn’t see any effect of T492 phosphorylation in SG granule dynamics, we strongly believe that other phosphosites from the Hsp70 chaperone code may have a role to play in regulating the dynamics. Further studies are required to understand the role of chaperone code in regulating these stress granule dynamics.

Chaperone phosphorylation reciprocally regulates CWI

Our study demonstrated the upstream involvement of CWI, which is also triggered by heat shock. Heat acts to cause membrane stretch, which is detected by the Mid2 mechanosensor. Activation of the cell integrity pathway leads to Pkc1-catalyzed phosphorylation of Ssa1 at T492, promoting a variety of cellular effects, including Ssa1-Hsf1 dissociation, correct disassembly of P-body, amplification of the CWI pathway and translational pausing. The complex involvement of the cell integrity pathway in other cellular processes is intriguing. Although heat activation of the cell integrity pathway has been known for several decades, how CWI and the HSR are spatially and temporally integrated has not been fully defined. In 2006, Wright and colleagues established the first direct connection between chaperone function and cell wall integrity signaling. Their seminal work demonstrated that overexpressing Mid2, a cell wall stress sensor, could rescue yeast strains lacking the co-chaperone Ydj1 growth defects, revealing an unexpected link between protein folding and cell wall maintenance pathways. (116). We identified Mid2 as the mechanosensor that is critical for the phosphorylation of Ssa1 T492 under heat stress. They also demonstrated that temperature-sensitive mutants of Hsp82 (G313N and G170D) that exhibited cell-wall

defects had improved growth at elevated temperatures by overexpression of Mid2 or Pkc1. We identified Pkc1 as the kinase that directly phosphorylates Ssa1 T492. Pkc1 directs various responses to heat shock through Ssa1 independent of the Bck1-Mkk1-Mpk1 MAPK cascade and may also explain the differences in knockout phenotypes for these proteins. While the loss of Pkc1 causes cell inviability, *bck1*Δ cells are viable but are temperature-sensitive (83). Studies have revealed intricate connections between molecular chaperones and cell wall integrity signaling. Neither Mid2 overexpression nor elevated PKC pathway components could rescue the temperature sensitivity of the Ssa1 T492 mutant, mirroring observations from the ssa1-45 thermosensitive mutant (177). (177). Hsp90 was identified as a Slt2 binding partner, suggesting that chaperones are a critical component of cell wall integrity signaling. Hsp90 preferentially binds dually phosphorylated Mpk1 to activate a downstream target. (112). Chaperones bind to a large number of kinases involved in signal transduction. Inhibition of chaperone function via mutation or small molecules leads to numerous kinases becoming destabilized and inactive (170). A major challenge in understanding chaperone-kinase interactions is their reciprocal nature. Chaperones can stabilize kinase, phosphorylating and fine-tuning chaperones (88). Our study reveals a complex interplay between the yeast chaperone Ssa1 and the Cell Wall Integrity (CWI) pathway. We found that phosphorylation of Ssa1 at T492 is both dependent on upstream CWI components and crucial for the pathway's downstream activation, particularly at high temperatures. Our study identified Bck1 as a novel interactor and bona fide client of the yeast chaperone systems. Bck1 is unique in yeast, possessing a classic kinase domain, while the remainder of its 163 kDa structure is minimally structured and likely intrinsically disordered. Bck1 levels are compromised in the mutant under heat

shock, leading to defective CWI signaling. Specifically, T492 phosphorylation promotes the stability of Bck1's C-terminal kinase domain. When this phosphorylation is absent, as in the T492 mutant, Bck1's defectiveness prevents the CWI cascade from transmitting activation signals to downstream kinases, explaining the observed defect in Slt2 activation. These findings collectively demonstrate a non-canonical amplification of CWI signaling through altered Pkc1 phosphorylation, highlighting the intricate regulatory mechanisms governing yeast cellular responses to heat stress. Truman et al. (2007) showed that loss of the CT domain of Hsf1 resulted in cell-wall integrity pathway defect at high temperatures. Deletion of the C-terminal region (amino acids 583-833) in Saccharomyces cerevisiae Hsf1 disrupts proper heat-induced activation of the Slt2 (Mpk1) MAP kinase (114). This defect leads to two major consequences: impaired expression of cell wall-related genes and compromised cell wall integrity at elevated temperatures. These findings highlight the established connection between heat shock response and the Cell Wall Integrity (CWI) signaling pathway. However, no linkage between the signaling events was ever established by a Ssa1 phosphorylation. However, a direct link between these two crucial stress response pathways remains elusive. Our study reveals a novel connection through the phosphorylation of Ssa1, a major Hsp70 chaperone. We demonstrate that heat-induced phosphorylation of Ssa1 is a critical bridge between these signal transduction pathways involved in the heat shock response. Specifically, we found that Pkc1, a key component of the CWI pathway, phosphorylates Ssa1. This phosphorylation event significantly impacts the fidelity and output of the global heat shock response.

This study demonstrates a fundamentally novel aspect of the heat shock response that explains how cells can respond so rapidly by activating Hsp70 phosphorylation.

Importantly it solves a long-standing question of how distinct features of the yeast shock response -Hsf1 activation, CWI pathway activation, ribosomal rearrangement, and heat-induced P-body resolving are integrated. Going forward, it will be interesting to understand how distinct features of the HSR, such as chaperone titration and heat-mediated HSF conformational changes, are co-regulated throughout cells and tissues. Overall, this implies modification of T492 can fine-tune client binding and processing as opposed to a binary on-off switch.

CHAPTER 5: CONCLUSIONS

This study provides a comprehensive mechanistic understanding of the regulation and functional impacts of heat-induced phosphorylation of threonine 492 (T492) on yeast Hsp70 (Ssa1). Our findings reveal a complex and multifaceted role for this highly conserved post-translational modification in coordinating various aspects of the cellular heat shock response. Ssa1 T492 phosphorylation is rapidly induced within 5 minutes of heat shock and is mediated by membrane stretch detected through the Mid2 mechanosensor. Yeast Protein Kinase C (Pkc1) was identified as the direct kinase responsible for T492 phosphorylation. Interactome remodeling: Phosphorylation of T492 significantly alters Ssa1's interaction network, affecting its associations with co-chaperones, client proteins, and various cellular machinery components involved in translation, RNA processing, and stress response. Heat Shock Response (HSR) regulation: T492 phosphorylation is critical for properly activating HSR through modulation of Ssa1-Hsf1 interactions. The T492A mutant fails to dissociate from Hsf1 upon heat shock, leading to impaired HSR activation-body dynamics: T492 phosphorylation is required for proper P-body disassembly during recovery from heat stress, while stress granule dynamics remain unaffected. Cell Wall Integrity (CWI) pathway: T492 phosphorylation promotes CWI signal amplification and is necessary for heat-induced activation of Mpk1. We also identified Bck1 as a novel client of Ssa1, with its stability dependent on T492 phosphorylation. Translational fidelity and protein synthesis: T492 phosphorylation plays a crucial role in maintaining translational fidelity and regulating global protein synthesis during heat stress. These findings collectively demonstrate that T492 phosphorylation serves as a critical regulatory switch, fine-tuning Hsp70 function across multiple cellular

processes in response to heat stress. This phosphorylation event integrates membrane stretch sensing with chaperone function, transcriptional regulation, mRNA processing, cell wall maintenance, and protein synthesis. Our work provides a unified model for understanding how a single post-translational modification on a key chaperone can orchestrate diverse cellular responses to heat stress. This research advances our understanding of stress response mechanisms in yeast. It provides insights that may apply to stress response systems in higher eukaryotes, given the high conservation of the T492 site across evolution.

Future studies can build upon this foundation to explore the potential therapeutic implications of modulating Hsp70 phosphorylation in stress-related disorders and to investigate similar regulatory mechanisms in other organisms.

FIGURES

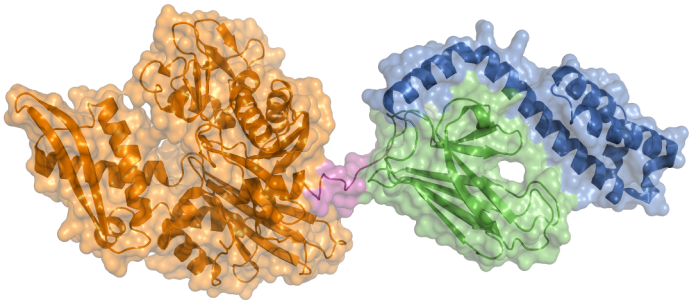

Figure 1. Domains of Hsp70 Domains of Ssa1 are colored as follows: NBD is the Nucleotide-binding domain is an ATPase domain that consists of two subdomains, forming a cleft in which adenine nucleotide binds where hydrolysis of ATP to ADP occurs. SBD is a substrate-binding domain that forms a peptide-binding pocket that accommodates polypeptide chains. The SBD and NBD are connected by a short, highly flexible linker, as labeled. CTD is the C-terminal domain that forms the lid on the substrate binding pocket. The blue circle is the substrate-binding pocket

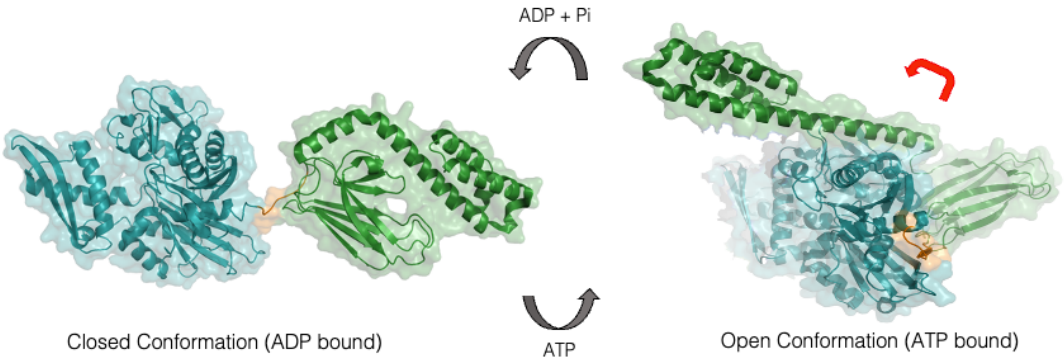

Figure 2. Regulation of Hsp70 Hsp70's activity depends on a conformational cycle controlled by nucleotide exchange factor and co-chaperones via allosteric regulation. When ATP binds, Hsp70 adopts a closed conformation. This configuration results in Hsp70 having a low affinity for misfolded proteins. When ATP is hydrolyzed to ADP, Hsp70 undergoes a substantial conformational change, increasing its affinity for misfolded proteins. J-protein brings the unfolded protein to the open state Hsp70.

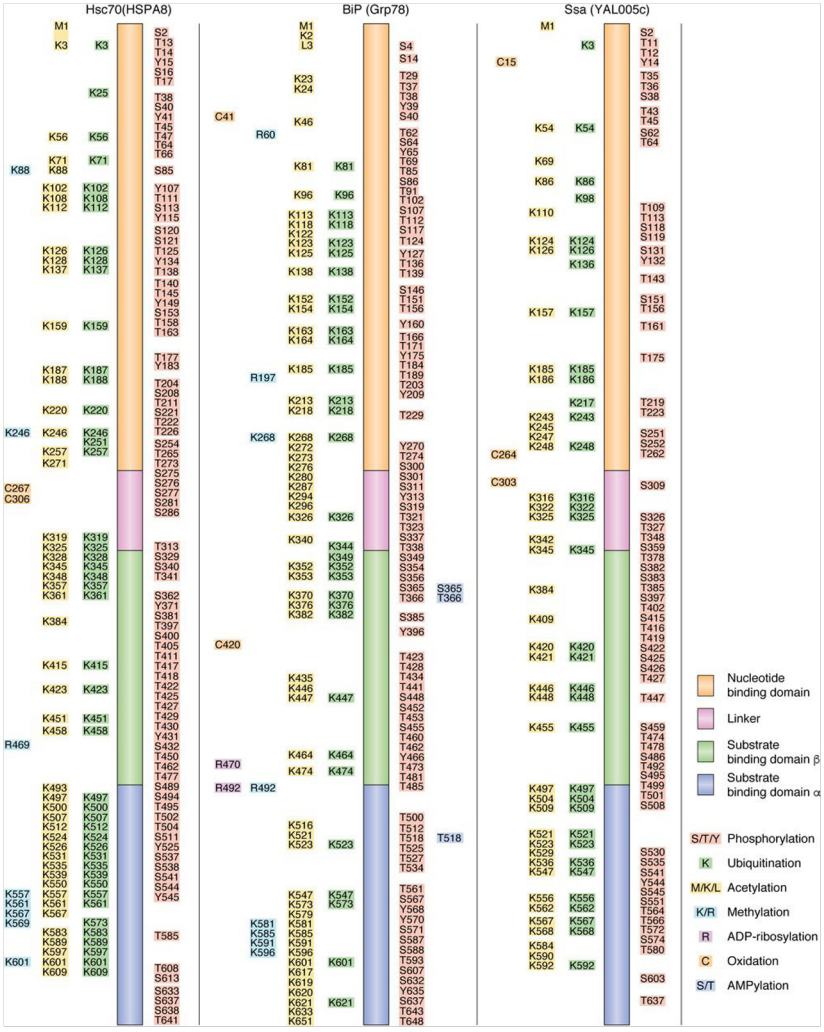

Figure 3. The Hsp70 chaperone code shown is a domain representation of the Hsp70 family members, with detected post-translational modifications (PTMs) marked with appropriate residue numbers. PTMs are labeled as follows: phosphorylation in red. PTMs significantly modify the Hsp70 family of proteins in yeast and mammalian cells. Little is known about the role and regulation of these PTMs. Figure reproduced from (1)

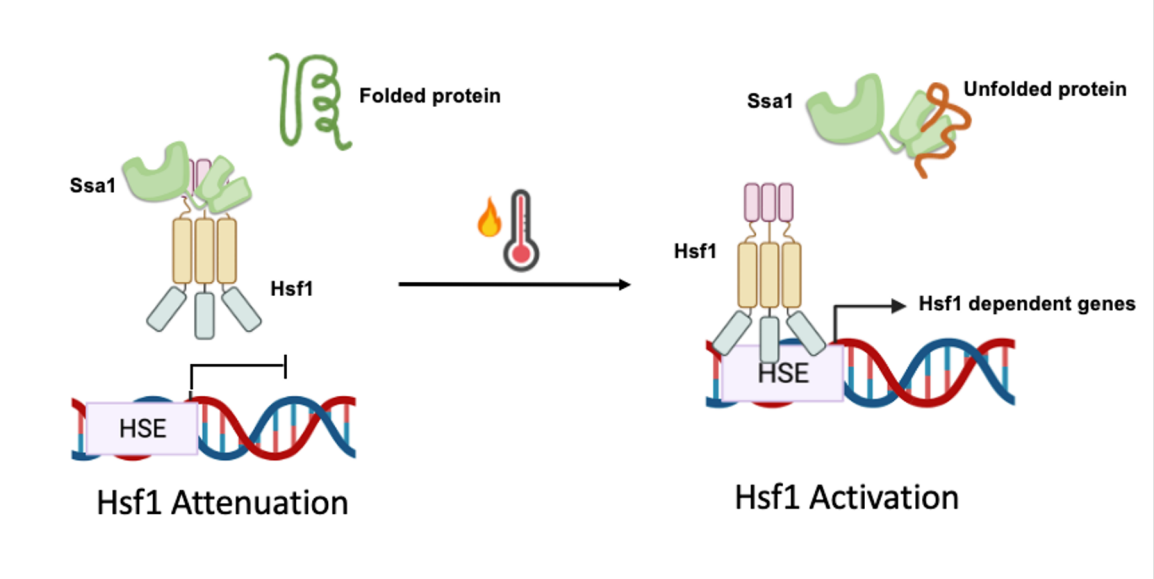

Figure 4. The traditional model for Yeast Heat-shock response (HSR) The transcription factor Hsf1 remains inactive in normal conditions through binding to the chaperone Ssa1.During heat shock, the accumulation of unfolded proteins in the cell competes for and draws away Ssa1 from Hsf1, leading to Hsf1 activation. The activated Hsf1 binds to Heat Shock Elements (HSE) in DNA, triggering increased transcription of heat shock response genes. This results in elevated production of molecular chaperones, which help restore proper protein folding. Once protein homeostasis is restored, excess chaperones bind back to Hsf1, returning the system to its inactive state.

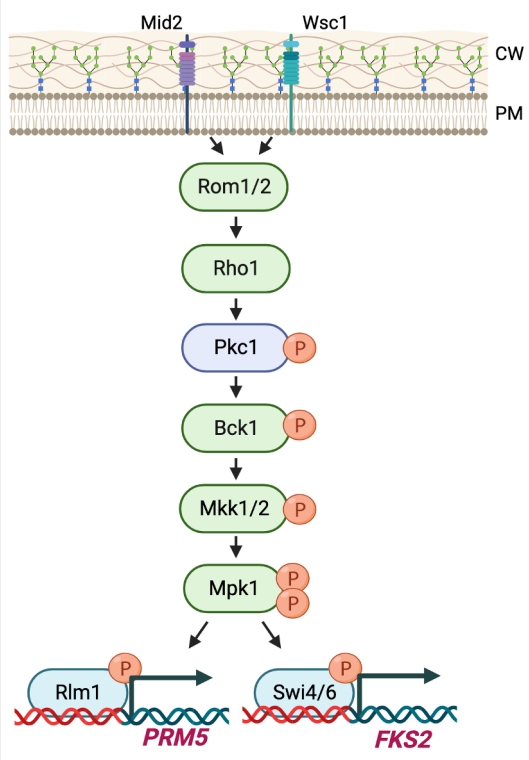

Figure 5. The cell integrity pathway. Cell wall agents activate the Mid2 and Wsc1 mechanosensors. The subsequent activation of Pkc1 leads to a series of phosphorylation events terminating in the phosphorylation of Rlm1 and Swi4 transcription factors, inducing genes that reinforce cell integrity.

A

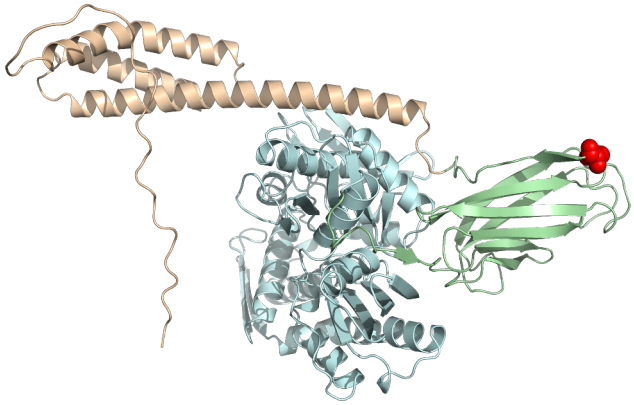

B

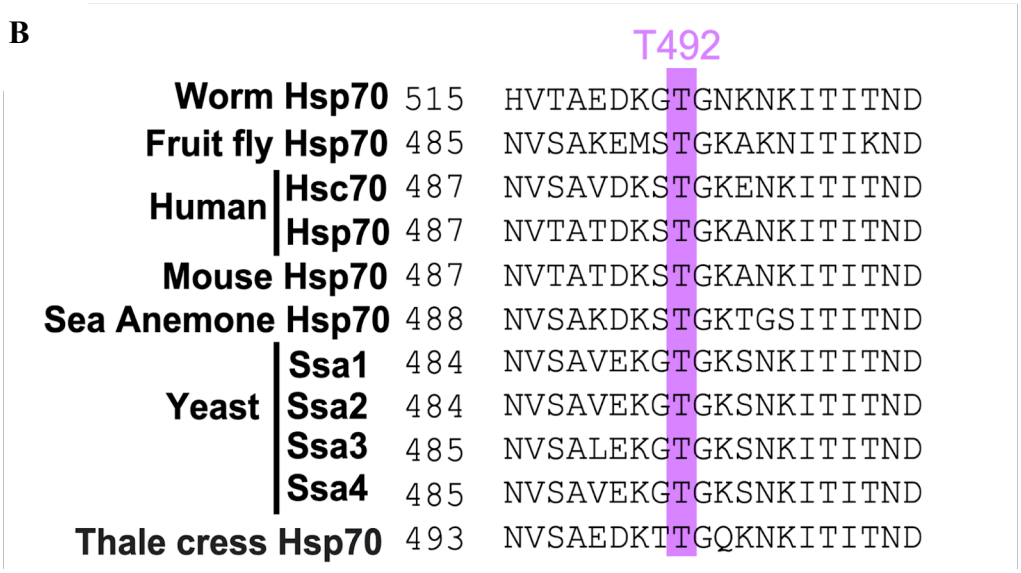

Figure 6. Ssa1 Threonine 492 is an evolutionarily conserved site located on the client binding region. (A) The open conformation of Ssa1 with T492 (red sphere). The domains of Ssa1 are colored as follows: nucleotide-binding domain (cyan), substrate-binding domain (green), and c-terminal lid region (brown). (B) Alignment of Hsp70 proteins from *Caenorhabditis elegans* (worm), *Drosophila melanogaster* (fruit fly), human cells, *Mus musculus* (mouse), *Nematostella vectensis* (sea anemone), *Saccharomyces cerevisiae* (yeast) and *Arabidopsis thaliana* (Thale cress). T492 is highlighted in purple.

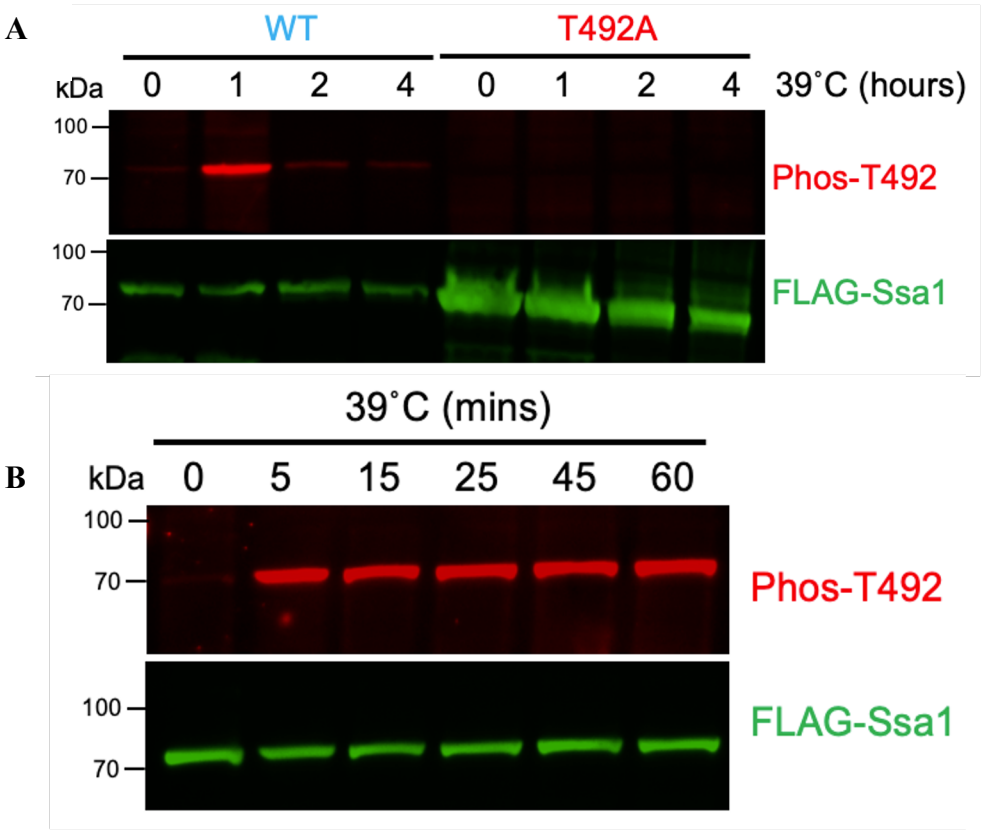

Figure 7. Threonine 492 (T492) on yeast Hsp70 is activated rapidly in response to heat stress. (A) Ssa1-4Δ background yeast cells were transformed with the LEU plasmid expressing either wild-type Flag-Ssa1 or non-phosphorylatable mutant Flag-T492A and cured on FOA. Cells were then grown in SD-LEU at 25 ˚C overnight and grown to the mid-log phase. Cells were stressed at 39 ℃, and aliquots of cells were collected at 0, 1,2, and 4 hours. Cell extracts were obtained, resolved on SDS-PAGE gels, and analyzed by immunoblotting for T492 activation (Phospho T492 antibody) and FLAG loading control (FLAG antibody). **(B)** Ssa1-4Δ background yeast cells were transformed with the LEU plasmid expressing wild-type Flag-Ssa1 cured on FOA. Cells were grown in SD-LEU at 25 ˚C overnight to mid-log phase. The cells were kept at 25 ℃ for unstressed conditions or stressed at 39 ℃. To study the rapid heat response, aliquots were collected at 0,5,15,25 and 45 minutes. Cell extracts were obtained, resolved on SDS-PAGE gels, and analyzed by immunoblotting for T492 activation (Phospho T492 antibody) and FLAG loading control (FLAG antibody).

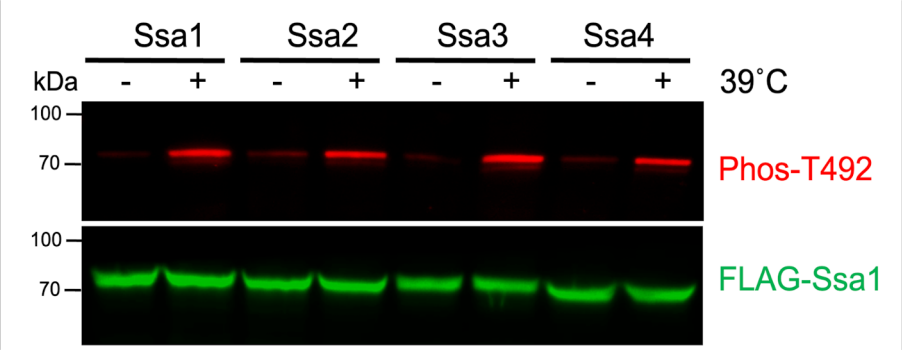

Figure 8. Threonine 492 phosphorylation is conserved in all yeast Hsp70 isoforms. Ssa1-4Δ background yeast cells expressing Flag-tagged Ssa1, 2, 3, 4 on constitutive Ssa2 promoters as the sole Ssa. Cells were then grown in SD-LEU at 25 ˚C overnight and grown to the mid-log phase. Cells were stressed at 39 ℃ for 1 hour. Cell extracts were obtained, resolved on SDS-PAGE gels, and analyzed by immunoblotting for T492 activation (Phospho T492 antibody) and FLAG loading control (FLAG antibody).

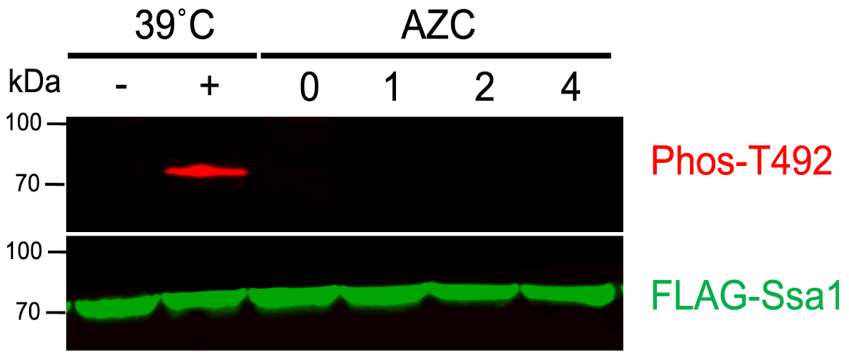

Figure 9. Heat-induced phosphorylation of T492 is independent of protein folding. Ssa1-4Δ background yeast cells were transformed with the LEU plasmid expressing either wild-type Flag-Ssa1 or non-phosphorylatable mutant Flag-T492A and cured on FOA. Cells were then grown in SD-LEU at 25 ˚C overnight and grown to the mid-log phase. Cells were AZC (azetidine-2-carboxylic acid), and aliquots of cells were collected at 0, 1,2, and 4 hours. Cell extracts were obtained, resolved on SDS-PAGE gels, and analyzed by immunoblotting for T492 activation (Phospho T492 antibody) and FLAG loading control (FLAG antibody).

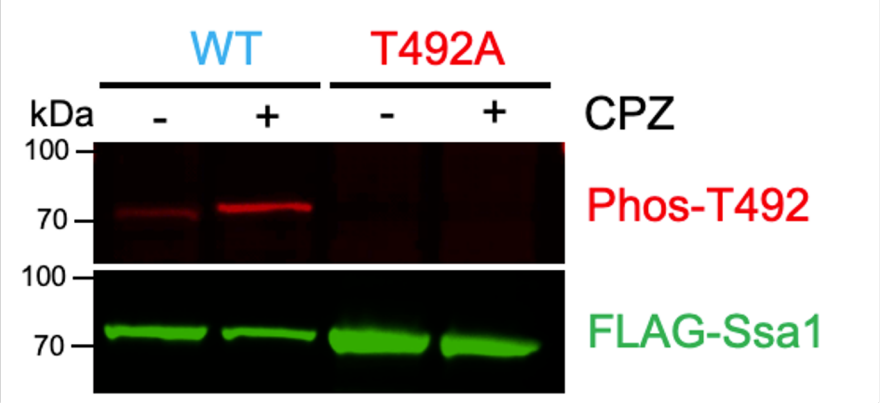

Figure 10. T492 phosphorylation is mediated by membrane stretch Ssa1-4Δ background yeast cells were transformed with the LEU plasmid expressing either wild-type Flag-Ssa1 or non-phosphorylatable mutant Flag-T492A and cured on FOA. Cells were then grown in SD-LEU at 25 ˚C overnight and grown to the mid-log phase. Lysate from FLAG-WT or T492A cells either untreated or treated with chlorpromazine (CPZ) for 1 hour were analyzed by Western Blotting using either FLAG or phospho-T492 antibody.

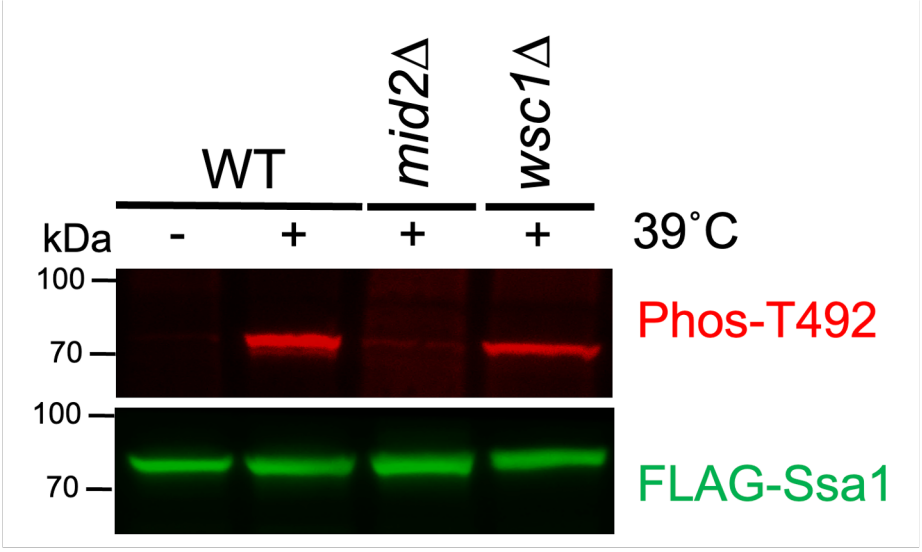

Figure 11. Heat-induced Ssa1 T492 phosphorylation is dependent on Mid2 mechanosensor Yeast strains deleted for either of the two mechanosensor-Mid2 or Wsc1 were grown in YPD media at 25 ˚C overnight and grown to mid-log phase. Cells were then heat-shocked at 39 ℃ for 1 hour. Cell extracts were obtained, resolved on SDS-PAGE gels, and analyzed by immunoblotting for T492 activation (Phospho T492 antibody) and Ssa1 antibody as loading control (FLAG antibody).

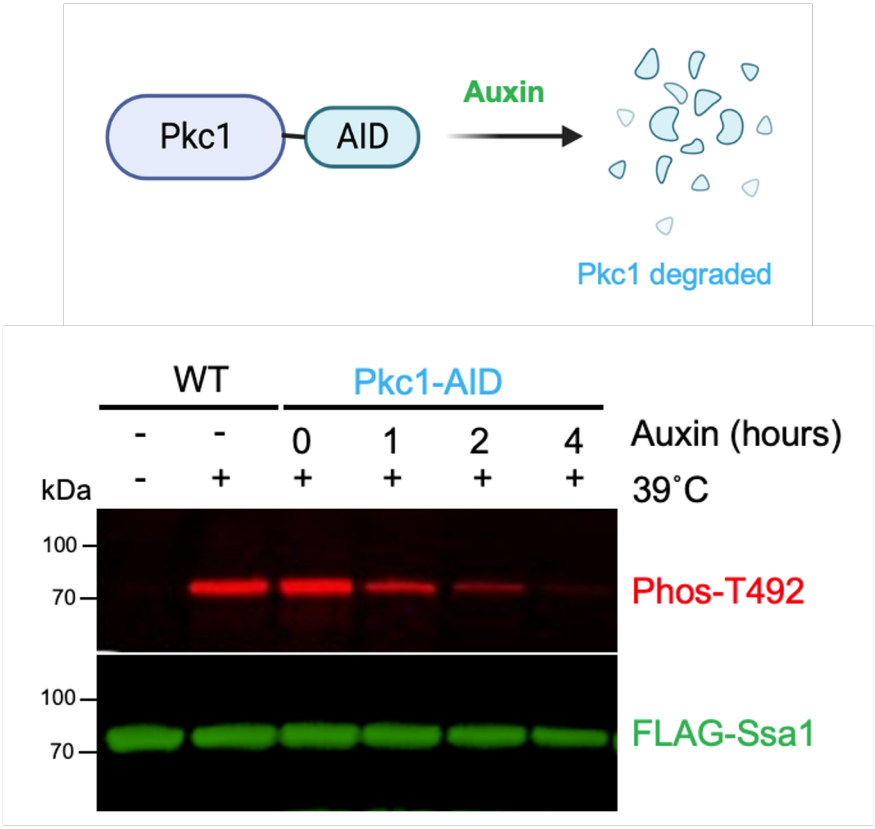

Figure 12. Ssa1 T492 phosphorylation is dependent on Pkc1 (A). Schematic of the mechanism used for auxin-induced degradation of Pkc1. (B) Ssa1-4Δ background yeast cells were transformed with the LEU plasmid expressing wild-type Flag-Ssa1 cured on FOA. In the cured FLAG-Ssa1 strain, Pkc1 was genomically AID-tagged. FLAG-Ssa1 (WT or with genomically AID-tagged Pkc1) cells were grown in SD-LEU or YPD at 25 ˚C overnight and grown to the mid-log phase. Cells were treated with auxin for the indicated time (0,1,2 and 4 hours), followed by heat shock at 39 ˚C for 1 hour. FLAG-Ssa1 WT cells were kept as control. Lysates were obtained, resolved on SDS-PAGE gels, and analyzed by immunoblotting for T492 activation (Phospho T492 antibody) and FLAG loading control (FLAG antibody).

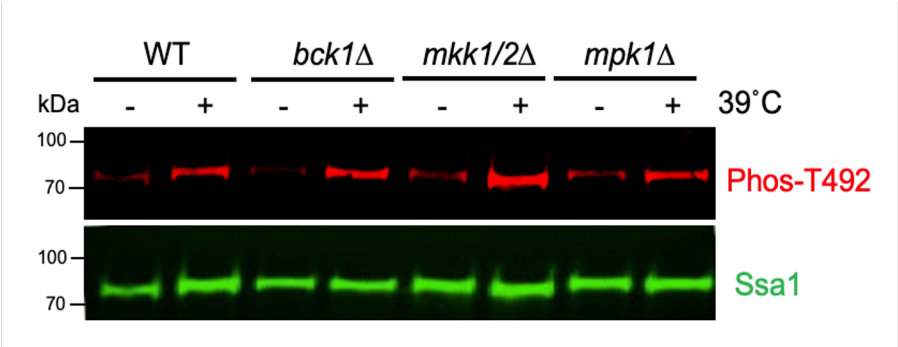

Figure 13. T492 phosphorylation is independent of Bck1, Mkk1, Mkk2 and Mpk1. Yeast with an EG123 strain background was used here. Strains deleted for indicated kinases (Bck1, Mkk1, and Mpk1) were grown in YPD at 25 ˚C overnight and grown to the mid-log phase. Cells were heat shocked at 39 ˚C for 30 minutes. WT cells were kept as control. Lysates were obtained, resolved on SDS-PAGE gels, and analyzed by immunoblotting for T492 activation (Phospho T492 antibody) and Ssa1 loading control (Ssa1 antibody).

A

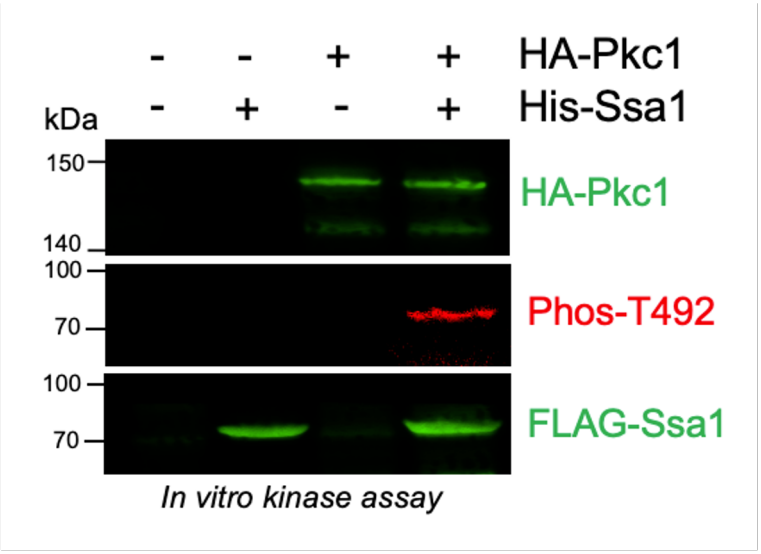

Figure14. Pkc1 directly phosphorylates Ssa1 T492 (A) Ssa1-4Δ background yeast cells with a plasmid expressing HA-PKC under galactose promoter. HA-Pkc1 was purified from a heat-shocked yeast strain using anti-HA antibody-conjugated beads. Recombinant His_6-Ssa1 was used as a substrate in an in vitro kinase assay with purified HA-Pkc1. 100μM of ATP was added to initiate kinase reaction. The reaction was incubated for 1 hour at room temperature. The reaction mixture was analyzed by Western Blotting using antisera to His, phospho-T492, or HA epitope.

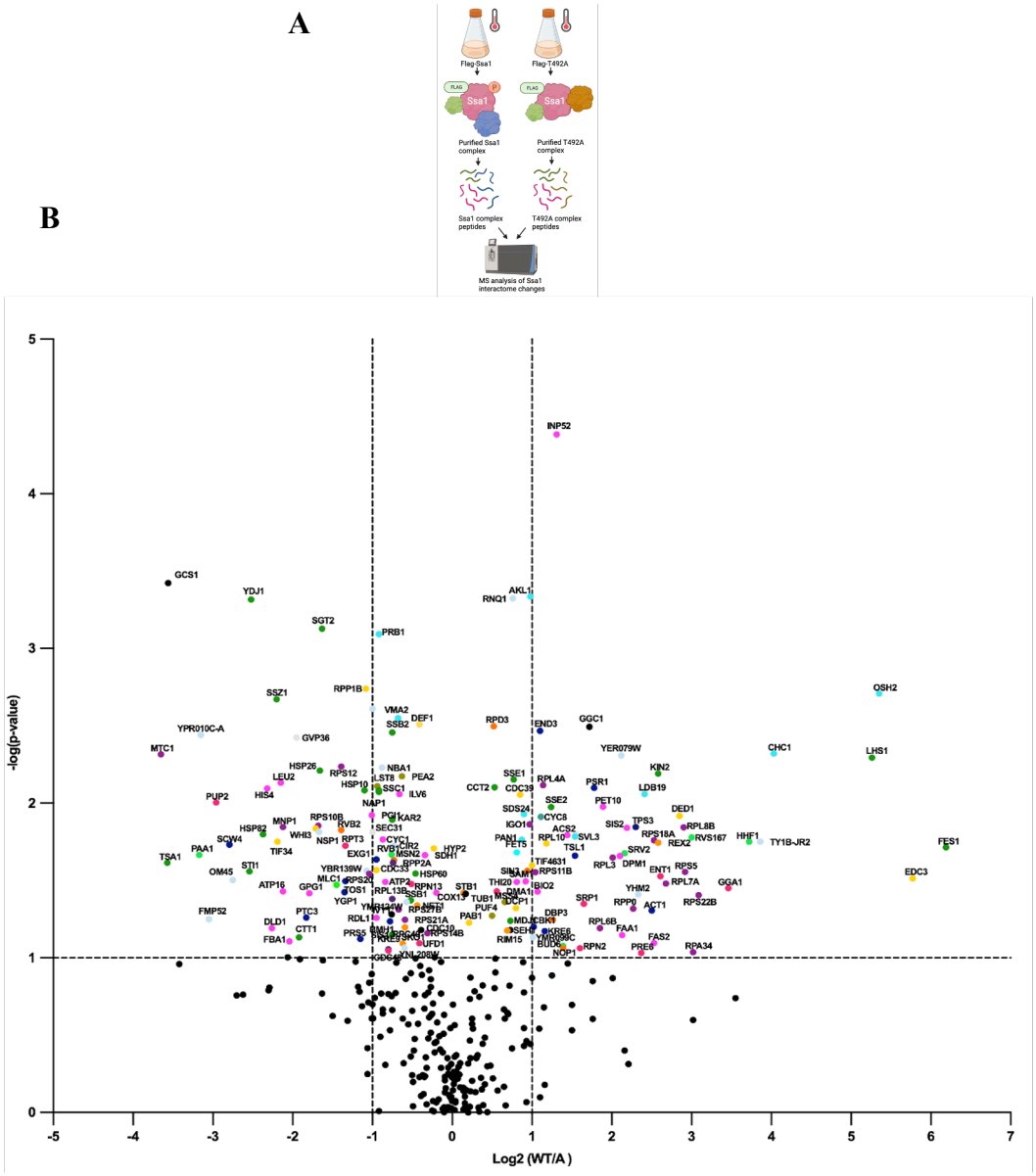

Figure 15. Phosphorylation of Ssa1 T492 fine-tunes the Hsp70 interactome **(A)** Proteomic workflow. **B)** Volcano plot of the interactome changes between WT and T492A cells. The log2 change (WT/T492A) and p-value for each interactor are plotted. The interacting proteins that are significantly downregulated were defined as $p < 0.05$ and have a $\log2 < -1$. For the significantly upregulated proteins, they have $p < 0.05$ and a $\log2 > 1$. Interactome visualization was performed using Prism 7 graphing software.

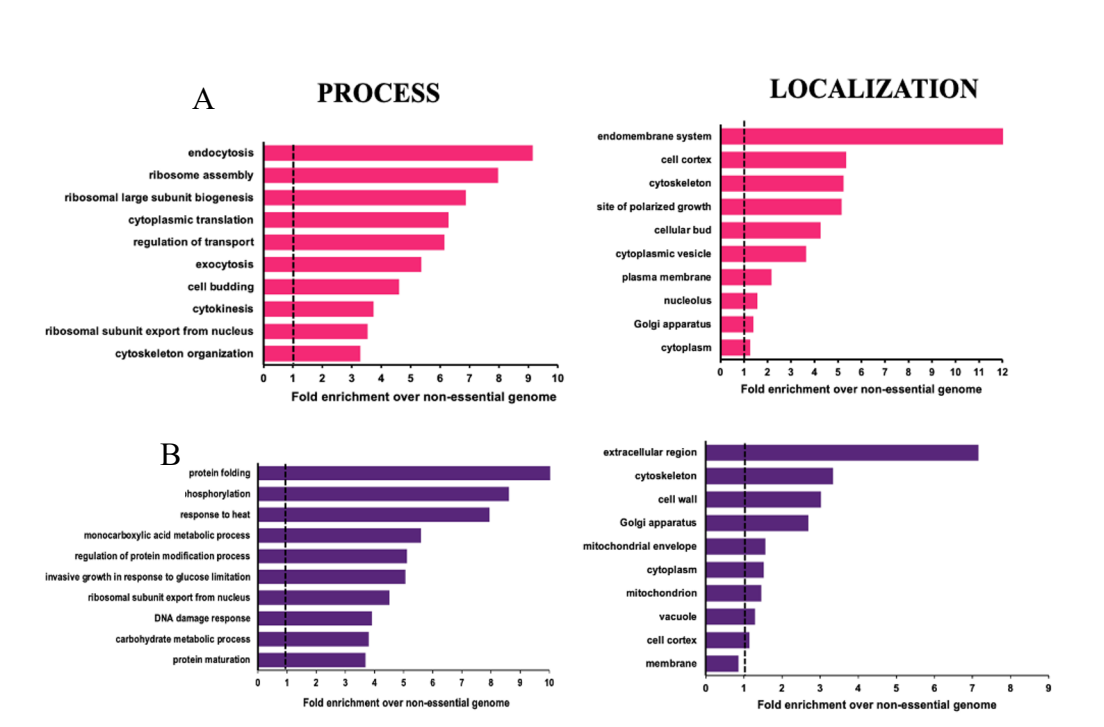

Figure 16. Gene ontology term analysis of Ssa1 Gene Ontology analysis was performed using GO Slim Mapper on the *Saccharomyces* Genome Database. For functional classification of the Ssa1 interactome. Ssa1 interactors were categorized by process and localization using GO Slim analysis and plotted by relative enrichment compared to occurrence in the nonessential genome. The top 10 enriched cellular processes are shown for each interactome. A) GO analysis for preferred interactors of WT Ssa1 under heat shock B) GO analysis for preferred interactors of Ssa1 T492A mutant under heat shock

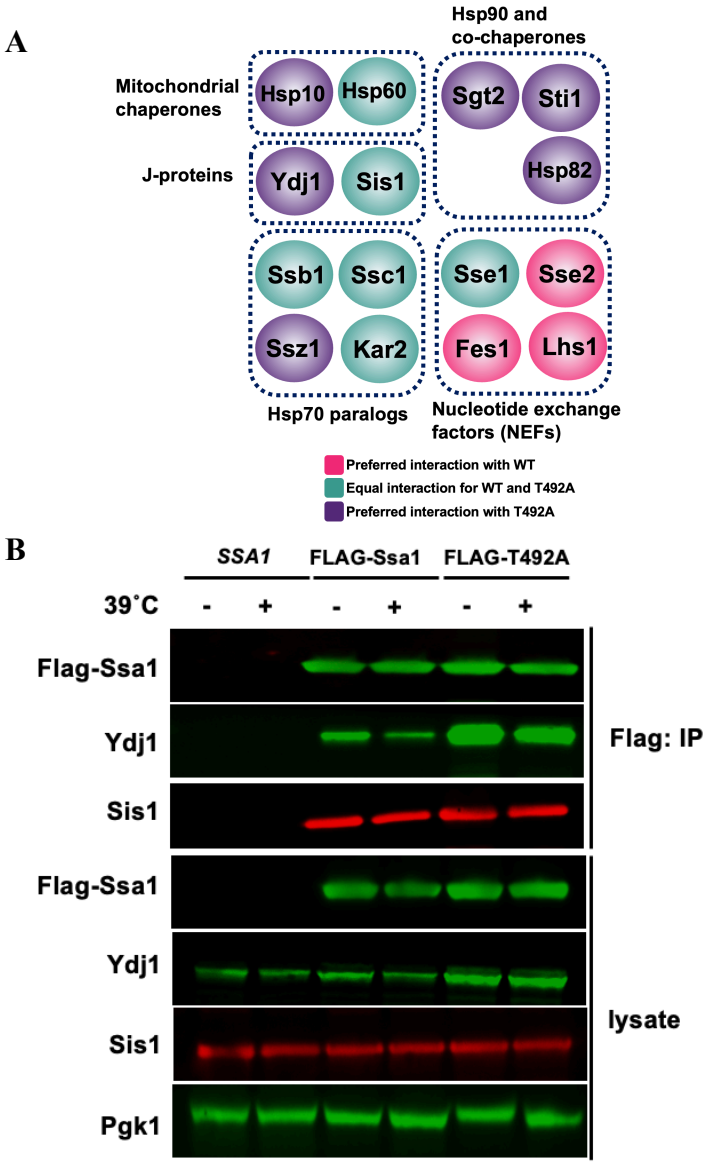

Figure 17. Altered Chaperone and co-chaperone interaction in the Ssa1 interactome (A) 15 chaperones and co-chaperone proteins were identified differently interacting with Ssa1 under phosphorylation. These interactors were analyzed using the STRING database and grouped based on homology and function. Interactors in pink are those that have preferred interaction with WT, while those in purple are interactors that have preferred interaction with mutant, and green are those with equal interaction with both (**B)** Flag-Ssa1 was immunoprecipitated using FLAG Dyna beads from WT and mutant. Western Blotting analyzed lysates and immunoprecipitated samples to check for Ydj1 and Sis1 coprecipitation using Ydj1 and Sis1 antibodies.

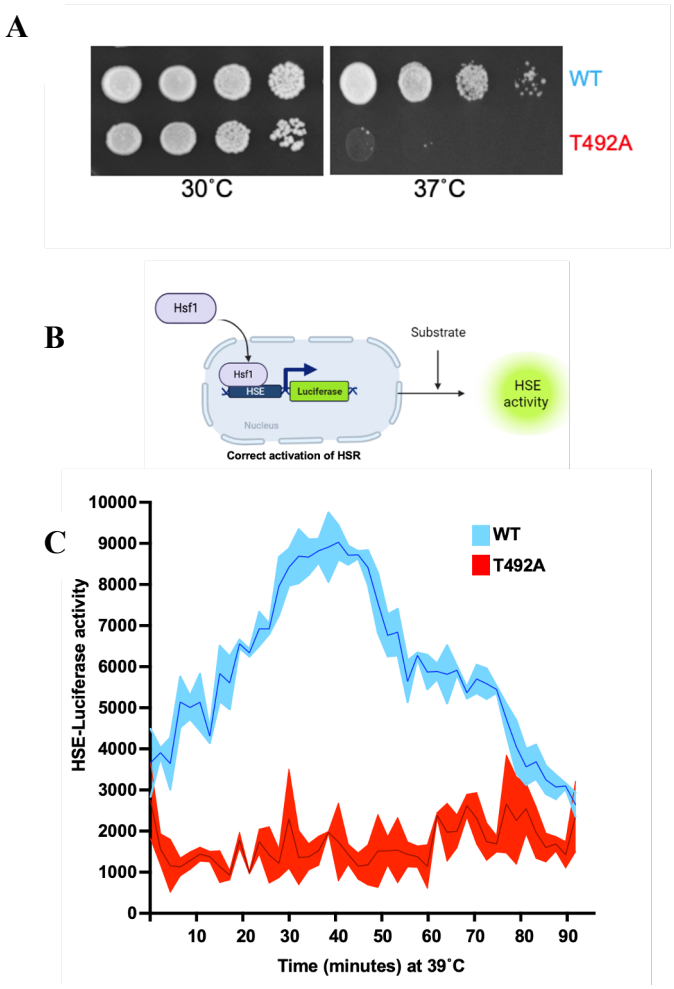

Figure 18. Phosphorylation of Ssa1 T492 is required for correct activation of heat shock response A) Ssa1 T492A is temperature-sensitive, WT and T492A cells were tenfold serially diluted, and spot assay was done on indicated media plates. Plates were incubated at 30 ˚C and 39 ˚C and photographed after 2 days. **(B)** Schematic for HSE-Luciferase assay **(C)** Lysate from FLAG-WT or T492A cells treated at 39 ˚C for 30 minutes were analyzed by HSE-luciferase activity of WT and T492A cells. Cells were transformed with a real-time destabilized secreted HSE-luciferase reporter. Cells were incubated at 39 ˚C and luciferase activity was measured. The values shown represent the mean, minimum, and maximum luciferase activity normalized to cell number for five replicates.

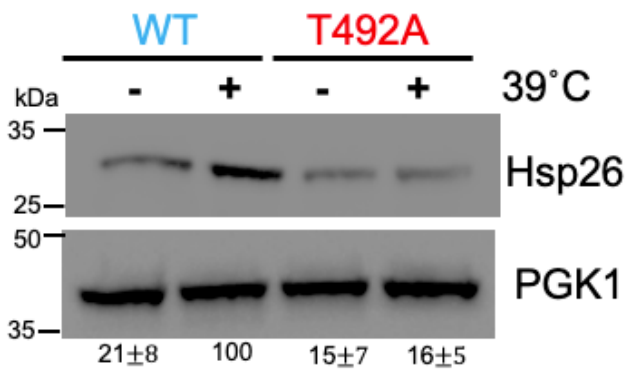

Figure 19. Ssa1 T492 mutant lacks Hsp26 inducibility Cured Ssa1-4Δ yeast cells expressing Flag-Ssa1 or Flag-T492A cells were grown in SD-LEU media at 25°C overnight. Cells were heat shocked at 39˚C for 30 minutes. Hsp26 native levels were checked using Western blot using Hsp26 antibody and Pgk1 as control

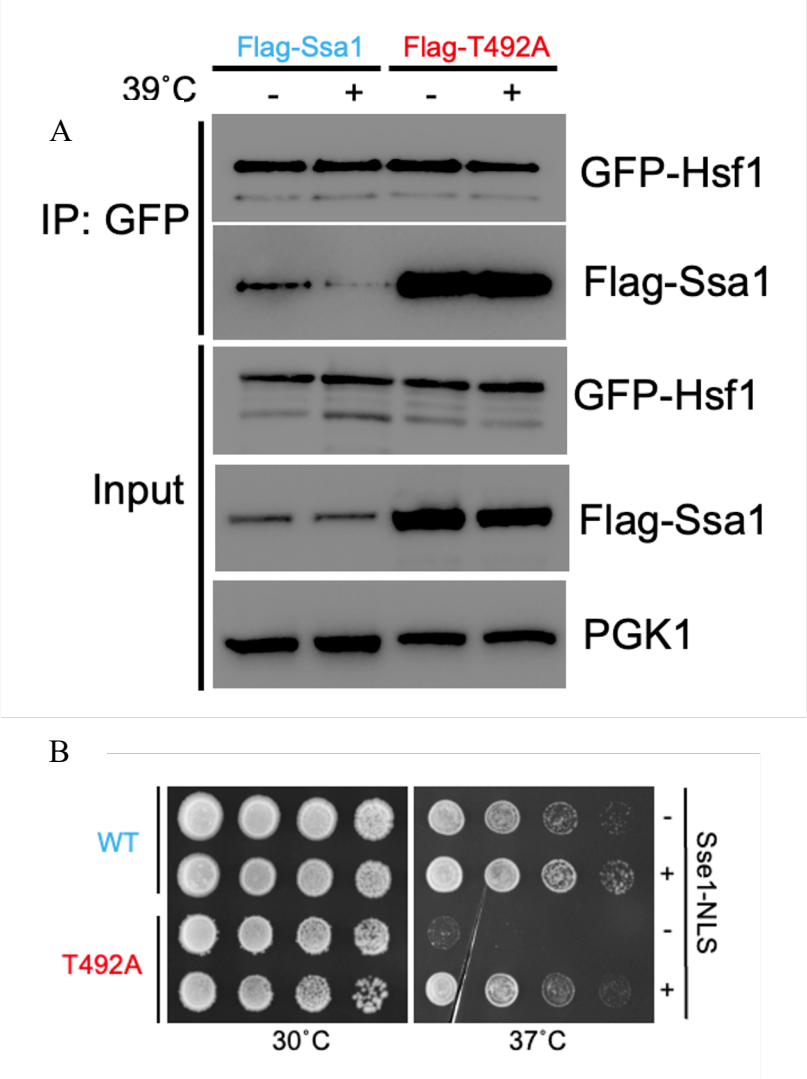

Figure 20. T492 phosphorylation mediates the Ssa1-Hsf1 interaction (A) Cured WT and mutant Ssa1 T492 cells were transformed with GFP-Hsf1 (N-AD 50-100 Hsf1-GFP-FLAG) plasmid. Hsf1 was purified from WT and mutant yeast in either untreated or heat-shocked conditions using GFP-Trap beads. Lysates and immunoprecipitated samples were analyzed by Western Blotting using GFP and FLAG Antibody **(B). Expression of Sse1-NLS suppresses the temperature-sensitive phenotype of mutant cells.** WT and T492A cells were transformed with control and Sse1-NLS plasmids. Cells were tenfold serially diluted, and spot assay was done onto indicated plates. Plates were incubated at 30 ˚C and 39 ˚C and imaged after 2 days

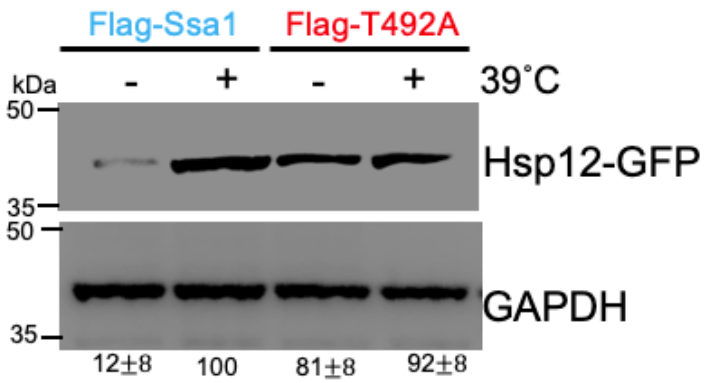

Figure 21. Ssa1 T492 mutant has an altered Msn2/4 regulation Hsp12 was genomically GFP tagged in Ssa1-4Δ background yeast cells. Epitope-tagged strains were further transformed with LEU-based plasmids for Flag-Ssa1 or Flag-T492A and then cured on FOA. Cells were grown in SD-LEU media at 25 ℃ overnight and grown to the mid-log phase. Cells were heat shocked at 39 ˚C for 30 minutes. WT cells were kept as control. Lysates were obtained, resolved on SDS-PAGE gels, and analyzed by immunoblotting using GFP antibody and Pgk1 for loading control

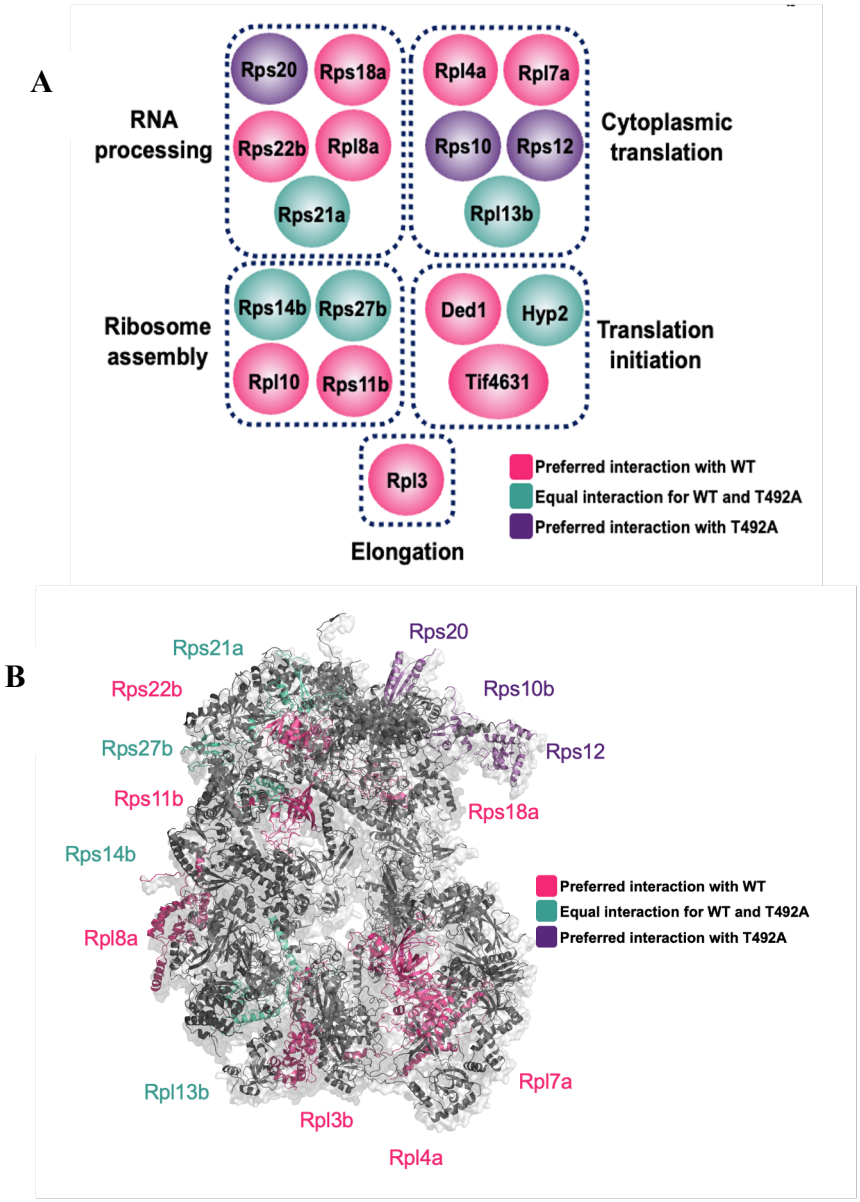

Figure 22. Ssa1 phosphorylation alters interactions with ribosomal proteins (A) From the interactome data, Ribosomal proteins and proteins involved in translation were identified to have altered interaction with Ssa1 under phosphorylation. These interactors were analyzed using the STRING database and grouped based on homology and function. Interactors in pink are those that have preferred interaction with WT, while those in purple are interactors that have preferred interaction with mutant, and green are those with equal interaction with both. **(B)** The yeast 80S ribosome PDB: 4V7R was mapped with protein interactors that showed an alteration in interaction upon Ssa1 T492 phosphorylation. Interactors in pink have preferred interaction with WT, while those in purple are interactors that have preferred interaction with mutants. Green are those with equal interaction with both.

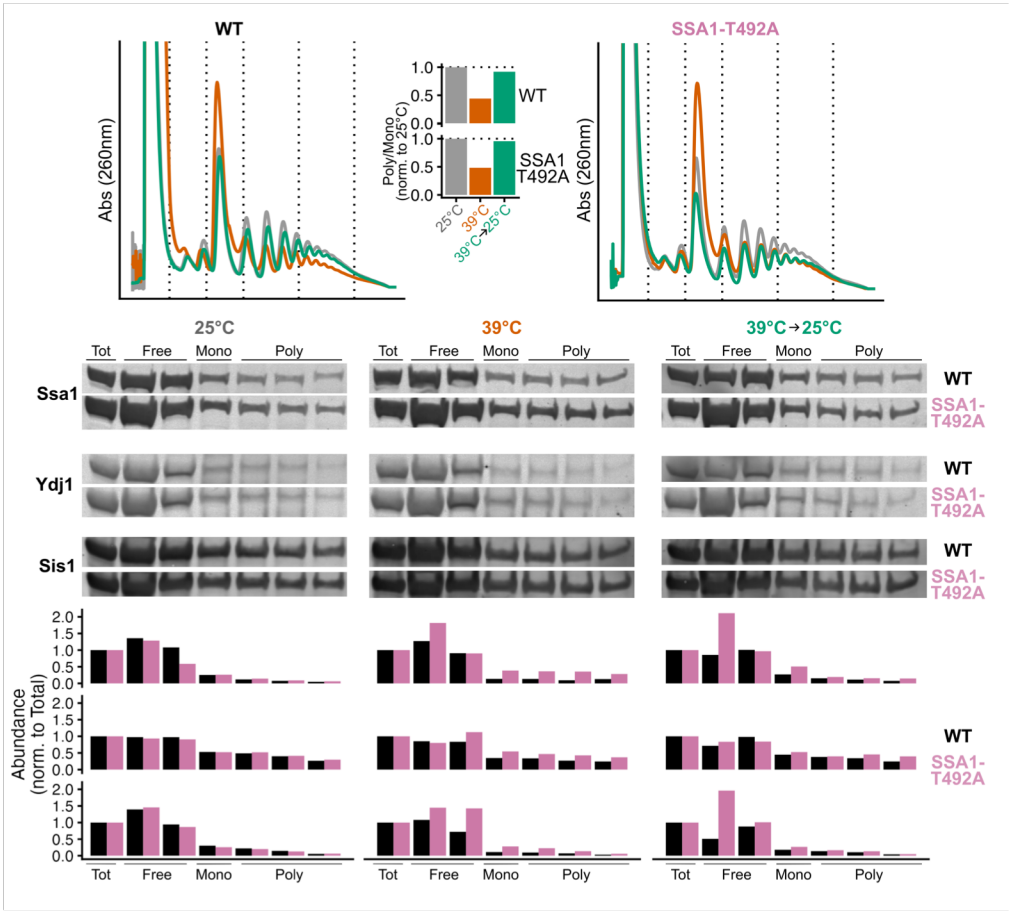

Figure 23. Polysome profiling Lysates from WT and mutant under unstressed, heat shock, and recovery were fractionated into polysomes. The graph is representative of the polysome UV trace taken at 260nm. The polysome-to-monosome ratio was plotted for both WT and mutants. The protein was precipitated, and western blots were run on all fractions to determine the amount of Ssa1, Ydj1, and Sis1 associated with the polysomes.

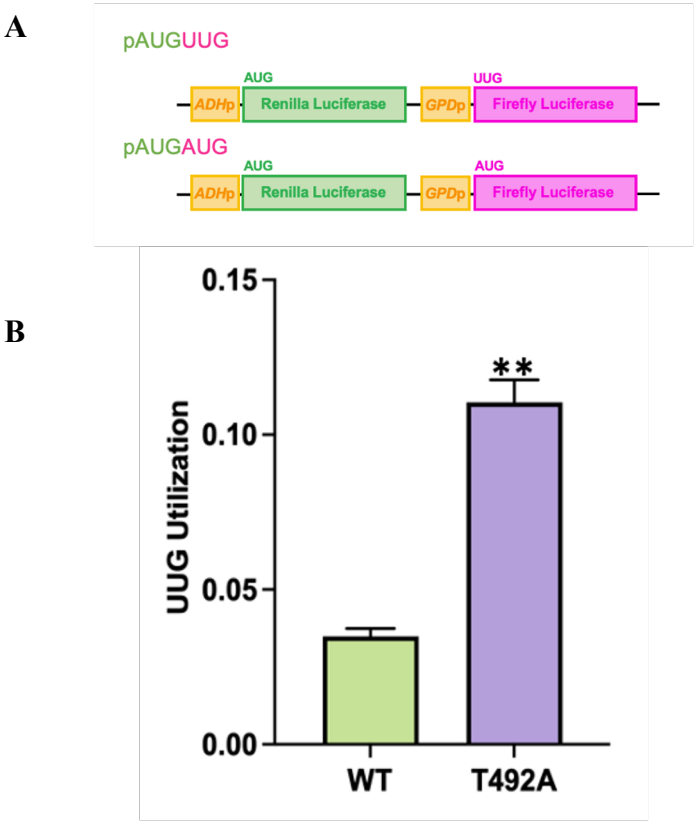

Figure 24. Hsp70 phosphorylation fine tunes translational fidelity(**A**) Schematic of the translational fidelity assay used. **(B)** WT and mutant cells (Ssa1-4Δ background yeast cells expressing Flag-Ssa1 or Flag-T492A) were transformed with pFJZ1052 (AUG) or pFJZ1054 (UUG). The fidelity of translation initiation was determined using the dual luciferase assay described in (156). The data shown for the assays are the mean and standard deviation of three biological replicates. Statistical significance was calculated via ANOVA. (*$p < 0.05$; **$p < 0.01$)

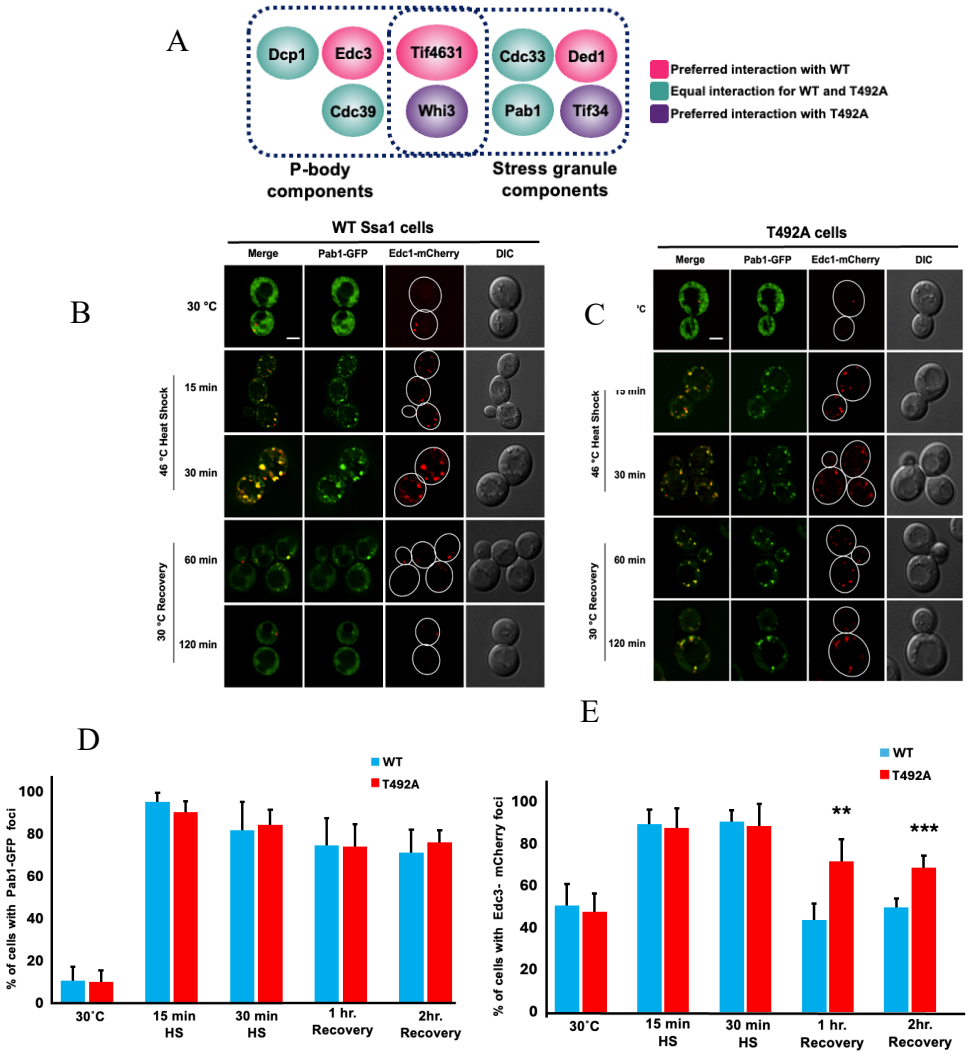

Figure 25. Ssa1 T492 phosphorylation is required for P-body disassembly (A) Interactors in pink are those that have preferred interaction with WT, while those in purple are interactors that have preferred interaction with mutant and green are those with equal interaction with both **(B) and (C)** Yeast cells from cultures grown to log phase (OD600 ≈ 0.5) were mounted in selective growth medium (C-URA) were imaged on a Delta Vision inverted microscope using a 100×1.4NA oil immersion lens. For heat shock experiments as described, cells were incubated in growth media at 39 °C for 15 minutes, 30 minutes, 1 hour, or 2 hours, then immediately mounted on slides for imaging**. (D) and (E)** Pab1 and Edc1 foci were analyzed in 100 cells for each time point. Statistical significance via ANOVA. (*$p < 0.05$; **$p< 0.01$) was calculated using mean and standard deviation for three replicates

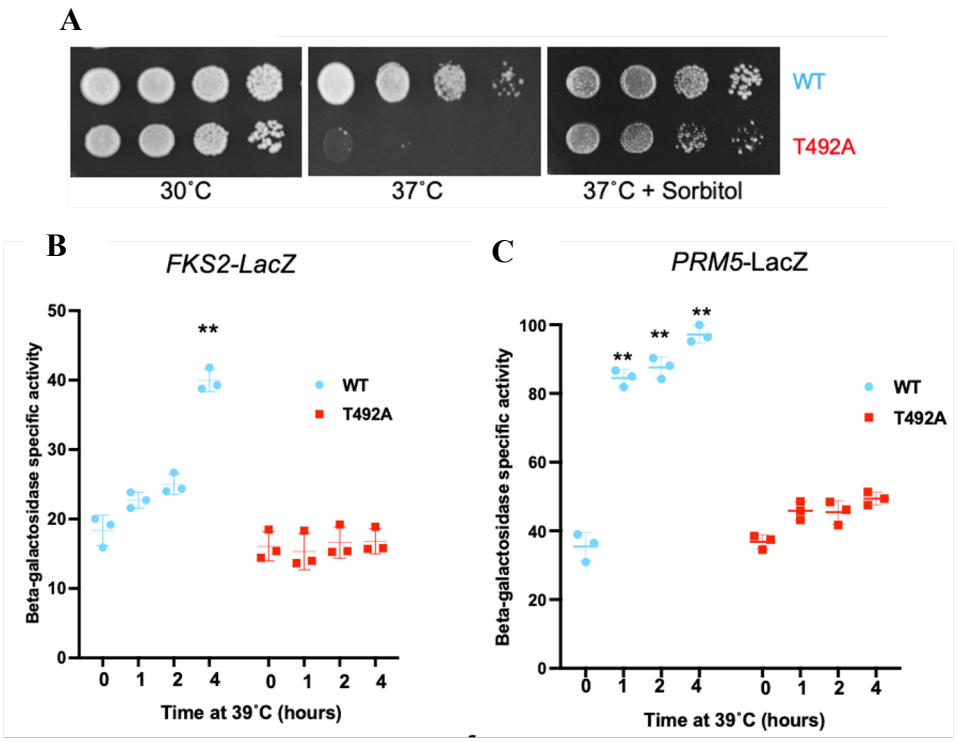

Figure 26. Heat-induced Ssa1 T492 phosphorylation promotes CWI amplification (A) Temperature sensitivity phenotype is suppressed with osmotic stabilization WT and T492A mutant cells were tenfold serially diluted, and spot assay was done onto indicated plates. Plates were incubated at 30 ℃ and 39 ℃ and imaged after 2 days **(B)** Ssa1-4Δ background yeast cells expressing Flag-Ssa1 or Flag-T492A were transformed with LacZ plasmids. Cells were grown in SD-URA media at 25℃ overnight and heat shocked at 39˚C for 30 minutes. Lysates were obtained, and LacZ assay was performed as described in (100). Statistical significance via ANOVA. (*p < 0.05; **p< 0.01) was calculated using mean and standard deviation for five replicates

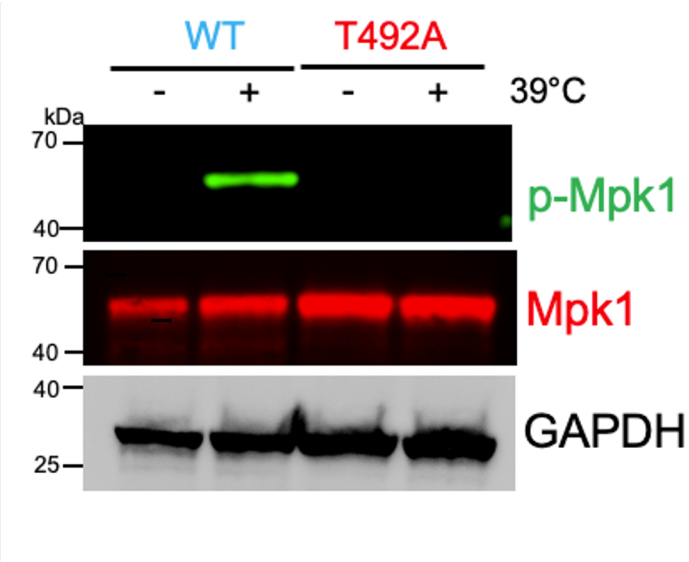

Figure 27. Mpk1 activation is dependent on Ssa1 T492 phosphorylation Ssa1-4Δ background yeast cells expressing Flag-Ssa1 or Flag-T492A were grown in SD-LEU media at 25 ˚C overnight and grown to mid-log phase. Cells were heat shocked at 39 ˚C for 30 minutes were obtained, resolved on SDS-PAGE gels, and analyzed by immunoblotting using dually phosphorylated (Thr190/Tyr192)-Slt2, commercial antibody raised against dually phosphorylated (Thr202/Tyr204)-p44/42 MAP kinase antibody and Mpk1 antibody for kinase stability and PGK1 for loading control.

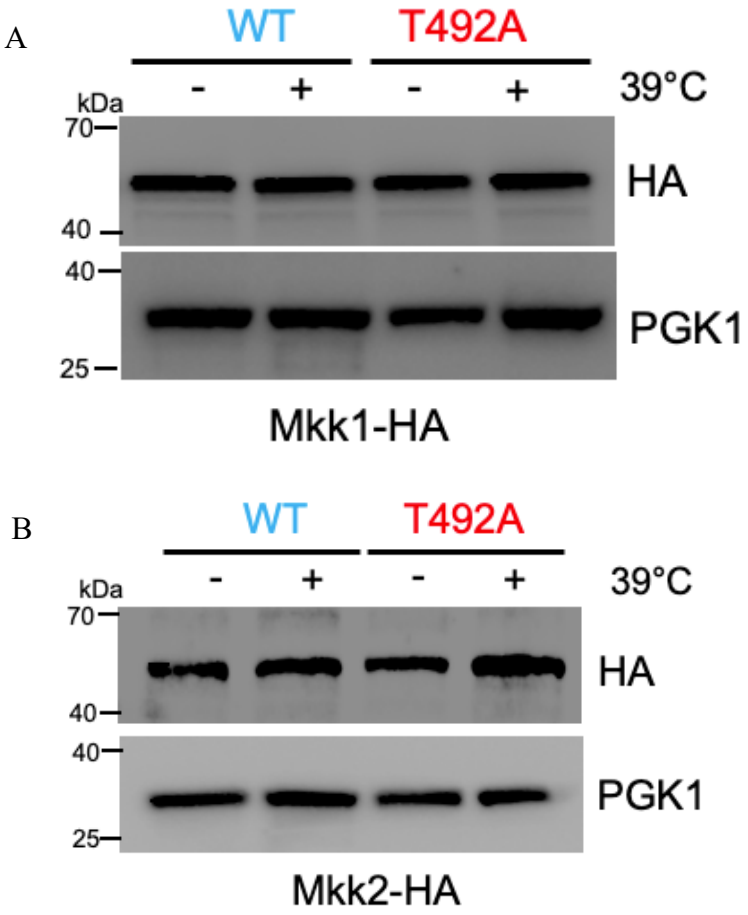

Figure 28. Levels of Mkk1 or Mkk2 remain unchanged in the mutant (A) Mkk1 was genomically HA tagged in Ssa1-4Δ background yeast cells. **(B)** Mkk2 was genomically HA tagged in Ssa1-4Δ background yeast. Epitope-tagged strains were further transformed with LEU-based plasmids for Flag-Ssa1 or Flag-T492A and then cured on FOA. Cells were grown in SD-LEU media at 25 ˚C overnight and grown to the mid-log phase. Cells were heat shocked at 39 ˚C for 30 minutes. Lysates were obtained, resolved on SDS-PAGE gels, and analyzed by immunoblotting using HA antibody and PGK1 for loading control.

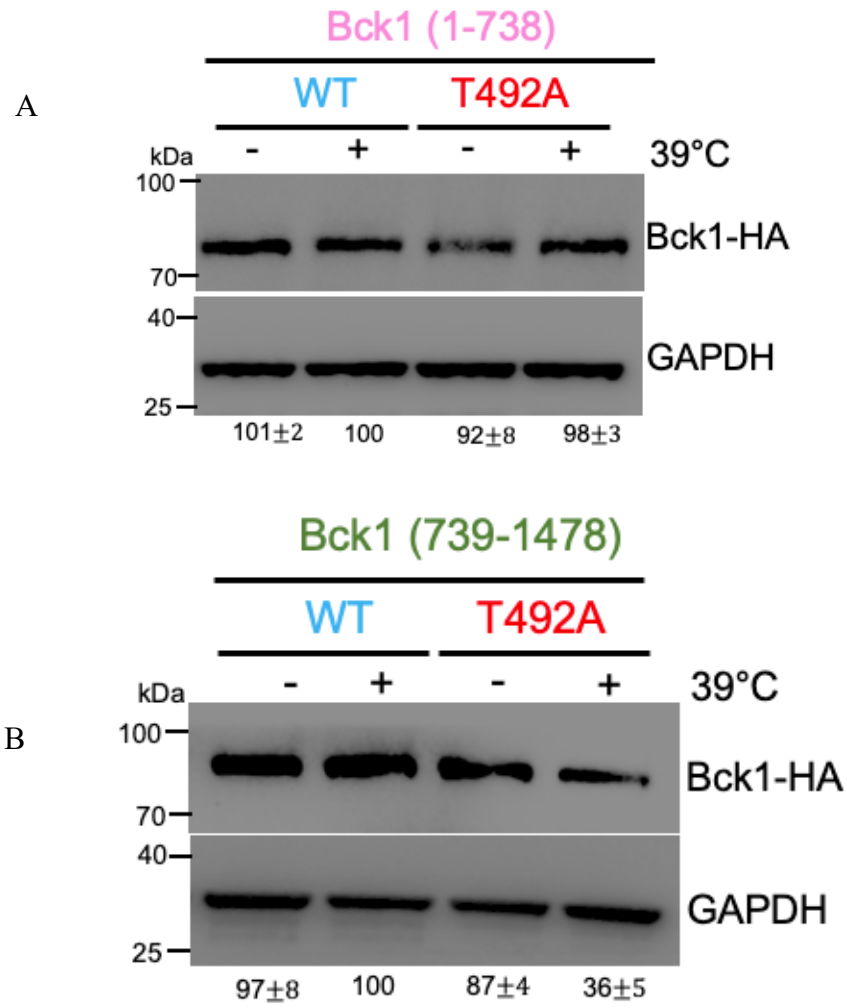

Figure 29. Levels of Bck1 are compromised in T492A mutant under heat shock. (A) Plasmid expressing Bck1 N-terminal Bck1 (residue 1-738) **(B)** Plasmid expressing C-terminal Bck1 (residue 739-1478) were transformed in WT and Ssa1 T492 mutant cells. Cells were grown in SD-HIS media at 25 ˚C overnight and grown to the mid-log phase. Cells were heat shocked at 39 ˚C for 30 minutes. Lysates were obtained, resolved on SDS-PAGE gels, and analyzed by immunoblotting using HA antibody and GAPDH for loading control.

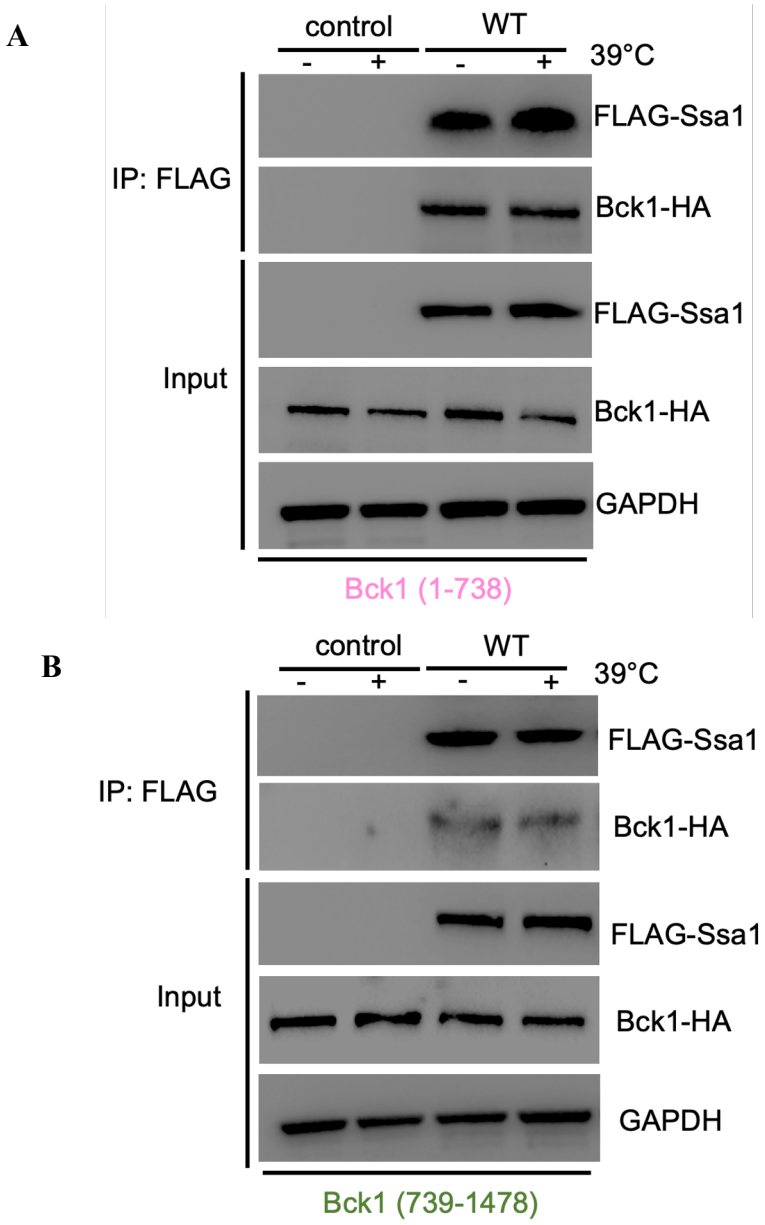

Figure 30. Bck1 is a novel interactor and bonafide client of yeast Hsp70 (A) Plasmid expressing the N- and (B) C--terminal domains of Bck1 (amino acids 1-738 and 739-1478) each with an HA tag were transformed in WT. Cells were grown in SD-HIS media overnight at 25 ˚C and then heat shocked at 39 ˚C for 30 minutes. Ssa1 was purified from WT in either untreated or heat-shocked conditions using FLAG-Dynabeads. Lysates and immunoprecipitated samples were analyzed by Western Blotting using HA and FLAG Antibody.

Table 1. **List of Plasmids**

Plasmid	Description	Reference/Source
pAT704	HSE-lucP+	49
pAT770	pMB743 (HA-PKC1)	95
pAT833	pGal1 HA-PKC R398A	95
pAT842	SKB4514, ADHIp-OsTIR1-9Myc	160
pAT843	SKB4510, IAA17-KanMX	160
pAT1102	pRS413-TEF-50- 100HGF	Peffer 2019
	pRP1657 Edc3-mCherry; Pab1-GFP (URA)	Buchan et al., 2008
	pRS313 (HIS3 centromeric plasmid)	Sikorski and Hieter, 1989
	pRS315 (LEU2 centromeric plasmid)	Sikorski and Hieter, 1989
	pRS316 (URA3 centromeric plasmid)	Sikorski and Hieter, 1989
	PRM5-LacZ	86
	FKS2-LacZ	86
	pFA6a-3HA-HIS3MX	Dr. Chi Lab
	pFA6a-GFP-HIS3MX	Dr. Chi Lab

Table 2. **Yeast strains used in the study**

Strain	**Genotype**	**Reference**
yAT143	MATa (MH272) ssa1Δ::trp1 ssa2::HisG ssa3::HisG ssa4::HisG (ssa1-4) [YCPlac33 SSA1]	-158
YAT525	MATa EG123 ura3-52 leu2-3,112 trp1-1 his4 can1r	Dr. David Levin lab
YAT526	MATa EG123 hsc77Δ (wsc1)::Leu2	Dr. David Levin lab
YAT527	MAT alpha mid2Δ: URA3	Dr. David Levin lab
YAT528	MAT alpha mid2Δ: URA3 hsc77Δ (wsc1): leu2	Dr. David Levin lab
YAT529	MAT alpha bck1Δ: URA3	Dr. David Levin lab
YAT530	MAT alpha pkc1Δ: LEU2	Dr. David Levin lab
YAT531	MAT alpha mkk1Δ:: LEU2 mkk2Δ ::URA3	Dr. David Levin lab
YAT532	MAT alpha mpk1Δ :: TRP1	Dr. David Levin lab
YAT533	MAT alpha pkc1Δ:: LEU2	Dr. David Levin lab
yAT143	MATa (MH272) ssa1Δ::trp1 ssa2::HisG ssa3::HisG ssa4::HisG (ssa1-4) [YCPlac33 SSA1]::HSP12-GFP-HIS3MX	This study
yAT143	MATa (MH272) ssa1Δ::trp1 ssa2::HisG ssa3::HisGssa4::HisG (ssa1-4) [YCPlac33 SSA1]::MKK1-3HA-HIS3MX	This study
yAT143	MATa (MH272) ssa1Δ::trp1 ssa2::HisG ssa3::HisGssa4::HisG (ssa1-4) [YCPlac33 SSA1]::MKK2-3HA-HIS3MX	This study

Table 3. **List of reagents used in the study**

Antibody	**Company**	**Source**
Anti-FLAG	Sigma (F3165-1MG)	This study
Anti-GFP	Thermo	
Anti-His	QIAGEN #34670	
Anti-HA	ThermoFisher (Cat#26183)	This study
Phospho-mpk1 p44/42	Cell-signaling #4695	This study
mpk1 antibody	Santacruz 133189	This study
pab1 antibody	EnCor	This study
Anti-HSP26	N/A	Dr. Johannes Buchner (36)
Anti-GAPDH	Invitrogen (MA5-15738)	This study
Anti-PGK	Invitrogen (459250)	This study
T492 phospho specific antibody	21st century biochemicals	This study
Ydj1	StressMarq	Cat# SMC166
Hsp82	StressMarq	Cat# SMC-135D
Ssa1	Enzo	Cat# BB79
Sis1		
Secondary Antibody-Mouse	GE (NA931V)	This study
Secondary Antibody-Rabbit	GE (NA934V)	This study

Anti-Flag M2 magnetic beads	Sigma	Cat# M8823
HA beads	Pierce	Cat# 88836
GFP beads	ChromeTek	Cat# GTMA-20
Luciferin	ApexBio	Cat# B6040
NuPAGE™ LDS sample buffer	Thermo Fisher Scientific	Cat# NP0007
M-PER	Thermo Fisher Scientific	Cat# 78501
NuPAGE™ 4 to 12% Bis-Tris, Mini Protein Gel	Thermo Fisher Scientific	Cat# NP0321BOX

Restore Western Blot Stripping Buffer	Thermo Fisher Scientific	Cat# 46430
Coomassie Protein Assay Kit	Thermo Fisher Scientific	Cat# 23236
Protease Inhibitor EDTA free	Thermo Fisher Scientific	Cat# A32961
Super Signal ECL	Thermo Fisher Scientific	Cat# 34577

Table 4: **Interactome data**

Gene Name	Accession	Log2(WT/T492A)	-log(p-value)
INP52	P50942	1.310	4.384
VMA2	P16140	-0.680	2.550
GCS1	P35197	-3.560	3.423
AKL1	P38080	0.980	3.337
RNQ1	P25367	0.760	3.323
YDJ1	P25491	-2.520	3.316
SGT2	Q12118	-1.630	3.127
PRB1	P09232	-0.920	3.093
RPP1B	P10622	-1.080	2.740
OSH2	Q12451	5.350	2.708
SSZ1	P38788	-2.200	2.671
TUP1	P16649	-1.000	2.611
VMA2	P16140	-0.680	2.550
DEF1	P35732	-0.410	2.509
RPD3	P32561	0.519	2.497
GGC1	P38988	1.719	2.493
END3	P39013	1.104	2.468
SSB2	P40150	-0.749	2.456
YPR010C-A	A5Z2X5	-3.154	2.441
GVP36	P40531	-1.946	2.423
CHC1	P22137	4.035	2.320
MTC1	P47018	-3.645	2.315
YER079W	P40052	2.115	2.308
LHS1	P36016	5.256	2.296
RPS12	P48589	-1.388	2.237
NBA1	Q08229	-0.880	2.230
MIG1	P27705	0.877	2.224
HSP26	P15992	-1.659	2.211
KIN2	P13186	2.583	2.192
PEA2	P40091	-0.627	2.174
SSE1	P32589	0.774	2.153
LEU2	P04173	-2.154	2.133
RPL4A	P10664	1.138	2.116
LST8	P41318	-0.941	2.110
CCT2	P39076	0.534	2.103
PSR1	Q07800	1.780	2.099

HIS4	P00815	-2.318	2.095
HSP10	P38910	-1.097	2.083
SSC1	P0CS90	-0.919	2.083
NAP1	P25293	-0.919	2.072
LDB19	Q12502	2.414	2.059
ILV6	P25605	-0.657	2.058
CDC39	P25655	0.846	2.055
PUP2	P32379	-2.958	2.004
PET10	P36139	1.886	1.977
SSE2	P32590	1.236	1.975
SDS24	P38314	0.899	1.930
PGI1	P12709	-1.005	1.922
DED1	P06634	2.847	1.917
CYC8	P14922	1.114	1.912
KAR2	P16474	-0.749	1.893
IGO1	P53897	0.973	1.863
RPS10B	P46784	-1.679	1.854
MNP1	P53163	-2.115	1.846
TPS3	P38426	2.298	1.845
RPL8B	P29453	2.902	1.845
SIS2	P36024	2.188	1.841
WHI3	P34761	-1.715	1.838
RVB2	Q12464	-1.388	1.826
SEC31	P38968	-0.999	1.815
NSP1	P14907	-1.671	1.814
NUP100	Q02629	1.547	1.803
HSP82	P02829	-2.366	1.798
ACS2	P52910	1.442	1.794
SVL3	Q03088	1.539	1.785
RVS167	P39743	3.002	1.780
CYC1	P00044	-0.871	1.766
PAN1	P32521	0.874	1.764
RPS18A	P0CX55	2.525	1.761
TY1B-JR2	P47100	3.858	1.752
HHF1	P02309	3.721	1.752
TIF34	P40217	-2.188	1.751
REX2	P54964	2.583	1.745
RPL10	P41805	1.185	1.740
SCW4	P53334	-2.788	1.732

RPT3	P33298	-1.345	1.725
CIR2	Q08822	-0.728	1.725
FES1	P38260	6.191	1.714
HYP2	P23301	-0.234	1.707
FET5	P43561	0.805	1.682
SRV2	P17555	2.163	1.676
RVB1	Q03940	-0.759	1.667
PAA1	Q12447	-3.170	1.665
SDH1	Q00711	-0.336	1.664
TSL1	P38427	1.543	1.661
DPM1	P14020	2.101	1.659
RPL3	P14126	2.009	1.648
EXG1	P23776	-0.947	1.636
MSN2	P33748	-0.734	1.632
RPP2A	P05319	-0.737	1.616
TSA1	P34760	-3.573	1.615
TIF4631	P39935	0.999	1.597
URA2	P07259	1.776	1.579
CDC33	P07260	-0.947	1.569
SIN3	P22579	0.944	1.563
YBR139W	P38109	-1.068	1.562
STI1	P15705	-2.537	1.560
RPS5	P26783	2.916	1.556
RPS11B	P0CX48	1.038	1.554
HSP60	P19882	-0.460	1.545
RPS20	P38701	-1.045	1.544
ENT1	Q12518	2.613	1.527
EDC3	P39998	5.770	1.513
OM45	P16547	-2.749	1.503
TOS1	P38288	-1.338	1.497
SAM1	P10659	0.925	1.494
THI20	Q08224	0.811	1.492
ATP2	P00830	-0.843	1.492
RPL7A	P05737	2.680	1.481
RPN13	O13563	-0.507	1.477
MLC1	P53141	-1.446	1.472
GGA1	Q06336	3.456	1.451
DMA1	P38823	0.558	1.431
ATP16	Q12165	-2.115	1.430

BIO2	P32451	1.074	1.427
YGP1	P38616	-1.352	1.425
COX13	P32799	-0.202	1.422
STB1	P42845	0.139	1.421
GPG1	P53130	-1.793	1.417
TUB1	P09733	0.168	1.415
YHM2	Q04013	2.329	1.410
RPS22B	Q3E7Y3	3.091	1.405
RPL13B	P40212	-0.752	1.380
SSB1	P11484	-0.516	1.371
YMR124W	P39523	-0.567	1.362
MSS4	P38994	0.657	1.362
SRP1	Q02821	1.647	1.350
NET1	P47035	-0.436	1.339
DCP1	Q12517	0.799	1.322
RPP0	P05317	2.272	1.317
RPS27B	P38711	-0.670	1.312
ACT1	P60010	2.503	1.305
ATP4	P05626	0.621	1.297
IVY1	Q04934	-0.759	1.281
PUF4	P25339	0.498	1.272
SEC16	P48415	0.576	1.261
PTC3	P34221	-1.834	1.261
RDL1	Q12305	-0.954	1.258
RAS2	P01120	0.802	1.252
FMP52	P40008	-3.054	1.250
RPS21A	P0C0V8	-0.591	1.246
DBP3	P20447	1.264	1.246
MDJ1	P35191	0.734	1.240
GRX2	P17695	0.639	1.238
BMH1	P29311	-0.777	1.236
KIC1	P38692	-0.679	1.229
PAB1	P04147	0.211	1.228
CBK1	P53894	1.025	1.202
RPC40	P07703	-0.594	1.198
RPL6B	P05739	1.847	1.192
DLD1	P32891	-2.257	1.192
CDC10	P25342	-0.392	1.180
SEH1	P53011	0.728	1.179

RIM15	P43565	0.691	1.176
KRE6	P32486	1.158	1.173
RPS14B	P39516	-0.313	1.159
SIS1	P25294	-0.752	1.150
FAA1	P30624	2.134	1.148
YMR099C	Q03161	1.005	1.134
CTT1	P06115	-1.925	1.133
SSA2	P10592	-0.032	1.122
PRS5	Q12265	-1.154	1.122
FBA1	P14540	-2.036	1.106
FAS2	P19097	2.531	1.097
UFD1	P53044	-0.407	1.094
SKO1	Q02100	-0.621	1.092
BUD6	P41697	1.391	1.077
YNL208W	P40159	-0.603	1.065
NOP1	P15646	1.388	1.064
RPN2	P32565	1.600	1.063
SIC1	P38634	0.469	1.057
KRE9	P39005	-0.802	1.054
CDC48	P25694	-0.799	1.047
RPA34	P47006	3.024	1.037
PRE6	P40303	2.371	1.032
ATP15	P21306	-2.059	1.004
RPP1A	P05318	-0.217	1.003
RPS21B	Q3E754	-0.460	0.996
MIC60	P36112	0.540	0.996
AHP1	P38013	-1.907	0.992
RPN11	P43588	-1.616	0.985
VMA7	P39111	-1.212	0.975
LAS17	Q12446	-0.136	0.974
TDH1	P00360	0.890	0.972
VMA6	P32366	-0.697	0.969
SRO9	P25567	1.453	0.963
ILV5	P06168	-3.419	0.959
CDC19	P00549	-0.398	0.947
PET9	P18239	-0.292	0.919
SUM1	P46676	0.537	0.906
RKR1	Q04781	-0.516	0.901
YHB1	P39676	-1.012	0.896

NSR1	P27476	-0.380	0.889
RPS0A	P32905	1.250	0.887
VMA1	P17255	0.226	0.872
BBC1	P47068	0.996	0.871
OLA1	P38219	2.014	0.869
PEP4	P07267	-0.579	0.865
YJL133C-A	Q3E7A3	-0.266	0.861
LYS20	P48570	1.760	0.851
GPM1	P00950	-1.045	0.839
RHO1	P06780	0.383	0.822
SUP45	P12385	0.725	0.820
TKL2	P33315	-1.178	0.813
NUP2	P32499	-0.266	0.812
YDR239C	Q03780	-2.293	0.807
RTN1	Q04947	0.531	0.805
PGK1	P00560	-2.298	0.791
SFL1	P20134	0.278	0.784
SRY1	P36007	-1.161	0.782
NGR1	P32831	0.903	0.777
ILV2	P07342	-0.298	0.776
EIS1	Q05050	-0.709	0.773
ATP7	P30902	-0.141	0.770
EFB1	P32471	-1.628	0.770
TPI1	P00942	-0.893	0.769
SEC13	Q04491	-0.799	0.765
DIG1	Q03063	-2.625	0.762
SPC19	Q03954	-0.466	0.762
RFS1	P38234	-0.345	0.760
ENO2	P00925	-2.698	0.756
TOM22	P49334	-0.759	0.752
TCB3	Q03640	0.342	0.748
SCJ1	P25303	-0.970	0.741
NCP1	P16603	3.553	0.740
RPL40B	P0CH09	0.220	0.735
SEC27	P41811	-1.054	0.712
AIM3	P38266	-0.243	0.705
SPT5	P27692	-1.002	0.699
ACF4	P47129	0.014	0.697
SDS23	P53172	1.498	0.697

ETT1	Q08421	-1.127	0.687
LEU1	P07264	1.154	0.681
PUP3	P25451	-0.348	0.672
CPS1	P27614	0.648	0.667
PEX14	P53112	-0.871	0.667
TDH3	P00359	-0.752	0.664
RPL32	P38061	-0.495	0.658
MIR1	P23641	0.691	0.645
GLT1	Q12680	-0.874	0.640
RIP1	P08067	-0.246	0.639
TEF1	P02994	0.703	0.637
CKS1	P20486	-0.098	0.631
MBF1	O14467	-0.272	0.628
DLD3	P39976	-1.502	0.624
ERG1	P32476	0.451	0.617
RPT5	P33297	-0.287	0.617
PFK2	P16862	-0.992	0.608
SFP1	P32432	-1.009	0.608
EGD1	Q02642	-0.615	0.607
RPL2B	P0CX46	0.252	0.607
YEF3	P16521	0.664	0.606
TEF4	P36008	1.755	0.606
COR1	P07256	3.016	0.598
RPS29A	P41057	-1.309	0.594
VMA10	P48836	-0.194	0.583
PTK2	P47116	-0.433	0.574
BFR1	P38934	0.246	0.572
MPM1	P40364	-0.546	0.571
YLR257W	Q06146	0.026	0.566
SNU13	P39990	-0.020	0.547
RXT2	P38255	0.899	0.546
RPL30	P14120	1.094	0.542
RPL19B	P0CX83	0.260	0.542
EFT1	P32324	-0.783	0.532
MCR1	P36060	1.498	0.531
RPS24A	P0CX31	-0.272	0.517
UME1	Q03010	-0.113	0.509
CCT8	P47079	-0.159	0.494
FPR1	P20081	-0.903	0.490

RPS23B	P0CX30	0.407	0.484
GPH1	P06738	-0.298	0.480
STM1	P39015	-0.469	0.475
RPS6B	P0CX38	0.223	0.466
RPP2B	P02400	0.931	0.461
ECM33	P38248	-0.197	0.458
SLA1	P32790	-0.223	0.450
LSP1	Q12230	0.383	0.444
RPL11B	Q3E757	0.979	0.443
TDH2	P00358	0.896	0.431
SUB2	Q07478	-1.058	0.416
SSA3	P09435	0.746	0.415
TKL1	P23254	-0.153	0.407
ARP2	P32381	-0.480	0.401
PMA1	P05030	2.163	0.401
WHI4	Q07655	-0.220	0.389
YEL043W	P32618	-0.121	0.389
RPL24A	P04449	0.322	0.371
GCN20	P43535	0.055	0.370
CYB5	P40312	-0.519	0.363
DCP2	P53550	0.035	0.361
TIF35	Q04067	-0.327	0.358
GLN1	P32288	0.298	0.355
RPL12A	P0CX53	0.295	0.352
RPL17A	P05740	0.226	0.351
PHB1	P40961	-0.063	0.351
SOK2	P53438	0.095	0.318
VMA8	P32610	-0.609	0.318
GSP2	P32836	0.197	0.317
RPT1	P33299	2.207	0.313
SSA1	P10591	-0.006	0.313
MDV1	P47025	-0.836	0.308
HSP104	P31539	0.480	0.303
AHA1	Q12449	0.439	0.299
RPS19A	P07280	0.078	0.296
TUB2	P02557	-0.052	0.291
ATP5	P09457	-0.322	0.290
PFK1	P16861	-0.139	0.289
TIF1	P10081	0.046	0.267

ASC1	P38011	0.023	0.262
SEC28	P40509	-0.046	0.251
ARG1	P22768	-1.064	0.249
PRE5	P40302	0.092	0.245
RPL26B	P53221	-0.501	0.242
RPS7B	P48164	-0.374	0.242
NUP145	P49687	-0.014	0.235
RPS15	Q01855	-0.339	0.234
ARO2	P28777	-0.089	0.231
NOP58	Q12499	0.061	0.231
QCR2	P07257	-0.348	0.230
JSN1	P47135	-0.407	0.229
TIM11	P81449	0.003	0.228
TOM40	P23644	0.363	0.225
RPS16B	P0CX52	0.510	0.221
CPR6	P53691	0.072	0.219
CST6	P40535	-0.089	0.208
HBT1	Q07653	0.029	0.207
MRC1	P25588	0.246	0.206
YPL247C	Q12523	-0.486	0.198
NUP60	P39705	0.020	0.184
IMD3	P50095	0.410	0.182
ILV1	P00927	1.158	0.179
RPT4	P53549	0.654	0.167
EDE1	P34216	0.104	0.163
LRE1	P25579	0.139	0.160
HSF1	P10961	-0.075	0.158
ADH1	P00330	0.374	0.149
EMP24	P32803	0.176	0.145
SWA2	Q06677	0.012	0.144
RNR4	P49723	0.573	0.143
UME6	P39001	0.136	0.141
LSM5	P40089	0.231	0.138
SMY2	P32909	0.287	0.131
MDY2	Q12285	-0.087	0.130
ATP3	P38077	-0.357	0.120
PRP5	P21372	-0.043	0.113
RPL27A	P0C2H6	-0.389	0.108
GLE2	P40066	0.162	0.104

HSP42	Q12329	-0.012	0.102
ENO1	P00924	1.104	0.099
RET3	P53600	-0.020	0.096
BTN2	P53286	-0.170	0.085
RPL28	P02406	-0.243	0.075
NUP116	Q02630	-0.003	0.075
SDH2	P21801	0.038	0.074
RPL34B	P40525	0.928	0.066
RPS7A	P26786	-0.197	0.066
TOM70	P07213	0.043	0.066
POR1	P04840	0.165	0.060
RPL15A	P05748	-0.325	0.053
NPA3	P47122	0.392	0.047
ERG6	P25087	0.667	0.046
RVS161	P25343	-0.492	0.042
TIF3	P34167	0.223	0.037
RSP5	P39940	-0.046	0.036
TIM44	Q01852	-0.098	0.033
CYC7	P00045	0.330	0.032
ATP1	P07251	0.156	0.031
FKH2	P41813	-0.009	0.029
HAA1	Q12753	-0.115	0.023
HSC82	P15108	0.139	0.020
RCN2	Q12044	-0.069	0.016
SSA4	P22202	0.035	0.016
RPL23A	P0CX41	-0.246	0.014
RPS8B	P0CX40	-0.915	0.009
PDC1	P06169	-0.226	0.009
PST2	Q12335	0.342	0.005
CPR1	P14832	0.436	0.003
VHS2	P40463	-0.098	0.002
PIL1	P53252	0.199	0.001

REFERENCES

1. Nitika, Porter CM, Truman AW, Truttmann MC. Post-translational modifications of Hsp70 family proteins: Expanding the chaperone code. *J Biol Chem*. 2020;295(31):10689-10708.
2. Mayer MP, Bukau B. Hsp70 chaperones: cellular functions and molecular mechanism. *Cell Mol Life Sci*. 2005;62(6):670-684.
3. Rosenzweig R, Nillegoda NB, Mayer MP, Bukau B. The Hsp70 chaperone network. *Nat Rev Mol Cell Biol*. 2019;20(11):665-680.
4. Kampinga HH, Craig EA. The HSP70 chaperone machinery: J proteins as drivers of functional specificity [published correction appears in Nat Rev Mol Cell Biol. 2010 Oct;11(10):750]. *Nat Rev Mol Cell Biol*. 2010;11(8):579-592.
5. Borchiellini C, Boury-Esnault N, Vacelet J, Le Parco Y. Phylogenetic analysis of the Hsp70 sequences reveals the monophyly of Metazoa and specific phylogenetic relationships between animals and fungi. *Mol Biol Evol*. 1998;15(6):647-655.
6. Gupta RS, Singh B. Phylogenetic analysis of 70 kD heat shock protein sequences suggest a chimeric origin for the eukaryotic cell nucleus. *Curr Biol*. 1994;4(12):1104-1114.
7. Wu B, Hunt C, Morimoto R. Structure, and expression of the human gene encoding major heat shock protein HSP70. *Mol Cell Biol*. 1985;5(2):330-341.
8. Zuiderweg ER, Hightower LE, Gestwicki JE. The remarkable multivalency of the Hsp70 chaperones. *Cell Stress Chaperones*. 2017;22(2):173-189.
9. Flaherty KM, DeLuca-Flaherty C, McKay DB. Three-dimensional structure of the ATPase fragment of a 70K heat-shock cognate protein. *Nature*. 1990;346(6285):623-628.
10. Freeman BC, Myers MP, Schumacher R, Morimoto RI. Identification of a regulatory motif in Hsp70 that affects ATPase activity, substrate binding and interaction with HDJ-1. *EMBO J*. 1995;14(10):2281-2292.
11. Kityk R, Vogel M, Schlecht R, Bukau B, Mayer MP. Pathways of allosteric regulation in Hsp70 chaperones. *Nat Commun*. 2015; 6:8308. Published 2015 Sep 18.
12. Vogel M, Mayer MP, Bukau B. Allosteric regulation of Hsp70 chaperones involves a conserved interdomain linker. *J Biol Chem*. 2006;281(50):38705-38711.
13. Zhuravleva A, Gierasch LM. Allosteric signal transmission in the nucleotide-binding domain of 70-kDa heat shock protein (Hsp70) molecular chaperones. *Proc Natl Acad Sci U S A*. 2011;108(17):6987-6992.
14. Verghese J, Abrams J, Wang Y, Morano KA. Biology of the heat shock response and protein chaperones: budding yeast (Saccharomyces cerevisiae) as a model system. *Microbiol Mol Biol Rev*. 2012;76(2):115-158.
15. Boorstein WR, Ziegelhoffer T, Craig EA. Molecular evolution of the HSP70 multigene family. *J Mol Evol*. 1994;38(1):1-17.

16. Kabani M, Martineau CN. Multiple hsp70 isoforms in the eukaryotic cytosol: mere redundancy or functional specificity? *Curr Genomics*. 2008;9(5):338-248.
17. Lotz SK, Knighton LE, Nitika, Jones GW, Truman AW. Not quite the SSAme: unique roles for the yeast cytosolic Hsp70s. *Curr Genet*. 2019;65(5):1127-1134.
18. Newcomb LL, Diderich JA, Slattery MG, Heideman W. Glucose regulation of Saccharomyces cerevisiae cell cycle genes. *Eukaryot Cell*. 2003;2(1):143-149.
19. Sharma D, Masison DC. Functionally redundant isoforms of a yeast Hsp70 chaperone subfamily have different antiprion effects. *Genetics*. 2008;179(3):1301-1311.
20. Qi R, Sarbeng EB, Liu Q, et al. Allosteric opening of the polypeptide-binding site when an Hsp70 binds ATP. *Nat Struct Mol Biol*. 2013;20(7):900-907.
21. Bhattacharya A, Kurochkin AV, Yip GN, Zhang Y, Bertelsen EB, Zuiderweg ER. Allostery in Hsp70 chaperones is transduced by subdomain rotations. *J Mol Biol*. 2009;388(3):475-490.
22. Cheetham ME, Caplan AJ. Structure, function and evolution of DnaJ: conservation and adaptation of chaperone function. *Cell Stress Chaperones*. 1998;3(1):28-36.
23. Greene MK, Maskos K, Landry SJ. Role of the J-domain in the cooperation of Hsp40 with Hsp70. *Proc Natl Acad Sci U S A*. 1998;95(11):6108-6113.
24. Kelley WL. Molecular chaperones: How J domains turn on Hsp70s. *Curr Biol*. 1999;9(8):R305-R308.
25. Sahi C, Craig EA. Network of general and specialty J protein chaperones of the yeast cytosol. *Proc Natl Acad Sci U S A*. 2007;104(17):7163-7168.
26. Harrison CJ. La cage aux fold: asymmetry in the crystal structure of GroEL-GroES-(ADP)7. *Structure*. 1997;5(10):1261-1264.
27. Alderson TR, Kim JH, Markley JL. Dynamical Structures of Hsp70 and Hsp70-Hsp40 Complexes. *Structure*. 2016;24(7):1014-1030.
28. Mukai H, Kuno T, Tanaka H, Hirata D, Miyakawa T, Tanaka C. Isolation, and characterization of SSE1 and SSE2, new members of the yeast HSP70 multigene family. *Gene*. 1993;132(1):57-66.
29. Beltrao P, Albanèse V, Kenner LR, et al. Systematic functional prioritization of protein posttranslational modifications. *Cell*. 2012;150(2):413-425.
30. Mann M, Jensen ON. Proteomic analysis of post-translational modifications. *Nat Biotechnol*. 2003;21(3):255-261.
31. Blom N, Sicheritz-Pontén T, Gupta R, Gammeltoft S, Brunak S. Prediction of post-translational glycosylation and phosphorylation of proteins from the amino acid sequence. *Proteomics*. 2004;4(6):1633-1649.
32. Cloutier P, Coulombe B. Regulation of molecular chaperones through post-translational modifications: decrypting the chaperone code. *Biochim Biophys Acta*. 2013;1829(5):443-454.
33. Hernando R, Manso R. Muscle fibre stress in response to exercise: synthesis, accumulation and isoform transitions of 70-kDa heat-shock proteins. *Eur J Biochem*.

1997;243(1-2):460-467.González B, Manso R. Induction, modification and accumulation of HSP70s in the rat liver after acute exercise: early and late responses. *J Physiol*. 2004;556(Pt 2):369-385.

34. Velasco L, Dublang L, Moro F, Muga A. The Complex Phosphorylation Patterns that Regulate the Activity of Hsp70 and Its Cochaperones. *Int J Mol Sci*. 2019;20(17):4122. Published 2019 Aug 23.
35. Griffith AA, Holmes W. Fine Tuning: Effects of Post-Translational Modification on Hsp70 Chaperones. *Int J Mol Sci*. 2019;20(17):4207. Published 2019 Aug 28
36. Truman AW, Kristjansdottir K, Wolfgeher D, et al. CDK-dependent Hsp70 Phosphorylation controls G1 cyclin abundance and cell-cycle progression. *Cell*. 2012;151(6):1308-1318.
37. Muller P, Ruckova E, Halada P, et al. C-terminal phosphorylation of Hsp70 and Hsp90 regulates alternate binding to co-chaperones CHIP and HOP to determine cellular protein folding/degradation balances. *Oncogene*. 2013;32(25):3101-3110.
38. Backe SJ, Sager RA, Woodford MR, Makedon AM, Mollapour M. Post-translational modifications of Hsp90 and translating the chaperone code. *J Biol Chem*. 2020;295(32):11099-11117.
39. Hornbeck PV, Zhang B, Murray B, Kornhauser JM, Latham V, Skrzypek E. PhosphoSitePlus, 2014: mutations, PTMs and recalibrations. *Nucleic Acids Res*. 2015;43(Database issue):D512-D520.
40. Craig R, Cortens JP, Beavis RC. The use of proteotypic peptide libraries for protein identification. *Rapid Commun Mass Spectrom*. 2005;19(13):1844-1850.
41. Pawson T, Scott JD. Protein phosphorylation in signaling--50 years and counting. *Trends Biochem Sci*. 2005;30(6):286-290.
42. Eckerdt F, Strebhardt K. Polo-like kinase 1: target and regulator of anaphase-promoting complex/cyclosome-dependent proteolysis. *Cancer Res*. 2006;66(14):6895-6898.
43. O'Regan L, Sampson J, Richards MW, et al. Hsp72 is targeted to the mitotic spindle by Nek6 to promote K-fiber assembly and mitotic progression. *J Cell Biol*. 2015;209(3):349-358.
44. Ballinger CA, Connell P, Wu Y, et al. Identification of CHIP, a novel tetratricopeptide repeat-containing protein that interacts with heat shock proteins and negatively regulates chaperone functions. *Mol Cell Biol*. 1999;19(6):4535-4545.
45. Connell P, Ballinger CA, Jiang J, et al. The co-chaperone CHIP regulates protein triage decisions mediated by heat-shock proteins. *Nat Cell Biol*. 2001;3(1):93-96.
46. Moss SM, Taylor IR, Ruggero D, Gestwicki JE, Shokat KM, Mukherjee S. A Legionella pneumophila Kinase Phosphorylates the Hsp70 Chaperone Family to Inhibit Eukaryotic Protein Synthesis. *Cell Host Microbe*. 2019;25(3):454-462.e6.
47. Weissman Z, Pinsky M, Wolfgeher DJ, Kron SJ, Truman AW, Kornitzer D. Genetic analysis of Hsp70 phosphorylation sites reveals a role in Candida albicans cell and

colony morphogenesis. *Biochim Biophys Acta Proteins Proteom*. 2020;1868(3):140135.
48. Alonso-Morales A, González-López L, Cázares-Raga FE, et al. Protein phosphorylation during Plasmodium berghei gametogenesis. *Exp Parasitol*. 2015;156:49-60
49. Peffer S, Gonçalves D, Morano KA. Regulation of the Hsf1-dependent transcriptome via conserved bipartite contacts with Hsp70 promotes survival in yeast. *J Biol Chem*. 2019;294(32):12191-12202
50. Sorger PK, Pelham HR. Purification and characterization of a heat-shock element binding protein from yeast. *EMBO J*. 1987;6(10):3035-3041
51. Wiederrecht G, Seto D, Parker CS. Isolation of the gene encoding the S. cerevisiae heat shock transcription factor. *Cell*. 1988;54(6):841-853.
52. Torres FA, Bonner JJ. Genetic identification of the site of DNA contact in the yeast heat shock transcription factor. *Mol Cell Biol*. 1995;15(9):5063-5070.
53. Yamamoto A, Ueda J, Yamamoto N, Hashikawa N, Sakurai H. Role of heat shock transcription factor in Saccharomyces cerevisiae oxidative stress response. *Eukaryot Cell*. 2007;6(8):1373-1379.
54. Sakurai H, Takemori Y. Interaction between heat shock transcription factors (HSFs) and divergent binding sequences: binding specificities of yeast HSFs and human HSF1. *J Biol Chem*. 2007;282(18):13334-13341.
55. Craig EA, Gross CA. Is hsp70 the cellular thermometer? *Trends Biochem Sci*. 1991;16(4):135-140.
56. Shi Y, Mosser DD, Morimoto RI. Molecular chaperones as HSF1-specific transcriptional repressors. *Genes Dev*. 1998;12(5):654-666.
57. Morimoto RI. The heat shock response: systems biology of proteotoxic stress in aging and disease. *Cold Spring Harb Symp Quant Biol*. 2011; 76:91-99.
58. Zheng X, Krakowiak J, Patel N, et al. Dynamic control of Hsf1 during heat shock by a chaperone switch and phosphorylation. *Elife*. 2016;5: e18638. Published 2016 Nov 10.
59. Krakowiak J, Zheng X, Patel N, et al. Hsf1 and Hsp70 constitute a two-component feedback loop that regulates the yeast heat shock response. *Elife*. 2018;7:e31668. Published 2018 Feb 2.
60. Cherkasov V, Hofmann S, Druffel-Augustin S, et al. Coordination of translational control and protein homeostasis during severe heat stress. *Curr Biol*. Solís EJ, Pandey JP, Zheng X, et al.
61. Solís EJ, Pandey JP, Zheng X, et al. Defining the Essential Function of Yeast Hsf1 Reveals a Compact Transcriptional Program for Maintaining Eukaryotic Proteostasis [published correction appears in Mol Cell. 2018 Feb 1;69(3):534. doi: 10.1016/j.molcel.2018.01.021]. *Mol Cell*. 2016;63(1):60-71.
62. Jakobsen BK, Pelham HR. Constitutive binding of yeast heat shock factor to DNA in vivo. *Mol Cell Biol*. 1988;8(11):5040-5042.

63. Vabulas RM, Raychaudhuri S, Hayer-Hartl M, Hartl FU. Protein folding in the cytoplasm and the heat shock response. *Cold Spring Harb Perspect Biol*. 2010;2(12):a004390.
64. Rüdiger S, Buchberger A, Bukau B. Interaction of Hsp70 chaperones with substrates. *Nat Struct Biol*. 1997;4(5):342-349.
65. Masser AE, Kang W, Roy J, et al. Cytoplasmic protein misfolding titrates Hsp70 to activate nuclear Hsf1. *Elife*. 2019;8:e47791. Published 2019 Sep 25.
66. Sorger PK, Pelham HR. Yeast heat shock factor is an essential DNA-binding protein that exhibits temperature-dependent phosphorylation. *Cell*. 1988;54(6):855-864.
67. Masser AE, Ciccarelli M, Andréasson C. Hsf1 on a leash - controlling the heat shock response by chaperone titration. *Exp Cell Res*. 2020;396(1):112246.
68. Morano KA, Grant CM, Moye-Rowley WS. The response to heat shock and oxidative stress in Saccharomyces cerevisiae. *Genetics*. 2012;190(4):1157-1195.
69. Garde R, Singh A, Ali A, Pincus D. Transcriptional regulation of Sis1 promotes fitness but not feedback in the heat shock response. *Elife*. 2023;12:e79444. Published 2023 May 9.
70. Feder ZA, Ali A, Singh A, et al. Subcellular localization of the J-protein Sis1 regulates the heat shock response. *J Cell Biol*. 2021;220(1):e202005165.
71. Budzyński MA, Puustinen MC, Joutsen J, Sistonen L. Uncoupling Stress-Inducible Phosphorylation of Heat Shock Factor 1 from Its Activation. *Mol Cell Biol*. 2015;35(14):2530-2540.
72. Triandafillou CG, Drummond DA. Heat Shock Factor 1: From Fire Chief to Crowd-Control Specialist. *Mol Cell*. 2016;63(1):1-2.
73. Ali A, Garde R, Schaffer OC, et al. Adaptive preservation of orphan ribosomal proteins in chaperone-dispersed condensates. *Nat Cell Biol*. 2023;25(11):1691-1703.
74. Dea A, Pincus D. The Heat Shock Response as a Condensate Cascade. *J Mol Biol*. 2024;436(14):168642.
75. Martínez-Pastor MT, Marchler G, Schüller C, Marchler-Bauer A, Ruis H, Estruch F. The Saccharomyces cerevisiae zinc finger proteins Msn2p and Msn4p are required for transcriptional induction through the stress response element (STRE). *EMBO J*. 1996;15(9):2227-2235.
76. Schmitt AP, McEntee K. Msn2p, a zinc finger DNA-binding protein, is the transcriptional activator of the multistress response in Saccharomyces cerevisiae. *Proc Natl Acad Sci U S A*. 1996;93(12):5777-5782.
77. Gasch AP, Spellman PT, Kao CM, et al. Genomic expression programs in the response of yeast cells to environmental changes. *Mol Biol Cell*. 2000;11(12):4241-4257.
78. Sadeh A, Movshovich N, Volokh M, Gheber L, Aharoni A. Fine-tuning of the Msn2/4-mediated yeast stress responses as revealed by systematic deletion of Msn2/4 partners. *Mol Biol Cell*. 2011;22(17):3127-3138.
79. Treger JM, Schmitt AP, Simon JR, McEntee K. Transcriptional factor mutations reveal regulatory complexities of heat shock and newly identified stress genes in Saccharomyces cerevisiae. *J Biol Chem*. 1998;273(41):26875-26879.
80. Eastmond DL, Nelson HC. Genome-wide analysis reveals new roles for the activation domains of the Saccharomyces cerevisiae heat shock transcription factor (Hsf1) during the transient heat shock response. *J Biol Chem*. 2006;281(43):32909-32921

81. Ruis H, Schüller C. Stress signaling in yeast. *Bioessays*. 1995;17(11):959-965.
82. Ciccarelli M, Masser AE, Kaimal JM, Planells J, Andréasson C. Genetic inactivation of essential *HSF1* reveals an isolated transcriptional stress response selectively induced by protein misfolding. *Mol Biol Cell*. 2023;34(10):ar101.
83. Levin DE. Regulation of cell wall biogenesis in Saccharomyces cerevisiae: the cell wall integrity signaling pathway. *Genetics*. 2011;189(4):1145-1175
84. Cid VJ, Durán A, del Rey F, Snyder MP, Nombela C, Sánchez M. Molecular basis of cell integrity and morphogenesis in Saccharomyces cerevisiae. *Microbiol Rev*. 1995;59(3):345-386.
85. Klis FM, Boorsma A, De Groot PW. Cell wall construction in Saccharomyces cerevisiae. *Yeast*. 2006;23(3):185-202.
86. Kim KY, Truman AW, Levin DE. Yeast Mpk1 mitogen-activated protein kinase activates transcription through Swi4/Swi6 by a noncatalytic mechanism that requires upstream signal. *Mol Cell Biol*. 2008;28(8):2579-2589.
87. Osumi M. The ultrastructure of yeast: cell wall structure and formation. *Micron*. 1998;29(2-3):207-233.
88. Levin DE. Cell wall integrity signaling in Saccharomyces cerevisiae. *Microbiol Mol Biol Rev*. 2005;69(2):262-291.
89. Dong Y, Pruyne D, Bretscher A. Formin-dependent actin assembly is regulated by distinct modes of Rho signaling in yeast. *J Cell Biol*. 2003;161(6):1081-1092.
90. Perez P, Rincón SA. Rho GTPases: regulation of cell polarity and growth in yeasts. *Biochem J*. 2010;426(3):243-253. Published 2010 Feb 24.
91. Ketela T, Green R, Bussey H. Saccharomyces cerevisiae mid2p is a potential cell wall stress sensor and upstream activator of the PKC1-MPK1 cell integrity pathway. *J Bacteriol*. 1999;181(11):3330-3340.
92. Verna J, Lodder A, Lee K, Vagts A, Ballester R. A family of genes required for maintenance of cell wall integrity and for the stress response in Saccharomyces cerevisiae. *Proc Natl Acad Sci U S A*. 1997;94(25):13804-13809.
93. Huang CY, Ferrell JE Jr. Ultrasensitivity in the mitogen-activated protein kinase cascade. *Proc Natl Acad Sci U S A*. 1996;93(19):10078-10083.
94. Levin DE, Fields FO, Kunisawa R, Bishop JM, Thorner J. A candidate protein kinase C gene, PKC1, is required for the S. cerevisiae cell cycle. *Cell*. 1990;62(2):213-224
95. Watanabe M, Chen CY, Levin DE. Saccharomyces cerevisiae PKC1 encodes a protein kinase C (PKC) homolog with a substrate specificity similar to that of mammalian PKC. *J Biol Chem*. 1994;269(24):16829-16836.
96. Lee KS, Levin DE. Dominant mutations in a gene encoding a putative protein kinase (BCK1) bypass the requirement for a Saccharomyces cerevisiae protein kinase C homolog. *Mol Cell Biol*. 1992;12(1):172-182.
97. Irie K, Takase M, Lee KS, et al. MKK1 and MKK2, which encode Saccharomyces cerevisiae mitogen-activated protein kinase-kinase homologs, function in the pathway mediated by protein kinase C. *Mol Cell Biol*. 1993;13(5):3076-3083.
98. Lee KS, Irie K, Gotoh Y, et al. A yeast mitogen-activated protein kinase homolog (Mpk1p) mediates signalling by protein kinase C. *Mol Cell Biol*. 1993;13(5):3067-3075.
99. Truman AW, Millson SH, Nuttall JM, et al. Expressed in the yeast Saccharomyces cerevisiae, human ERK5 is a client of the Hsp90 chaperone that complements loss of

the Slt2p (Mpk1p) cell integrity stress-activated protein kinase. *Eukaryot Cell*. 2006;5(11):1914-1924.

100. Martín H, Rodríguez-Pachón JM, Ruiz C, Nombela C, Molina M. Regulatory mechanisms for modulation of signaling through the cell integrity Slt2-mediated pathway in Saccharomyces cerevisiae. *J Biol Chem*. 2000;275(2):1511-1519.
101. Kim KY, Truman AW, Levin DE. Yeast Mpk1 mitogen-activated protein kinase activates transcription through Swi4/Swi6 by a noncatalytic mechanism that requires upstream signal. *Mol Cell Biol*. 2008;28(8):2579-2589.
102. Dodou E, Treisman R. The Saccharomyces cerevisiae MADS-box transcription factor Rlm1 is a target for the Mpk1 mitogen-activated protein kinase pathway. *Mol Cell Biol*. 1997;17(4):1848-1859.
103. Watanabe Y, Irie K, Matsumoto K. Yeast RLM1 encodes a serum response factor-like protein that may function downstream of the Mpk1 (Slt2) mitogen-activated protein kinase pathway. *Mol Cell Biol*. 1995;15(10):5740-5749.
104. Jung US, Sobering AK, Romeo MJ, Levin DE. Regulation of the yeast Rlm1 transcription factor by the Mpk1 cell wall integrity MAP kinase. *Mol Microbiol*. 2002;46(3):781-789.
105. Kim KY, Levin DE. Transcriptional reporters for genes activated by cell wall stress through a non-catalytic mechanism involving Mpk1 and SBF. *Yeast*. 2010;27(8):541-548.
106. Truman AW, Kim KY, Levin DE. Mechanism of Mpk1 mitogen-activated protein kinase binding to the Swi4 transcription factor and its regulation by a novel caffeine-induced phosphorylation. *Mol Cell Biol*. 2009;29(24):6449-6461.
107. Kamada Y, Jung US, Piotrowski J, Levin DE. The protein kinase C-activated MAP kinase pathway of Saccharomyces cerevisiae mediates a novel aspect of the heat shock response. *Genes Dev*. 1995;9(13):1559-157
108. Martín H, Rodríguez-Pachón JM, Ruiz C, Nombela C, Molina M. Regulatory mechanisms for modulation of signaling through the cell integrity Slt2-mediated pathway in Saccharomyces cerevisiae. *J Biol Chem*. 2000;275(2):1511-1519
109. Jung US, Sobering AK, Romeo MJ, Levin DE. Regulation of the yeast Rlm1 transcription factor by the Mpk1 cell wall integrity MAP kinase. *Mol Microbiol*. 2002;46(3):781-789.
110. Kuranda K, Leberre V, Sokol S, Palamarczyk G, François J. Investigating the caffeine effects in the yeast Saccharomyces cerevisiae brings new insights into the connection between TOR, PKC and Ras/cAMP signalling pathways. *Mol Microbiol*. 2006;61(5):1147-1166.
111. Morano KA, Santoro N, Koch KA, Thiele DJ. A trans-activation domain in yeast heat shock transcription factor is essential for cell cycle progression during stress. *Mol Cell Biol*. 1999;19(1):402-411.
112. Millson SH, Truman AW, King V, Prodromou C, Pearl LH, Piper PW. A two-hybrid screen of the yeast proteome for Hsp90 interactors uncovers a novel Hsp90 chaperone requirement in the activity of a stress-activated mitogen-activated protein kinase, Slt2p (Mpk1p). *Eukaryot Cell*. 2005;4(5):849-860.
113. Trotter EW, Berenfeld L, Krause SA, Petsko GA, Gray JV. Protein misfolding and temperature up-shift cause G1 arrest via a common mechanism dependent on heat

shock factor in Saccharomyces cerevisiae. *Proc Natl Acad Sci U S A*. 2001;98(13):7313-7318.
114. Truman AW, Millson SH, Nuttall JM, Mollapour M, Prodromou C, Piper PW. In the yeast heat shock response, Hsf1-directed induction of Hsp90 facilitates the activation of the Slt2 (Mpk1) mitogen-activated protein kinase required for cell integrity. *Eukaryot Cell*. 2007;6(4):744-752.
115. Simons JF, Ebersold M, Helenius A. Cell wall 1,6-beta-glucan synthesis in Saccharomyces cerevisiae depends on ER glucosidases I and II, and the molecular chaperone BiP/Kar2p. *EMBO J*. 1998;17(2):396-405.
116. Wright CM, Fewell SW, Sullivan ML, Pipas JM, Watkins SC, Brodsky JL. The Hsp40 molecular chaperone Ydj1p, along with the protein kinase C pathway, affects cell-wall integrity in the yeast Saccharomyces cerevisiae. *Genetics*. 2007;175(4):1649-1664.
117. Shaner L, Gibney PA, Morano KA. The Hsp110 protein chaperone Sse1 is required for yeast cell wall integrity and morphogenesis. *Curr Genet*. 2008;54(1):1-11.
118. Buchan JR, Muhlrad D, Parker R. P bodies promote stress granule assembly in Saccharomyces cerevisiae. *J Cell Biol*. 2008;183(3):441-455.
119. Parker R, Sheth U. P bodies and the control of mRNA translation and degradation. *Mol Cell*. 2007;25(5):635-646.
120. Youn JY, Dyakov BJA, Zhang J, et al. Properties of Stress Granule and P-Body Proteomes. *Mol Cell*. 2019;76(2):286-294.
121. Cougot N, Babajko S, Séraphin B. Cytoplasmic foci are sites of mRNA decay in human cells. *J Cell Biol*. 2004;165(1):31-40.
122. Buchan JR, Parker R. Eukaryotic stress granules: the ins and outs of translation. *Mol Cell*. 2009;36(6):932-941.
123. Kedersha N, Stoecklin G, Ayodele M, et al. Stress granules and processing bodies are dynamically linked sites of mRNP remodeling. *J Cell Biol*. 2005;169(6):871-884.
124. Roy R, Das G, Kuttanda IA, Bhatter N, Rajyaguru PI. Low complexity RGG-motif sequence is required for Processing body (P-body) disassembly. *Nat Commun*. 2022;13(1):2077. Published 2022 Apr 19
125. Giménez-Barcons M, Díez J. Yeast processing bodies and stress granules: self-assembly ribonucleoprotein particles. *Microb Cell Fact*. 2011;10:73. Published 2011 Sep 24.
126. Decker CJ, Parker R. P-bodies and stress granules: possible roles in the control of translation and mRNA degradation. *Cold Spring Harb Perspect Biol*. 2012;4(9):a012286. Published 2012 Sep 1.
127. Coller JM, Tucker M, Sheth U, Valencia-Sanchez MA, Parker R. The DEAD box helicase, Dhh1p, functions in mRNA decapping and interacts with both the decapping and deadenylase complexes. *RNA*. 2001;7(12):1717-1727.
128. Ho Y, Gruhler A, Heilbut A, et al. Systematic identification of protein complexes in Saccharomyces cerevisiae by mass spectrometry. *Nature*. 2002;415(6868):180-183.
129. Hata H, Mitsui H, Liu H, et al. Dhh1p, a putative RNA helicase, associates with the general transcription factors Pop2p and Ccr4p from Saccharomyces cerevisiae. *Genetics*. 1998;148(2):571-579.

130. Fenger-Grøn M, Fillman C, Norrild B, Lykke-Andersen J. Multiple processing body factors and the ARE binding protein TTP activate mRNA decapping. *Mol Cell*. 2005;20(6):905-915.
131. Teixeira D, Sheth U, Valencia-Sanchez MA, Brengues M, Parker R. Processing bodies require RNA for assembly and contain nontranslating mRNAs. *RNA*. 2005;11(4):371-382.
132. García R, Pulido V, Orellana-Muñoz S, et al. Signalling through the yeast MAPK Cell Wall Integrity pathway controls P-body assembly upon cell wall stress [published correction appears in Sci Rep. 2019 Nov 7;9(1):16650. doi: 10.1038/s41598-019-52664-x]. *Sci Rep*. 2019;9(1):3186. Published 2019 Feb 28.
133. Kedersha NL, Gupta M, Li W, Miller I, Anderson P. RNA-binding proteins TIA-and TIAR link the phosphorylation of eIF-2 alpha to the assembly of mammalian stress granules. *J Cell Biol*. 1999;147(7):1431-1442
134. Kimball SR, Horetsky RL, Ron D, Jefferson LS, Harding HP. Mammalian stress granules represent sites of accumulation of stalled translation initiation complexes. *Am J Physiol Cell Physiol*. 2003;284(2):C273-C284.
135. Nonhoff U, Ralser M, Welzel F, et al. Ataxin-2 interacts with the DEAD/H-box RNA helicase DDX6 and interferes with P-bodies and stress granules. *Mol Biol Cell*. 2007;18(4):1385-1396.
136. Anderson P, Kedersha N. Stress granules: the Tao of RNA triage. *Trends Biochem Sci*. 2008;33(3):141-150.
137. Kedersha N, Anderson P. Stress granules: sites of mRNA triage that regulate mRNA stability and translatability. *Biochem Soc Trans*. 2002;30(Pt 6):963-96
138. Cherkasov V, Hofmann S, Druffel-Augustin S, et al. Coordination of translational control and protein homeostasis during severe heat stress. *Curr Biol*. 2013;23(24):2452-2462.
139. Hoyle NP, Castelli LM, Campbell SG, Holmes LE, Ashe MP. Stress-dependent relocalization of translationally primed mRNPs to cytoplasmic granules that are kinetically and spatially distinct from P-bodies. *J Cell Biol*. 2007;179(1):65-74.
140. Buchan JR, Yoon JH, Parker R. Stress-specific composition, assembly and kinetics of stress granules in Saccharomyces cerevisiae. *J Cell Sci*. 2011;124(Pt 2):228-239.
141. Grousl T, Ivanov P, Malcova I, et al. Heat shock-induced accumulation of translation elongation and termination factors precedes assembly of stress granules in S. cerevisiae. *PLoS One*. 2013;8(2):e57083.
142. Cowart LA, Gandy JL, Tholanikunnel B, Hannun YA. Sphingolipids mediate formation of mRNA processing bodies during the heat-stress response of Saccharomyces cerevisiae. *Biochem J*. 2010;431(1):31-38.
143. Hofmann S, Cherkasova V, Bankhead P, Bukau B, Stoecklin G. Translation suppression promotes stress granule formation and cell survival in response to cold shock. *Mol Biol Cell*. 2012;23(19):3786-3800.
144. Wallace EW, Kear-Scott JL, Pilipenko EV, et al. Reversible, Specific, Active Aggregates of Endogenous Proteins Assemble upon Heat Stress. *Cell*. 2015;162(6):1286-1298.
145. Woolford JL Jr, Baserga SJ. Ribosome biogenesis in the yeast Saccharomyces cerevisiae. *Genetics*. 2013;195(3):643-681.

146. Kolhe JA, Babu NL, Freeman BC. The Hsp90 molecular chaperone governs client proteins by targeting intrinsically disordered regions. *Mol Cell*. 2023;83(12):2035-2044.e7.
147. Nitika, Zheng B, Ruan L, et al. Comprehensive characterization of the Hsp70 interactome reveals novel client proteins and interactions mediated by posttranslational modifications. *PLoS Biol*. 2022;20(10):e3001839. Published 2022 Oct 21.
148. Klinge S, Woolford JL Jr. Ribosome assembly coming into focus. *Nat Rev Mol Cell Biol*. 2019;20(2):116-131.
149. Gautschi M, Mun A, Ross S, Rospert S. A functional chaperone triad on the yeast ribosome. *Proc Natl Acad Sci U S A*. 2002;99(7):4209-4214.
150. Deuerling E, Gamerdinger M, Kreft SG. Chaperone Interactions at the Ribosome. *Cold Spring Harb Perspect Biol*. 2019;11(11):a033977. Published 2019 Nov 1.
151. Deuerling E, Bukau B. Chaperone-assisted folding of newly synthesized proteins in the cytosol. *Crit Rev Biochem Mol Biol*. 2004;39(5-6):261-277.
152. Hartl FU, Bracher A, Hayer-Hartl M. Molecular chaperones in protein folding and proteostasis. *Nature*. 2011;475(7356):324-332. Published 2011 Jul 20.
153. Rakwalska M, Rospert S. The ribosome-bound chaperones RAC and Ssb1/2p are required for accurate translation in Saccharomyces cerevisiae. *Mol Cell Biol*. 2004;24(20):9186-9197.
154. Albert B, Kos-Braun IC, Henras AK, et al. A ribosome assembly stress response regulates transcription to maintain proteome homeostasis. *Elife*. 2019;8:e45002. Published 2019 May 24.
155. Bresson S, Shchepachev V, Spanos C, Turowski TW, Rappsilber J, Tollervey D. Stress-Induced Translation Inhibition through Rapid Displacement of Scanning Initiation Factors. *Mol Cell*. 2020;80(3):470-484.e8.
156. Ballinger DG, Pardue ML. The control of protein synthesis during heat shock in Drosophila cells involves altered polypeptide elongation rates. *Cell*. 1983;33(1):103-113.
157. Shalgi R, Hurt JA, Krykbaeva I, Taipale M, Lindquist S, Burge CB. Widespread regulation of translation by elongation pausing in heat shock. *Mol Cell*. 2013;49(3):439-452.
158. Jaiswal H, Conz C, Otto H, et al. The chaperone network connected to human ribosome-associated complex. *Mol Cell Biol*. 2011;31(6):1160-1173.
159. Güldener U, Heck S, Fielder T, Beinhauer J, Hegemann JH. A new efficient gene disruption cassette for repeated use in budding yeast. *Nucleic Acids Res*. 1996;24(13):2519-2524.
160. Nishimura K, Fukagawa T, Takisawa H, Kakimoto T, Kanemaki M. An auxin-based degron system for the rapid depletion of proteins in nonplant cells. *Nat Methods*. 2009;6(12):917-922.
161. Knighton LE, Saa LP, Reitzel AM, Truman AW. Analyzing the Functionality of Non-native Hsp70 Proteins in *Saccharomyces cerevisiae*. *Bio Protoc*. 2019;9(19):e3389.
162. Takacs JE, Neary TB, Ingolia NT, et al. Identification of compounds that decrease the fidelity of start codon recognition by the eukaryotic translational machinery. *RNA*. 2011;17(3):439-452.

163. Shattuck JE, Paul KR, Cascarina SM, Ross ED. The prion-like protein kinase Sky1 is required for efficient stress granule disassembly. *Nat Commun*. 2019;10(1):3614. Published 2019 Aug 9.
164. Knighton LE, Nitika, Waller SJ, et al. Dynamic remodeling of the interactomes of Nematostella vectensis Hsp70 isoforms under heat shock. *J Proteomics*. 2019;206:103416.
165. Werner-Washburne M, Braun EL, Crawford ME, Peck VM. Stationary phase in Saccharomyces cerevisiae. *Mol Microbiol*. 1996;19(6):1159-1166.
166. Mascaraque V, Hernáez ML, Jiménez-Sánchez M, et al. Phosphoproteomic analysis of protein kinase C signaling in Saccharomyces cerevisiae reveals Slt2 mitogen-activated protein kinase (MAPK)-dependent phosphorylation of eisosome core components. *Mol Cell Proteomics*. 2013;12(3):557-574.
167. Nishikawa K, Toker A, Johannes FJ, Songyang Z, Cantley LC. Determination of the specific substrate sequence motifs of protein kinase C isozymes. *J Biol Chem*. 1997;272(2):952-960.
168. Omkar S, Rysbayeva A, Truman AW. Understanding chaperone specificity: evidence for a 'client code'. *Trends Biochem Sci*. 2023;48(8):662-664.
169. Wolfgeher D, Dunn DM, Woodford MR, et al. The dynamic interactome of human Aha1 upon Y223 phosphorylation
170. Mollapour M, Tsutsumi S, Truman AW, et al. Threonine 22 phosphorylation attenuates Hsp90 interaction with cochaperones and affects its chaperone activity. *Mol Cell*. 2011;41(6):672-681.
171. Haslbeck M, Walke S, Stromer T, et al. Hsp26: a temperature-regulated chaperone. *EMBO J*. 1999;18(23):6744-6751.
172. Millson SH, Truman AW, Piper PW. Hsp90 and phosphorylation of the Slt2(Mpk1) MAP kinase activation loop are essential for catalytic, but not non-catalytic, Slt2-mediated transcription in yeast. *Cell Stress Chaperones*. 2022;27(3):295
173. Martín H, Rodríguez-Pachón JM, Ruiz C, Nombela C, Molina M. Regulatory mechanisms for modulation of signaling through the cell integrity Slt2-mediated pathway in Saccharomyces cerevisiae. *J Biol Chem*. 2000;275(2):1511-1519.
174. Jiménez-Sánchez M, Cid VJ, Molina M. Retrophosphorylation of Mkk1 and Mkk2 MAPKKs by the Slt2 MAPK in the yeast cell integrity pathway. *J Biol Chem*. 2007;282(43):31174-31185.
175. Diezmann S, Michaut M, Shapiro RS, Bader GD, Cowen LE. Mapping the Hsp90 genetic interaction network in Candida albicans reveals environmental contingency and rewired circuitry. *PLoS Genet*. 2012;8(3):e100256
176. Caplan T, Polvi EJ, Xie JL, et al. Functional Genomic Screening Reveals Core Modulators of Echinocandin Stress Responses in Candida albicans. *Cell Rep*. 2018;23(8):2292-2298.
177. Needham PG, Patel HJ, Chiosis G, Thibodeau PH, Brodsky JL. Mutations in the Yeast Hsp70, Ssa1, at P417 Alter ATP Cycling, Interdomain Coupling, and Specific Chaperone Functions. *J Mol Biol*. 2015;427(18):2948-2965.
178. Gillies AT, Taylor R, Gestwicki JE. Synthetic lethal interactions in yeast reveal functional roles of J protein co-chaperones. *Mol Biosyst*. 2012;8(11):2901-2908.

179. Mudholkar K, Fitzke E, Prinz C, Mayer MP, Rospert S. The Hsp70 homolog Ssb affects ribosome biogenesis via the TORC1-Sch9 signaling pathway. *Nat Commun*. 2017;8(1):937. Published 2017 Oct 16.
180. Tye BW, Churchman LS. Hsf1 activation by proteotoxic stress requires concurrent protein synthesis. *Mol Biol Cell*. 2021;32(19):1800-1806.
181. Hilliker A, Gao Z, Jankowsky E, Parker R. The DEAD-box protein Ded1 modulates translation by the formation and resolution of an eIF4F-mRNA complex. *Mol Cell*. 2011;43(6):962-972.
182. Yeter-Alat H, Belgareh-Touzé N, Huvelle E, Banroques J, Tanner NK. The DEAD-Box RNA Helicase Ded1 Is Associated with Translating Ribosomes. *Genes (Basel)*. 2023;14(8):1566. Published 2023 Jul 31.
183. Lindquist S. Varying patterns of protein synthesis in Drosophila during heat shock: implications for regulation. *Dev Biol*. 1980;77(2):463-479.
184. Walters RW, Muhlrad D, Garcia J, Parker R. Differential effects of Ydj1 and Sis1 on Hsp70-mediated clearance of stress granules in Saccharomyces cerevisiae. *RNA*. 2015;21(9):1660-1671.
185. Sulima SO, Gülay SP, Anjos M, et al. Eukaryotic rpL10 drives ribosomal rotation. *Nucleic Acids Res*. 2014;42(3):2049-2063.